MICROPATTERNABLE MULTIFUNCTIONAL NANOCOMPOSITE POLYMERS FOR FLEXIBLE SOFT MEMS APPLICATIONS

by

Ajit Khosla
M.Sc, University of Wales Bangor, UK

THESIS SUBMITTED IN PARTIAL FULFILLMENT OF
THE REQUIREMENTS FOR THE DEGREE OF

DOCTOR OF PHILOSOPHY

in the
School of Engineering Science
Faculty of Applied Sciences

SIMON FRASER UNIVERSITY

Fall 2011

APPROVAL

Name: **Ajit Khosla**

Degree: **Ph.D**

Title of Thesis: **Micropatternable Multifunctional Nanocomposite Polymers for Flexible Soft MEMS Applications**

Examining Committee:

Chair: **Prof. John Jones, P. Eng**

_____

Prof. B. L. Gray, P. Eng
Senior Supervisor

_____

Prof. Glenn Chapman, P. Eng
Supervisor

_____

Prof. M. Parameswaran, P.Eng
Supervisor

_____

Prof. Marinko V. Sarunic, P. Eng
Supervisor

_____

Prof. Daniel. B. Leznoff
Internal Examiner, SFU

_____

Dr. James. W. Herchenorder
External Examiner
Vice President Engineering,
Magnequench International, Inc.

Neo-Materials Inc.

Date Defended/Approved: 25 October 2011
_____

Declaration of
Partial Copyright Licence

ABSTRACT

This thesis describes the fabrication, micro-machining, and characterization of novel multifunctional nanocomposite polymers for flexible microsystems. Various elastomers, primarily polydimethylsiloxane (PDMS), a silicone based elastomer, are chosen as substrate materials to create new flexible microsystems because of numerous benefits of PDMS including flexibility, biocompatibility, low cost, low toxicity, high oxidative and thermal stability, optical transparency, low permeability to water, low electrical conductivity, and ease of micropatterning. However, most devices to date based on PDMS are passive, as making active devices out of PDMS is extremely challenging. When PDMS is bonded to substrates with conventionally-realized active components like electrodes, heaters, sensors, actuators, etc., it is rendered inflexible – defeating one of its key benefits. For example, the common method of bonding PDMS with glass renders the resulting devices completely inflexible. If metals or alloys are deposited on PDMS, the weak adhesion between them and PDMS leads to microcracks when the substrates are flexed, bent, or twisted. This leads to electrical disconnection and device failure.

The focus of this thesis is the development of novel approaches to the realization of active-component based highly flexible microsystems employing PDMS and/or other elastomer materials. To overcome problems with

incorporating active devices while maintaining system flexibility, various new materials and methods of microfabricating them are developed. These newly developed electrically conductive and magnetic nanocomposite polymers deliver flexibility similar to undoped and insulating PDMS, yet provide functionality for active device development similar to the inclusion of inflexible metals and other functional materials. These new polymers can also be easily micromicromolded using conventional PDMS processing, such as soft lithography techniques. A new hybrid microfabrication process for combining micromolded nanocomposite with undoped PDMS polymer is also developed to demonstrate the potential of the new polymers to be incorporated into fully flexible systems containing active components. Poly(methyl methacrylate) (PMMA) is also explored as a new molding substrate for small and large area microfabrication such that 12 inch by 24 inch flexible sheets containing active nanocomposite polymer devices can be realized on a large scale.

Applications of these multifunctional nanocomposites include shape-conformable microelectrodes, hard magnetic microactuators, signal routing for Lab on a Chip (LOC) and many other devices requiring flexible microsystems and electronics.

Keywords: Polymers, Nanocomposites, PDMS, Micromolding, Hybrid fabrication, Flexible microsystem, Nanoparticles, μTAS, LOC

DEDICATION

To my father

Mom this is for you, your son did it !!!

:)

ACKNOWLEDGEMENTS

I would like to thank my supervisor Prof B. L Gray, for her support and the freedom she gave me to work; I could not have asked for more. Credit to all my success goes to Prof. B. L. Gray and Prof. R. Pethig (supervisor for M.Sc). It is because of Prof. R. Pethig that I learned the value and importance of filing in patents.

Thanks go out to Manu Pallapa, Steve Whitmore, Mike Sjoerdsma, Prof. Ash. M. Parameswaran, Prof. John Jones, Prof D. B. Leznoff, Barry Shell, Marius Haiducu, Raj Pabla, Ryan Rosner, Devan Huber,Bill Woods, Andres,all my lab mates, friends, and enemies.

Without the support of Amit Khosla and Charu Khosla, I would not have been able to be where I am today.

TABLE OF CONTENTS

Approval ..... **ii**

Abstract ..... **iii**

Dedication ..... **v**

Acknowledgements ..... **vi**

Table of Contents ..... **vii**

List of Figures ..... **x**

List of Tables ..... **xiii**

Glossary ..... **xiv**

Chapter 1: Introduction **1**

Chapter 2: Prior art **10**

2.1 Defining nanoparticles 11
2.2 Shape of nanoparticles 11
2.3 Carbon nanotubes 12
2.4 Polymer nanocomposites 13
2.5 Why nanoparticles 14
2.6 Percolation threshold 15
2.7 Dispersion mechanisms of nanoparticles in polymers 17
2.8 Prior work on micropatternable electrically conductive PDMS 19
Carbon Black-PDMS: 19
Carbon Nanotubes-PDMS 20
Silver micro and nanoparticles in PDMS 22
2.9 Prior art on magnetic PDMS and issues 25
2.10 Summary of chapter 2 26

Chapter 3: Nanocomposite polymers: Fabrication and micropatterning **28**

3.1 Nanocomposite fabrication and patterning process 30
General fabrication process for polymeric nanocomposites 30
Examples PDMS based nanocomposite fabrication 31
Electrically conducting multi-walled carbon nanotube-PDMS nanocomposite 32
Electrically conducting Silver nanoparticle (Ag-n) doped PDMS nanocomposite 36
Hard magnetic neodymium iron boron based composite 38

Hard magnetic powder used 39
NdFeB ($Nd_{0.7}Ce_{0.3})_{10.5}Fe_{83.9}B_{5.6}$) doped hard magnetic PDMS 41
3.2 SU-8 micromold fabrication 41
Substrate cleaning 44
Glass substrate 44
Silicon substrate 44
Adhesion layer 45
Micromold structural layer 46
3.3 General hybrid nanocomposite micromolding process 47
3.4 Summary, contributionsand discussion 51

Chapter 4: PMMA as Micromold Material 56

4.1 Deep-UV lithography of commercial grade PMMA 57
4.2 CO_2 laser ablation of PMMA 63
4.3 Summary, contributions and discussion 68

Chapter 5: Results and discussion 70

5.1 Electrically conductive MWCNT-PDMS results and discussion 71
Resistivity and percolation threshold measurements 71
MWCNT-PDMS microribbon cable fabrication and testing 74
Negative Temperature Coefficient of Resistivity Results 77
Summary 79
5.2 Electrically conductive Ag-n-PDMS results and discussion 80
Percolation threshold and electrical properties 80
Summary 83
5.3 Soft magnetic Ni-PDMS nanocomposite properties and testing 84
Magnetic characterization 84
Mechanical characterization 86
Electrical characterization 87
Summary 89
5.4 NdFeB-PDMS and micromagnet testing 90
Micromagnets characterization 90
Summary 92
5.5 Summary table for properties of multifunctional 93
Nanocomposites 93

Chapter 6: Future work and conclusion 95

6.1 Future work 95
Feature size 95
PMMA etching improvements 95
Cyclic olefin copolymer as structural mold material 96
Other microfabrication techniques 96
Device fabrication 96
6.2 Contributions 97
6.3 Conclusion 99

Appendices 101
Appendix 1 Positive mask layout for electrodes fabricated in figures 13 and 32 101
Appendix 2 Negative mask layout for electrodes fabricated in figures 13 and 32 102
Appendix 3 Layout of .cdr file for CO_2 laser ablation of 12inch x 24 inch large scale PMMA micromold 103
Appendix 4 Layout of .cdr file for CO_2 laser ablation of PMMA micromold for ribbon cables 104
Appendix 5 RCA run sheet: cleaning Silicon and glass substrates 105
Appendix 6 Thick SU8 100 processing parameters 106
Appendix 7 Commercial Plexiglass mirrors and MEMS: New approach toward low cost polymer microsystems 108
Introduction 108
Experimental 110
Micromachining Mirrored-Extruded Acrylic 110
Electrical properties 111
Summary 115
Reference List 116

LIST OF FIGURES

Figure 1 Chemical structure of polydimethylsiloxane (PDMS) 4

Figure 2 Microcracks on sputtered gold on PDMS under mechanical stretch cycles: (a) Cycle1, strain 0; (b) Cycles 2 Strain 20%; (c) Cycles 101, strain 0. 7

Figure 3 Resistivity versus weight percentage of nanoparticle filler in polymer matrix for conductive nanocomposite polymer. The percolation threshold *(p_c)*is labelled. 16

Figure 4 Conductivity vsweight fraction of CNT in PDMS matrix (Yi Kuen Li *et al*) [81] 22

Figure 5 Conductivity vsweight percentage of silver 1-2 micron particles in PDMS matrix [83] 23

Figure 6 Process flow chart illustrating the patterning of conductive PDMS by plastering by X. Z. Niu [84]: a) Micropatterning of the conductive PDMS as follows; b–d) SEM images showing the various fabricated conductive patterns. 24

Figure 7 Photographs showing steps involved in fabrication of MWCNT-PDMS nanonanocomposites: a) MWCNT's; b) MWCNT's in heptane; c) high frequency ultrasonicted MWCNT's in heptane; d) shear mixing of MWCNT-PDMS using magnetic stirrer. 34

Figure 8 SEM photographs of COOH- functionalized MWCNTs at different (increasing) magnifications in PDMS showing uniform dispersal. Scale bar: a) 1µm ; b) 200 nm; c) 100nm; d) 20nm. 35

Figure 9 SEM graphs of Ag-n at different magnifications in PDMS. Scale bar: a) 2µm ; b) 500 nm; c) 2µm; d) 200nm 37

Figure 10 SEM micrograph of MQFP magnetic powder with an average particle size of 5µm 40

Figure 11 Chemical structure of SU-8 photoresist 42

Figure 12 Fabrication process step for SU-8 micromold preparation via UV-light photopatterning of SU-8. 43

Figure 13 SU-8 micromold fabricated via UV-lightmicropattering of SU8 100 photoresist on 4 inch silicon wafer. 47

Figure 14 Hybrid fabrication process for combining micromolded nanocomposite with undoped PDMS polymer. A) SU-8 micromold, b) PDMS nanocomposite poured on SU-8 micromold, c) Excess nanocomposite scraped off from the surface of micromold, d) PDMS poured on the surface of mold, e) Pealed off nanocomposite microstructures on PDMS nonconductive/magnetic polymer 49

Figure 15 Optical micrographs of fabricated conductive microstructures on non-conducting PDMS: a) MWCNT-PDMS (4 wt.%)nanocomposite array of microelectrodes of lengths ranging from 1mm to 10mm, height of 30 µm and width of 100 µm; b) Ag-n PDMS (50 wt.%) array of m microelectrodes of lengths ranging from 1mm to 10mm height of 30 µm and width of 100 µm..... 50

Figure 16 SEM and optical micrograph of: a) NdFeB micromolded hard micromagnets; b) 50nm nickel nanoparticle doped PDMS microcoils..... 51

Figure 17 Optical micrograph of stiction of Ag-n PDMS nanocomposite to SU-8 micromold..... 54

Figure 18 Deep-UV exposure of PMMA: fabrication process steps [104]..... 58

Figure 19 SEM micrographs of Deep UV patterned PMMA..... 61

Figure 20 SEM micrographs of micromolded magnetic nanocomposite: a) cantilevers; b) bridges; c) cantilever tip/edge; d) parallel bridges. 62

Figure 21 Cross-sectional area of CO_2 laser etched PMMA..... 64

Figure 22 Optical micro graph top view of 150µm CO_2 Laser etch PMMA 65

Figure 23 Effect of laser power (a) and beam speed (b) on the channel depth. The relative values are based on the maximum laser power of 65 W and beam speed of 1143 mm/s. Data points are measurement results and solid lines are fitting curves. The substrate material is 5mm thick. 66

Figure 24 Optical micrograph of large scale micro patterning of MWCNT-PDMS nano composite-Hybrid microfabrication process against a 12 inch x 24 inch substrate..... 67

Figure 25 Test fixture to measure the resistivity of MWCNT-PDMS nanocomposite samples..... 72

Figure 26 Resistivity verses COOH- functionalized MWCNT wt.% in the PDMS matrix 73

Figure 27 Microribboncabel fabrication: a) laser etched PMMA micromold; b) PMMA micromold after Damascene-like process, filled with MWCNT-PDMS nanocomposite; c) optical micrograph of etched PMMA; d) demolded MWCNT-PDMS ribbon cable close up; e) cured PDMS on PMM..... 75

Figure 28 Micro ribbon cables (a) curved in (b) curved out. For the curved in structures, the ribbon cable structures are on the surface on the inside curve, and the opposite (on the outside of the rolled sheet) for the outside curved. 76

Figure 29 Negative temperature coefficient of resistivity of COOH-functionalized MWCNT in PDMS for different weight percentages of nanotubes. 79

Figure 30 Optical micrographs of fabricated microelectrodes on nonconducting PDMS: array of microelectrodes of lengths ranging from 1mm to 10mm..... 81

Figure 31 Electrical properties of Ag-n PDMS nanocomposite micropatternable polymer: a) resistivity vs. weight percentage of silver nanoparticles in PDMS matrix; b) I-V characteristics of microelectrodes of different lengths. 82

Figure 32 Saturation magnetization (Msat) per gram of composite as a function of mass percent of Ni in the Ni-PDMS composites. 85

Figure 33 Young Modulus's versus nickel weight percentage (Wt%) in PDMS matrix 87

Figure 34 Resisitivity versus nickel wt. % in PDMS matrix. 88

Figure 35 a) SEM micrograph of an array of micromolded magnets and b) typical remanent magnetization (M) vs. coercitvity (H) hysteresis loop of a micromagnetic polymer sample at 300 K 91

Figure 36 Fabrication flow for micromachining Mirrored-Extruded Acrylic metal..... 113

Figure 37 Micrographs of micromachined extruded mirrored acrylic aluminium. 114

LIST OF TABLES

Table 1 Materials and suppliers for nanoparticles and polymers fabricated as part of this thesis..... 29

Table 2 Comparison Deep UV vs CO_2 micromaching of PMMA..... 69

Table 3 Standard and relativestandard deviation of resistivity of 45 ribbon cables..... 76

Table 4 Effects on resistance of MWCNT-PDMS microribbon cables due to curving..... 77

Table 5 Coercivity (Hc) and remanent magnetization (Mr) of five different 50μm, height 30μm micromolded magnet samples. 91

Table 6 Multifunctional nanocomposite polymers & properties..... 93

Table 7 Comparison of electrical resistivity of bulk elements verses nanocomposites 94

GLOSSARY

ABS	Acrylonitrile butadiene styrene
CNT	Carbon nano tube
COC	Cyclic olefin copolymer
CVD	Chemical vapour deposition
DI	Deionized water
DMM	Digital multimeter
IC	Integrated circuit
IPA	Isopropyl alcohol
HF	Hydrofluoric acid
KOH	Potassium hydroxide
LIGA	Lithography, electrodeposition and moulding (German acronym for “LithographieGalvanoformungAbformung”)
LOC	Lab-On-a-Chip
MEMS	Micro Electro Mechanical Systems
MQFP	Magnequench fine powder, 5micron, NdFeB based powder
MWCNT	Multiwalled Carbon Nanotube
NPs	Nanoparticles
NTCR	Negative temperature coefficient of resistiviy
PDMS	Poly(dimethylsiloxane)
PET	Poly(ethylene terephthalate)
PMMA	Poly(methylmethacrylate)

PVC	Poly(vinyl chloride)
PZT	Lead ZirconateTitanate
SWCNT	Single waleed carbon nano tube
SMA	Shape memory alloy
SEM	Scanning Electron Microscope
SQUID	Superconducting Quantum Interference Device
SU-8	Epoxy Resin
UV	Ultraviolet Light
nm	Nanometer
VSM	Vibrating Sample Magnetometer
µTAS	Micro Total Analysis System
µm	Micrometer

CHAPTER 1: INTRODUCTION

Nanotechnology is set to have a major impact on our society and the way we live andis defined as the study, control of phenomena and materials, at length scales below 100 nm [1]. For explanation, often the length scale comparison is made with a human hair, which is about 80,000 nm wide. The bulk properties of materials often change dramatically with brought down to the nano regime [2]. Two main properties of nanomaterials are increased relative surface area and quantum effects. These two factors can change or enhance properties such as reactivity, mechanical strength, magnetic and electrical characteristics.With a reduction in particle size, a more atoms are found at the surface compared to those inside the particle. For example, a particle of size 30 nm has 5% of its atoms on its surface, at 10 nm 20% of its atoms, and at 3 nm 50% of its atoms [3]. Hence, smaller nanoparticles have a relatively higher surface area per unit mass compared to larger nano or micron sized particles. Hence, for a given mass of material in nano regime will be much more reactive than the same mass of material made up of larger particles.

Because of new properties associated with nanomaterials, such materials have already brought advances to many fields of engineering; e.g., self-cleaning windows [4], high efficiency solar cells [5], energy-efficient LED lighting [6], cleantech [7], and super-hydrophobic nanomaterials resistant to ice accumulation

[8]. New developments are seen in atomic force microscope probes [9], high performance ultra-capacitors [10], single electron transistors [11], high density memories [12], field emission displays [13], textiles [14], agriculture [15], nanoparticle reinforced lighter and tougher nanocomposite steel and plastics/polymers [16], composite fabric/textile with nano-sized particles, and chemical sensors [17]. Nanotechnology could soon deliver medical breakthroughs such as drug delivery, cancer detection and other advances that have a significant potential to revolutionize our daily life [18].

One particular area of interest is developing ***nanoparticle doped functional polymers*** for applications in aviation, space, smart textiles, wearable electronics-health monitoring systems, sensors, microfluidics and micro-electro mechanical systems (MEMS). Nanoparticles have opened doors to many applications in the area of nanocomposite materials [19],addressed in chapter 2.

The definition of nanocomposite materials has broadened significantly to encompass a large variety of systems such as one-dimensional, two-dimensional, three-dimensional and amorphous materials, that are fabricated with distinctly dissimilar components and mixed at the nanometer scale. The general class of nanocomposite organic/inorganic materials is a growing area of research. Significant effort is focused on the ability to obtain control of the nanoscale structures via innovative synthetic approaches, such as chemical vapour deposition (CVD) [20]. The properties of nano-composite materials depend not only on the properties of their parents but also on their morphology and interfacial characteristics. The latter can derive by combining properties from

the parent constituents into a single material, resulting in the possibility of new properties that are unknown in the parent constituent materials [21].

Experimental work carried out by researchers worldwide has shown that virtually all types and classes of nanocomposite materials lead to new and improved properties when compared to their macrocomposite counterparts [22]. Therefore, nanocomposites promise new applications in many fields such as mechanically reinforced lightweight components, non-linear optics, battery cathodes and ionics, nano-wires, sensors and other systems.

By judiciously engineering the polymer-nanoparticles, nanocomposites maybe produced with a broad range of properties. Polymers possess well-defined, ordered intralamellar space potentially accessible by foreign species, enabling them to act as matrices or hosts for polymers, yielding interesting hybrid nano-composite materials [23].

Although micromachining and MEMS originated within the silicon-based IC community, more recently, as new and wider applications of MEMS have been forthcoming, new materials and fabrication technologies have been developed, including polymer microfabrication techniques such as soft lithography/micromolding and microinjectionmolding [24]. MEMS, with microfluidics, can enable precise control of fluids on micro-nano litre scales e.g. drug delivery systems.In order to realize such systems, all of the required components needed must be miniaturized and interconnected into a complete functional system. These systems may include multiple components for sample/drug storage, chemical reaction chambers, fluid control, analyte

separation and detection, and data acquisition, to accomplish complex tasks such as the detection of disease markers or environmental toxins in small (e.g., nanoliter) samples of fluid and monitoring.

While many materials have been employed to realize flexible MEMS and microfluidic devices such as stated above, polydimethylsiloxane (PDMS), a silicone based elastomer, has been widely used because of its biocompatibility, low cost, low toxicity, high oxidative and thermal stability, optical transparent, low permeability to water, low electrical conductivity, and ease of micropatterning [25]. PDMS is a thermosetting polymer and is particularly known for its unusual rheological (or flow-self levelling) properties. The chemical formula for PDMS is $CH_3[Si(CH_3)_2O]_nSi(CH_3)_3$, where n is the number of repeating monomer $[SiO(CH_3)_2]$ units. Chemical structure of PDMS is shown in figure 1.

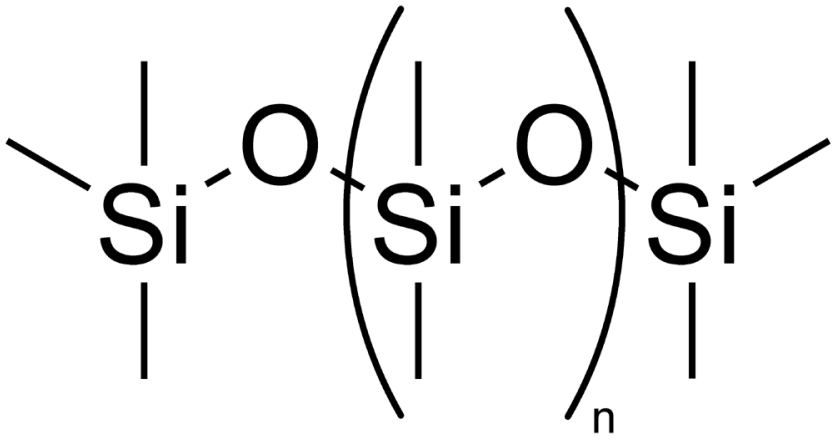

Figure 1[1] Chemical structure of polydimethylsiloxane (PDMS)

[1] Permission is granted to copy and use the figure, under the terms of the GNU Free Documentation License

Various standalone MEMS and microfluidic devices have been fabricated by micromolding PDMS against SU-8 photopolymer masters (called soft lithography) including imicromixers, microchannels, valves, pumps, and interconnect structures for a wide variety of applications for lab-on-a-chip (LOC) analysis [26].However, most devices based on PDMS are passive and, if active devices are fabricated, then they are bonded to substrates like glass whichmay contain active components like electrodes, heaters etc patterned on it. This is because it has proven difficult to integrate, embed or pattern conducting lines, magnetic materials on PDMS because of the weak adhesion between PDMS and metals [27]. Integrating of functional material (electrically conductive and magnetic) structures in bulk PDMS is extremely important for signal routing, interfacing to signal processing electronics, for powering active devices, and actuation purposes. In the case of metal/metal-alloys patterning, microcracks appear on the surface of the patterned conductive lines on being flexed, bent, or twisted, leading to electrical disconnection [28]. Figure 1 shows microcracks appearing on sputtered gold on PDMS under mechanical stretch cycles leading to discontinuity of sputtered gold. The gold on PDMS was tested for their different mechanical strain cycles: (a) Cycle1, strain 0; (b) Cycles 2 Strain 20%; (c) Cycles 101, strain 0. In all the cases, microcracks are observed as shown by SEM analysis. Hence, in order to elevate the problem of microcracks appearing on sputtered metals on PDMS surfaces such as shown in figure 1, it is important to develop PDMS-based active materials of similar flexibility to the undoped and insulating PDMS; so that they can also be easily micromolded using similar soft

lithography techniques in order to provide robust system electrical routing. In addition, for MEMS and microfluidic systems, the ability to manipulate fluid on chip (fluid control) via on-chip microvalves and pumps is usually required. Magnetically actuated valves and pumps are asuperior choice due to the high energy density of magnetic actuation schemes [29]. While PDMS is inherently electrically insulating and non-magnetic, these properties can be modified by introducing conducting and/or magnetic nanoparticles in the polymer matrix [30]. Such active polymers are of great interest to the microelectronic, MEMS, microfluidic and lab-on-a-chip (LOC) communities for packaging, microsensor, and microactuator applications [31], which may lead to developing of fully integrated flexible systems. Thus, there is a need to develop both conductive and magnetic PDMS-based micropatternable nanocomposite polymers

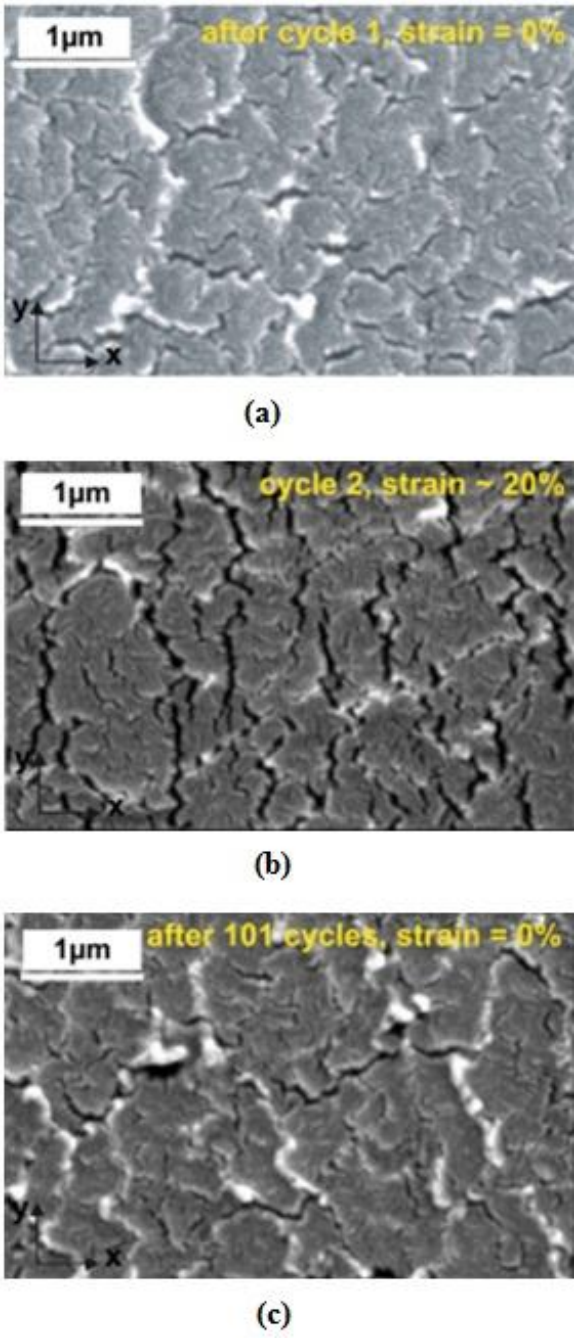

Figure 2[2] Microcracks on sputtered gold on PDMS under mechanical stretch cycles: (a) Cycle1, strain 0; (b) Cycles 2 Strain 20%; (c) Cycles 101, strain 0.

[2] Copyright obtained: Licensee: Ajit Khosla, License Date: Nov 19, 2011, License Number: 2792680508109 Publication: Applied Physics Letters, Title: Mechanisms of reversible stretchability of thin metal films on elastomeric substrates, Type Of Use: Thesis/Dissertation

The main thrust of this thesis is to develop process which alleviate problems with materials mismatch between flexible nonconductive polymers and metals/Alloys or less flexible conductive polymers for soft (polymer) MEMS and flexible lab-on-chip systems.

In order to solve the problem of combining electronic and magnetic functionality with passive PDMS devices, nanoparticle doped multifunctional polymers, which either are electrically conducting, magnetic in nature, or both, are developed and described in detail in this thesis. The idea of developing silicone based elastomers which are electrically conducting, magnetic and both in nature is not new [32, 33, 34, 35, 36]; however, micropatternability and stability of these elastomers has always remained a challenge, which is the major focus of this thesis. This thesis substantially contributes to the fields of flexible MEMS and microfluidics through the development, fabrication, and characterization of nanocomposite polymer materials and devices. The contribution of this thesis will be as follows:

1. Development of general fabrication process for micromoldable multifunctional nanocomposite polymer materials, including
    i. Materials suitable for microfabrication of nanocomposite polymers
    ii. Microfabrication of those materials
    iii. Nanoparticle dispersion techniques best suited for PDMS based nanocomposite polymermicrodevices and systems
    iv. Choice of substrate for micropatternable nanocomposite polymers

2. Development of new fabrication methods for conductive and magnetic nanocomposite polymers including

i. Comparison of micropatterning against various master molds

ii. Large scale micropatterning over large areas

iii. Hybrid process for combining nanocomposite polymers with unfilled polymers

3. Demonstration of these new materials and methods for active MEMS devices tointegrate with flexible microsystems

i. Microelectrodes

ii. Ribbon Cables

iii. Micromagnets

This thesis has five main sections: 1) background/prior art, 2)nanocomposite polymer: fabrication and micropatterning, 3) poly(methyl methacrylate) as a new micromold material, 4)results anddiscussion, 5) future work and conclusion.

CHAPTER 2: PRIOR ART

In this chapter, we will discuss the basics of nanoparticles, nanocomposite polymers, various dispersion mechanisms of nanoparticles in polymers, percolation threshold (in the case of electrically conducting polymers) and the prior work done in the field of nanocomposite electrically conductive and magnetic PDMS in preparation for discussing of my work in new methods of fabricating and micropatterning nanocomposite polymers. This chapter is divided into the following sub sections:

2.1. Defining nanoparticles

2.2. Shape and Size of nanoparticles

2.3. Carbon nanotubes

2.4. Polymer nanocomposites

2.5. Why nanoparticles

2.6. Percolation threshold

2.7. Dispersion mechanism of nanoparticles in polymers

2.8. Prior work on micropatternable electrically conductive PDMS

2.9. Prior work on micropatternable magnetic PDMS

2.10. Summary of chapter 2

2.1 Defining nanoparticles

There is no accepted international definition of a nanoparticle, but one given in the new Publicly Available Specification 71 (PAS71) document developed in United Kingdom is:“A particle having one or more dimensions of the order of 100nm or less”. However, a note associated with this definition further refers to the characteristics of such particles: “Novel properties that differentiate nanoparticles from the bulk material typically develop at a critical length scale of under 100nm” [37]. A nanopowder is “an agglomeration of noncrystalline nanostructural subunits with at least one dimension less than 100nm.”

2.2 Shape of nanoparticles

Nanoparticles come in different shapes: spheres, flakes, rods, tubes, fibers, wires and random assortments that may contain all of these shapes [38]. Nanoparticles can have a very high aspect ratio of 1:1000000, or they can be simple spheres [39]. These shapes and sizes play an important role in determining the percolation threshold (see section 2.7), the ability to uniformly mix particles, and calculating mechanical changes (e.g., Young’s modulus) to the polymer matrix after addition of nanoparticles. Aspect ratio (length to width ratio) is thought to play a large role in percolation threshold, as it seems that conductive percolation paths are, in general, more easily set up between long and thin nanoparticles [40].

Different metal nanoparticles and elemental nanoparticles, as well as nanoparticles composed of alloys, borides, carbides, nitrides, oxides,

phosphides, and sulfides are commercially available [41]. Out of all these, nanoparticles consisting of metal (silver, gold, aluminum, copper etc.), elements (carbon, fullerenes, graphene, CNT's etc), alloys (Zinc Iron, Hafnium, Niobium etc), borides (NdFeB etc.) and oxides (Iron III oxide etc) are of great interest to us in this work because of their higher conductivity (for electrically conducting nanocomposites employing metals, alloys, or elementals) and high magnetization (for magnetic nanocomposites employing magnetic materials). Most of these nanoparticles have not been employed to fabricate nanocomposite polymers to date, or have been incompletely characterized.

2.3 Carbon nanotubes

In order to understand carbon nanotubes (CNT), it is important to define graphene. Graphene is an allotrope of carbon, whose structure is one-atom-thick planar sheets of carbon atoms that are densely packed in a honeycomb crystal lattice [42]. A carbon nanotube consists of either one cylindrical graphene sheet (single-wall carbon nanotube, SWCNT) or of several nested cylinders with an interlayer spacing of $0.34 – 0.36$ nm that is close to the typical spacing of turbostratic graphite (multiwall carbon nanotube, MWCNT) [43].

Different types of carbon nanotubes, which are commercially available, are: 1) single wall carbon nanotubes (SWCNT), 2) double wall carbon nanotubes (DWCNT), 3) multiwall carbon nanotubes (MWCNT), 4) torus (doughnut shape), 5) Nanobuds ("buds" are covalently bonded to each other's outer sidewalls.

However, the SWCNTs and MWCNTs are most commonly used carbon nanotubes because of ease of bulk fabrication [44].

In this thesis, we have employed MWCNTs for preparation of electrically conducting micropatternable nanocomposites. Some of the MWCNTs that we employ are functionalised with OH- and COOH- bonds for easy dispersion [45]. This reason for this is explained in detail in section 2.7 of this chapter.

2.4 Polymer nanocomposites

Polymer nanocomposites are polymer matrices reinforced with nanoparticles [46], whereas conventional polymer composites contain micrometer scale particles. In the simplest case, polymer nanocomposites are prepared by adding nanoparticles in a polymer. Different particles have been used to prepare polymer/inorganic particle nanocomposites by other researchers; however, micropatternability has not been previously demonstrated for many of these nanocomposites.Particles of interest include:

1. Metal (for example: Al, Fe, Au, Ag, W, Cu, Mo etc.)
2. Metal oxide (for example: ZnO, Al_2O_3, $CaCO_3$, TiO_2 etc.)
3. Nonmetal oxide (for example: SiO_2)
4. Rare earth alloy (for example: NdFeB, SmCo)
5. Other (for example: SiC, C including CNT’s)

Different methods used to prepare polymer-inorganic materials include in-situ polymerization, melt compounding by twin-screw extrusion, solution blending, high shear mixing, high and low frequency ultrasonics, ball milling and bead milling and chemical methods (using surfacents and functionalizing) [47]. Some of these processes like shear mixing and high frequency ultrasonics, which are used for fabricating PDMS based polymer nanocomposites in this thesis are discussed in detail in section 2.7 of this chapter and also in chapter 3.

2.5 Why nanoparticles

Nanoparticles exhibit size-related properties that differ significantly from those observed in micron sized particles or bulk materials. Nanoparticles can be embedded in many different polymer matrices, such as polycarbonate, polystyrene, nylon, PMMA, PDMS, silicone rubbers, polyamide, ABS, polyethylene etc [48, 49, 50, 51].From these materials,nanocomposites based on PDMS are of interest to us for soft MEMS applications as discussed in theIntroduction. These nanocomposites exhibit enhanced properties of high performance materialsare mainly due to the high aspect ratio and/or the high surface area of the fillers, since nanoparticulates have extremely high surface area to volume ratios when homogeneous dispersion is achieved [52]. This new class of composite materials show enhanced optical, electrical, magnetic and dielectric properties compared to microparticles reinforced polymers [53]. So, it is

likely that we should be able to develop PDMS nanocomposites with unique capabilities which can be micropatterened similarly to ordinary PDMS.

2.6 Percolation threshold

Silicone based polymers can be made electrically conductive by filling them with conductive particles [54]. The particles are called fillers, and the material in which they are put is called the matrix; the total of matrix with fillers is called a composite. When the size of the particles is of the order of 10^{-9}m to 10^{-7}m a composite is also called a nanocomposite [55]. When the fillers form a continuous path from one side of the material to the other, the material is above its critical filler fraction/concentration(figure 2, indicated by point B) and a direct current (DC) can flow through it. For fewer particles, no continuous path is formed from one side to the other and the material is below its critical filler fraction (figure 2, indicated by point A). It is desired to have a critical filler fraction that is as low as possible, in order to have a conductive material already for a low amount of fillers [56]. Figure3shows resistivity versus weight percentage of nanoparticle filler in a polymer matrix for a conductive nanocomposite polymer. It can be clearly seen that after the percolation threshold *(p_c)*, resistivity drops down drastically.The advantage of such a material is that the properties of the matrix (like transparency, hardness, stiffness, etc) are largely maintained [57]. Above the critical filler fraction/concentration (figure 3, indicated by point C), the resistivity is generally hardly dependent on the amount of fillers [58].

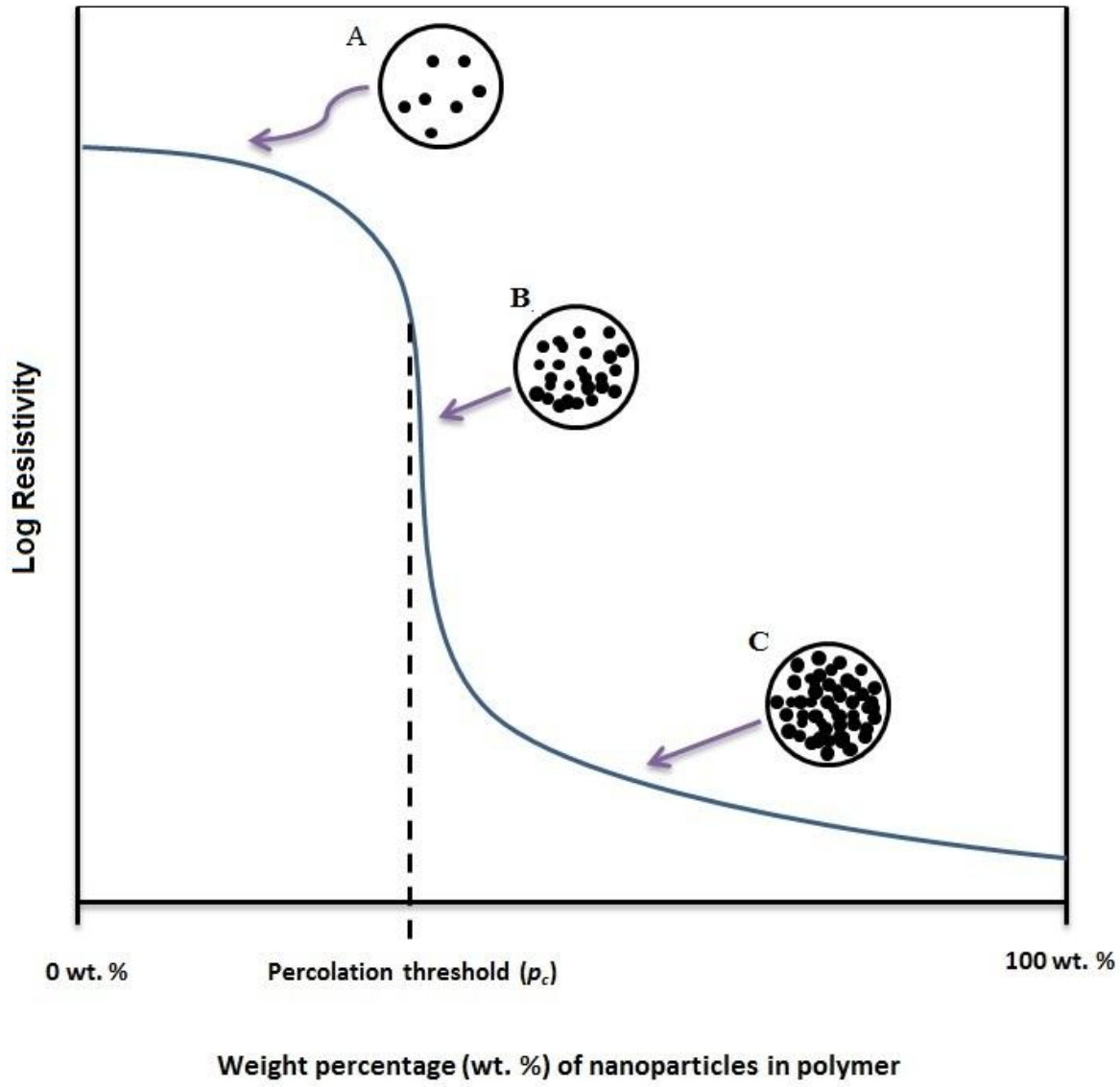

Figure 3 Resistivity versus weight percentage of nanoparticle filler in polymer matrix for conductive nanocomposite polymer. The percolation threshold *(p_c)*is labelled.

2.7 Dispersion mechanisms of nanoparticles in polymers

In order to fabricate nanocomposites with enhanced properties such as electrical conductivity or magnetization, for their fill percentage or weight percentage (percentage of nanoparticles in the polymer matrix), the nanoparticles must be mixed substantially homogeneously and uniformly distributed within the polymer matrix [59]. Dispersion is the key to developing a high quality nanocomposite with uniform properties.

Typical methods of nanoparticle dispersion in polymers are classified into two main categories: physical dispersion and chemical dispersion [60]. Physical dispersion method involves separating agglomerates of nanoparticles, nanorods or a bundle of CNTs which are tied up or clumped up together by van der Waals forces [61]. Three main physical dispersion mechanisms which are commonly used: 1) ultrasonic agitation, 2) shear mixing,3) ball milling [62]. The most popular technique is ultrasonic agitation, in which the nanoparticles are first manually stirred in a solvent and then exposed to ultrasonic waves/irradiation [63]. There are two different types of ultrasonic waves which can be used. The first type is low frequency ultrasonics (~ 20-24 kHz), in which the composite is placed in an ultrasonic bath and is agitated for a specified time depending on the type of nanoparticles. The second type involves using high frequency ultrasonics (~ 42-50 kHz) in which an ultrasonic probe is immersed into the composite. Usually, the probe is operated in pulse mode, which provides mixing by repeatedly allowing the sample to resettle under the probe after each burst. The

shock waves generated by ultrasonic pulses lead to collisions between nanoparticles. Consequently, the agglomerated nanoparticles are eroded and split by the collisions [64]. One of the major problems with ultrasonic agitation is that heat is produced; hence it is recommended to operate the ultrasonic bath or the probe in pulse mode. In the case of CNT's it has been observed that prolonged exposure to ultrasonic waves can damage the CNT's [65]. Thus, other mixing methods may be required, such as prolonged shear mixing for 6 to 7 hours [66].

For viscous monomers/polymers and photoresists (e.g., PDMS, SU8 100, SU8-2050 etc.) shear mixing is the preferred method as it allows direct dispersion of nanoparticles in the polymer matrix. The nanoparticle aggregates are forced apart by high speed shear mixing. The viscosity of the solvent/polymer matrix does not allow the nanoparticles to re-aggregate [67]. One of the most common ways for shear mixing is to use a magnetic stirrer (usually at 1000 to 5000 rpm depending on the viscosity of polymer or monomer); however, magnetic stirring is, for obvious reasons, not recommended for magnetic nanoparticles like nickel, iron hexferrites, NdFeB etc.

Ball milling is another technique used for nanoparticle dispersion and it is usually preferred for CNT dispersion because of the bundle size of CNTs [68]. It consists of a rotary cylinder along with iron or plastic balls to break the clumps of carbon nanotubes. However, it is not widely used at research level and tends to break the carbon nanotubes [69]. Bead milling, which is a technique similar to ball milling, has proved efficient in dispersing nanoparticles in which balls of

micrometer scale diameter are used to disperse nanoparticles to the primary particle size [70]. Among all the three physical dispersion methods ultrasonic is preferred because it is quick, easy to use and the dispersion is good as compared to other physical methods.

Chemical dispersion methods are classified as covalent and non-covalent methods. Extensive research is being carried out in chemical dispersion techniques for CNT based polymer nanocomposites. Covalent method consists of functionalizing the surface of CNT's with –OH or –COOH groups and non-covalent method makes use of surfactants which attach to CNT's and prevents them from aggregating. Functionalizing of other nanoparticles dispersion method is still a heavily researched on topic [71]. Chemical dispersion methods are highly promising for fabrication of uniformly dispersed nanoparticles composites [72].

2.8 Prior work on micropatternable electrically conductive PDMS

Prior to this thesis, the most common types of conductive fillers used to make PDMS conductive are carbonblack (CB), carbon nanotubes (CNTs) and silver micro-and nano-particles.

Carbon Black-PDMS:

Carbon black (CB) has been widely used for making polymers conductive. In fact, Colmer filed the first patent in 1952 [73]. However, micropatternability was not investigated at that time. Recently, Quake *et al* [74] used the same technique

presented by Colmer to fabricated conductive PDMS by the adding of a fine carbon black (Vulcan XC72; Cabot, Billerica, MA) at 10% or higher concentration by weight [74]. They observed that electrical conductivity increased with carbon black concentration from 5.6×10^{14} to ~5×10^{1} (Ω-m). In 2001, S.P. Rwei *et al* at the Institute of Organic and Polymeric Materials, National Taipei University of Technology, Taiwan, improved on the work done by Quake et al, by showing that electric conductivity increases from 10^{-6} to 10^{-1} (Ω-m) when less than 3% CB aggregates were dispersed into the PDMS [75].

Carbon Nanotubes-PDMS

Since the discovery of CNT's by Iijima [76] in 1991, many potential applications have been proposed that exploit their extraordinary properties, such as nano-electronics, chemical and physical sensors, biosensors, actuators, and scanning probes [77]. In 2007, Yi Kuen Li *et al*manufactured MWCNT-PDMS samples. As shown in figure 4, the conductivity highly depends on the CNT concentration. They showed a percolation threshold of 4-weight percentage [78].Junyong Lu et al, in 2007, showed that CNT-PDMS nanocomposite can be easily used as a novel piezoresistor using low-cost MEMS technology; this nanomaterial has decent potential in nanosensors and PDMS-based microfluidic systems [79]. In 2009, Chao-Xuan Liu and Jin-Woo Choi showed amicrocontact printing technique, for patterning conductive poly(dimethylsiloxane) (PDMS) composites fabricated by mixing multi-walled carbon nanotubes (MWCNTs) embedded into bulk PDMS [80]. One problem with CNT's that is worth

mentioning is that it extremely difficult to get purely metallic CNT's (usually we get 40% metallic and 60% semiconducting) and there are no suppliers currently available who provide them. This is a concern not often addressed in the literature.

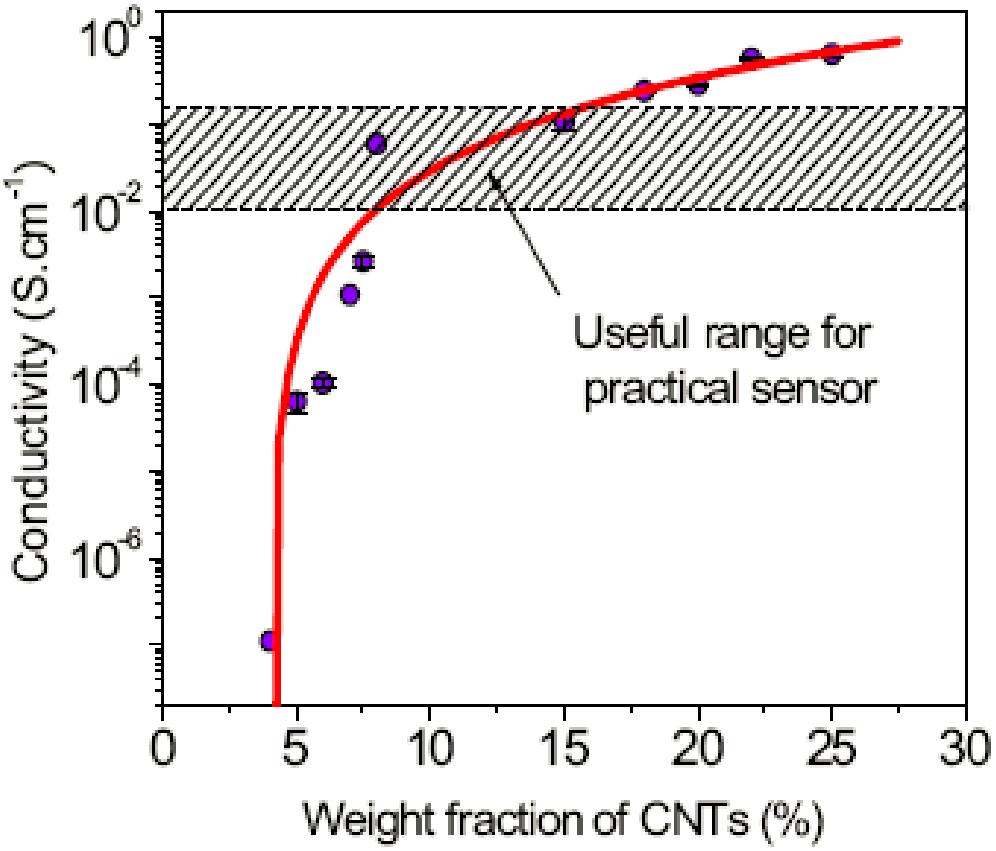

Figure 4[3] Conductivity vsweight fraction of CNT in PDMS matrix (Yi Kuen Li *et al*) [81]

Silver micro and nanoparticles in PDMS

Silver has the highest conductivity among all metals and is available in powder form. X. Z. Niu et al, in 2007 exploited this property of silver powder and were the first to demonstrate micromolding of silver-PDMS-based electrically conducting composite. They used silver particles of 1-2 μm in diameter and were able to achieve conductivity of 10^{2} $(\Omega\text{-m})^{-1}$ at 86 wt.% of silver in PDMS matrix (figure 5) [82].

[3] Copyright obtained : For Thesis / Dissertation Reuse, The IEEE does not require individuals working on a thesis to obtain a formal reuse license. Attached is print out of permission in Appendix.

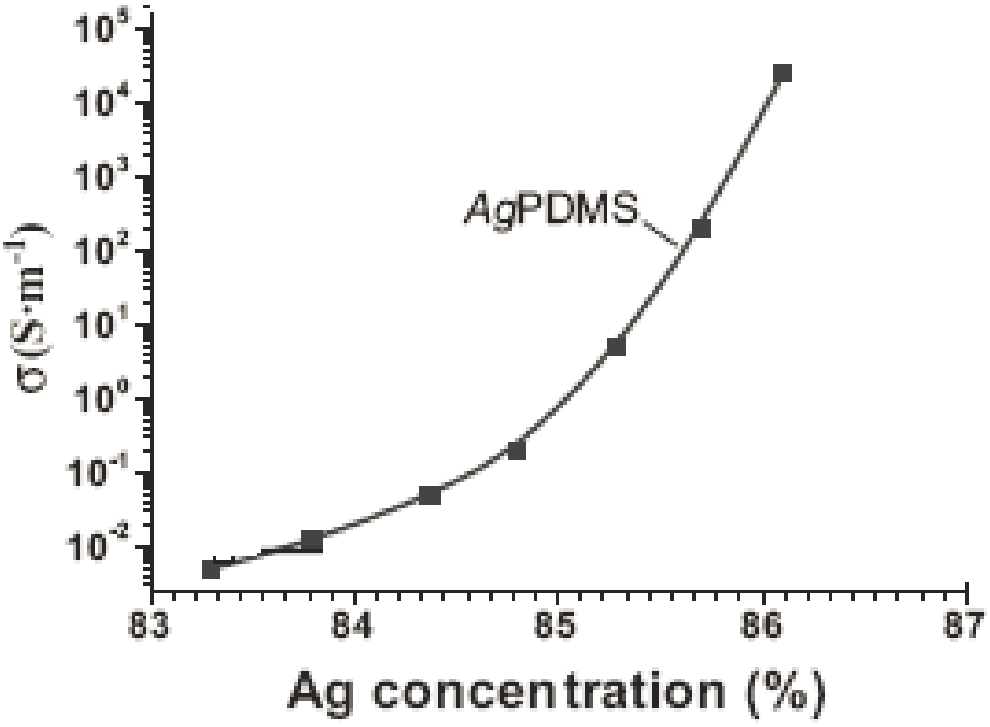

Figure 5[4] Conductivity vsweight percentage of silver 1-2 micron particles in PDMS matrix [83]

Figure 6 summarises the lithography technique adopted by X. Z. Niu *et al* to fabricate peg and line like structures [84]. The plastering technique was employed in order to micropattern the conductive PDMS in to holes (made on the master using AZ photoresist).

[4] Copyright obtained : Licensee: AjitKhosla, License Date: Nov 19, 2011, License Number: 2792690363694, Publication: Advanced Materials, Title: Characterizing and Patterning of PDMS-Based Conducting Composites, Type Of Use: Dissertation/Thesis

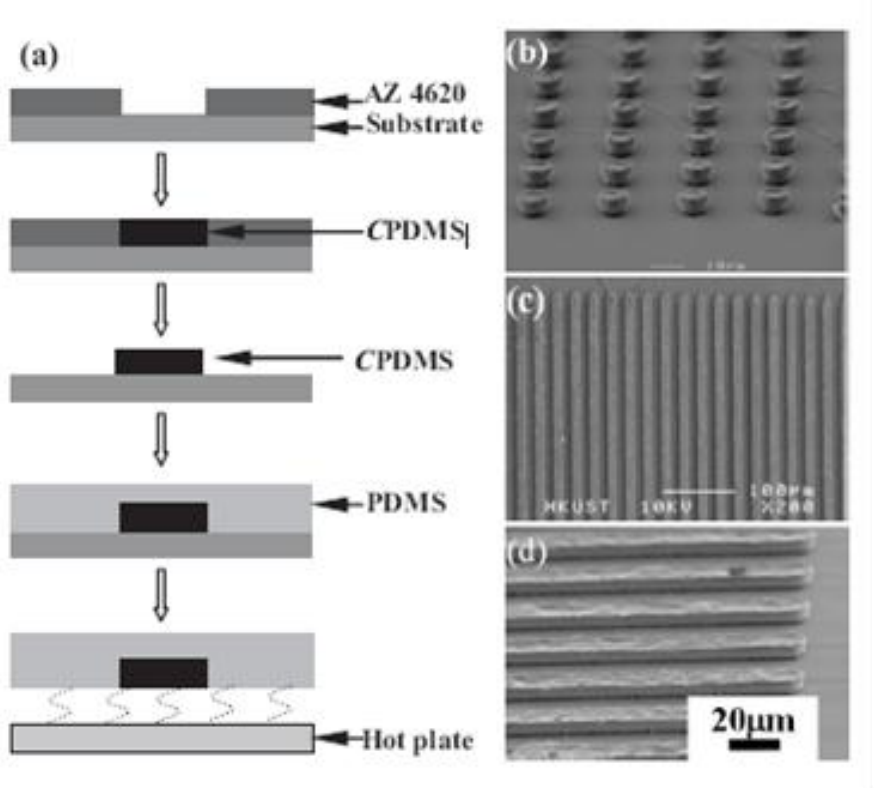

Figure 6[5] Process flow chart illustrating the patterning of conductive PDMS by plastering by X. Z. Niu [84]: a) Micropatterning of the conductive PDMS as follows; b–d) SEM images showing the various fabricated conductive patterns.

H. Cong and T. Pan, in 2008, developed electrically conductive conductivephotopatternable polydimethylsiloxane (PDMS) nanocomposites. The developed photosensitive silver-PDMS nanocomposite was sensitive only to light below 365 nm, and could be photopatterned with feature sizes of 60 μm in the positive photoresist and 10 μm in the negative photoresist [86].

[5] Copyright obtained : Licensee: Ajit Khosla, License Date: Nov 19, 2011, License Number: 2792690363694, Publication: Advanced Materials, Title: Characterizing and Patterning of PDMS-Based Conducting Composites, Type Of Use: Dissertation/Thesis

2.9 Prior art on magnetic PDMS and issues[6]

Over the last decade, many researchers in the micro-electro-mechanical-systems (MEMS) community have been involved in fabricating rare earth, hard micromagnets for the purposes of producing microactuation. Magnetic microactuation can generate high forces over comparatively long working distances, which is attractive for, among other things, manipulation of fluids in micro-total-analysis-systems (μTAS) that require actuation to facilitate fluid transport and mixing [85]. The novel hard micromagnets presented here are capable of generating large bi-directional forces with long working lengths. Their advantages that they can be actuated with external fields, operated in a variety of contaminated or dirty environments, have the ability to generate large forces over large distances, can provide a‘latching’ action, can be micromolded into complex shapes, and can be remotely actuated. These properties are due to the inherent properties of hard rare earth magnetic materials: they are permanently magnetic (as opposed to ferromagnetic) and have high remanent magnetization.

Various techniques have been reported to fabricate rare earth micro magnets such as screen printing [86], resin bonding [87], wax bonding [88], polymer bonding [89], tape casting [90], and sputtering [91]. However, none of these techniques is easily compatible with PDMS.Hence, there is a need to develop PDMS-based active materials of similar flexibility to the undoped and insulating PDMS, that can also be easily micromolded using similar soft

[6] Adapted from: A. Khosla, J. L. Korčok, B. L. Gray, D. B. Leznoff, J. W. Herchenroeder, D. Miller and Z. Chen, "Fabrication and testing of integrated permanent micromagnets for microfluidic systems", Proc. SPIE 7593, 759316 (2010); doi:10.1117/12.840942

lithography techniques so as to manipulate fluid on chip (fluid control) via on-chip microvalves and pumps. Magnetically actuated valves and pumps are a good choice due to the high energy density of magnetic actuation schemes. One of the obstacles to widespread use of micromagnetic actuation is the inclusion or permanent magnetic materials in micro systems. In a similar way as described by Jaffer et al who fabricated iron composite PDMS structures via micromolding against a SU8 master [88], Farhani and others showed iron oxide nanoparticles – PDMS polymer matrix microstructures for lab on a chip actuation [89]. One of the main issues with Iron oxide is that it's a weak magnetic material and requires large external magnetic fields for bi-directional actuation as compared to rare earth magnetic materials.

2.10 Summary of chapter 2

We have discussed the basics of polymer nanocomposites, nanoparticles, discussedpercolation threshold and dispersion mechanisms for nanoparticles in polymers. These definitions and explanations form the basis of my work and will help to understand the remainder of this thesis.

Prior work done on micromoldable electrically conductive PDMS shows that electrical conductivity of a PDMS conducting composite depends upon various factors including filler particle size, the shape of the particles, and the filler composition. Conductivity levels offered by carbon black-PDMS, CNT-PDMS composite, although good enough for sensor as shown by Yi Kuen Li *et*

al).In all these cases, at high weight percentages of conductive particles, PDMS lost its self leveling properties, resulting in polymers that formed like clay, thus requiring a more difficult plastering method of patterning as opposed to spin-coating.

However, CNT's and silver micron-sized particles have shown promising results. Use of –OH or COOH functionalized CNT's overcome the dispersion problem associated with as prepared CNT's in PDMS matrix. Another problem with CNT's is that it is extremely difficult to get purely metallic CNT's (usually we get 40%metallic and 60% semiconducting) and there are no suppliers currently available who provide them.

The levels of conductivity obtained are highly dependent on the type of particles used such as which type of carbon black is employed to fabricate conductive PDMS, particle size and how well it is dispersed in PDMS matrix, and by what method. The dispersion of particles in PDMS polymer matrix still remains a challenging issue and will be explained in chapter 3.

The next chapterfocuses on defining a general fabrication process for all types of PDMS based nanocomposites such as electrically conducting and magnetic nanocomposites. Also, a new hybrid micromolding process is developed that enables hybrid systems with combined micropatterned PDMS based nanocomposites and undoped PDMS, which provides a greater degree of flexibility in fabrication of system containing these functional polymers.

CHAPTER 3: NANOCOMPOSITE POLYMERS: FABRICATION AND MICROPATTERNING [7]

In this chapter,wediscussand define a general fabrication and micropatterning process for polymeric nanocomposites which can be electrically conductive, magnetic, or both in nature, and combined with non-doped polymer substrates. Before defining a general fabrication process for PDMS based nanocomposites, a summary of the materials used for developing the multifunctional micropatternable nanocomposite polymers is necessary. Table 1 lists the materials and suppliers which have been used throughout this research,

[7] Adapted version of :

[1] *A. Khosla and B. L Gray; "Preparation, characterization and micromolding of multi-walled carbon nanotube polydimethylsiloxane conducting nanocomposite polymer", Materials Letters Volume 63, Issues 13-14, 31 May 2009, Pages 1203-1206*

[2] *A. Khosla and B. L. Gray, " Preparation, Micro-Patterning and Electrical Characterization of Functionalized Carbon-Nanotube Polydimethylsiloxane Nanocomposite Polymer", Macromolecular Symposia: Special Issue: Polymers and Organic Chemistry, Volume 297, Issue 1, pages 210–218, November-2010*

[3] *A. Khosla, B. L Gray "Properties of Conductive Micromoldable Thermosetting Polymer for Electronic Routing in Highly Flexible Microfluidic Systems" SPIE Proceedings Vol. 7593, Microfluidics, BioMEMS, and Medical Microsystems VIII*

[4] *A. Khosla, B. L Gray "Fabrication of Multiwalled Carbon Nanotube Polydimethylsiloxne Nanocomposite Polymer Flexible Microelectrodes for Microfluidics and MEMS." SPIE Proceedings Vol. 7642 Electroactive Polymer Actuators and Devices (EAPAD) 2010.*

[5] *A. Khosla, B.L. Gray, "CONDUCTIVE ELASTOMERIC MATERIAL AND USES THEREFOR" US Patent No. 61/113998*

[6] *A. Khosla, B. L Gray, J. L. Korčok, D. B. Leznoff, "NOVEL MAGNETIC NANOCOMPOSITES WITH PREPARATION AND METHODS OF PATTERNING SAME". US Patent No. 61/288,244*

of which a subset will be provided as examples. The examples provided are fabrication of: electrically conducting MWCNT and sliver nanoparticle doped PDMS; permanent magnetic NdFeB doped PDMS; and soft magnetic-electrically conductive nickel nanoparticle doped PDMS.

Table 1 Materials and suppliers for nanoparticles and polymers fabricated as part of this thesis.

Supplier	Material
Dow Corning, USA.	Polydimethylsiloxane (Sylgard 184 Elastomer Kit), consisting of a base elastomer and curing agent.
NanoamorInc	Silver
	Carbon nanotubes
	Copper
	Nanowires
	Nanorods
	Gold
	Nanowhiskers
	Alloys and metal oxides
HC Stark Enterprises, USA	Baytron™ FHC
Agfa Materials, Germany	Orgacon™
Cheap tubes Inc, USA	Carbon nanotubes
	Fullrenes
	Carbon fiber
MagnequenchInc, Canada	NdFeB magnetic material
Microchem, USA	SU-8 and SU-8 Developer
Alfa Aesar, USA	Barium hexferrites
Industrial Plastics & Paints,	PMMA-Cast Grade

3.1 Nanocomposite fabrication and patterning process

Two different processes were developed to fabricate nanocomposite polymers using PDMS as a matrix material. These processes mainly differed in the method used to uniformly disperse the nanoparticles: process 1 employed shear mixing, while process 2 used ultrasonic processing. We observed that for electrically conducting nanocomposites, a combination of shear mixing and ultrasonic processing yielded better dispersion as compared to process 1 or process 2 on their own.However, high frequency ultrasonics is preferred over low frequency ultrasonics as better dispersion is achieved in shorter time. Also, it is worth noting that ultrasonic baths do not yield good results, meaning that agglomeration of nanoparticles is observed as discussed in section 2.7 in chapter 2. However, high frequency ultrasonicsovercomes this problem when a horn tip probe is used. In the case of magnetic nanocomposites, the same processes defined above works, but the use of a magnetic stirrer for shear mixing is not recommended.

General fabrication process for polymeric nanocomposites

The general process defined here works for all of thedifferent micropatternable PDMS based nanocomposites thathave been discussed in this thesis.After conducting a series of experiments in order to determine a general fabrication process, a simple four-step protocolwas developed:

1. The desired quantity of nanoparticles is distributedin an organic solvent, such as heptane or toluene,via high frequency ultrasonics(42

kHz) employing a horn tip probe in pulse mode (10 seconds on and 15 seconds off) for a total time of two minutes.

2. The base elastomer/monomer is added to the nanoparticle- organic solvent emulsion, followed by high frequency agitation.
3. The polymer curing/crosslinking agent is added in ratio of 10:1;i.e., 10 parts of base elastomer and one part of curing agent, as recommended by the supplier (Dow Corning Inc. USA). It is important to add the curing agent “after”the high frequencyultrasonic process as a lot of heat is produced during the ultrasonication process, which canstart to solidify (cure) the nanocomposite during mixing.
4. The prepared PDMS based nanocomposite is shear mixed until the heptane evaporates. The evaporation of organic solvent from the PDMS nanocomposite may be determined visually, by weight, or by calculating the volume of the nanocomposite.
5. The prepared nanocomposite is placed in vacuum for 30 minutes to remove air bubbles and any excess solvent.

The nanocomposite is now ready to be micropatterened.

Examples PDMS based nanocomposite fabrication

In this section, we discuss examples of fabrication of PDMS basednanocomposites, which are prepared by different nanoparticles such as 1) multi walled carbon nanotube, 2) silver, 3) nickel, 4) NdFeB.

Electrically conducting multi-walled carbon nanotube-PDMS nanocomposite

The electrically conducting MWCNT-PDMS nanocomposites were prepared by first manually stirring and then ultrasonically dispersing(using a horn tip VC 750 (Sonics Inc, USA.) programmable ultrasonic processor) COOH-functionalized MWCNTs in heptane. The COOH-MWCNTs used had an average outer diameter of 10nm and length of 30μm. Organic solvents such as heptane and toluene are compatible with PDMS, meaning that PDMS dissolves homogeneously in heptane/toluene. Hence, nanoparticles, in this case COOH-MWCNTs are first de-agglomerated in heptane and then PDMS is added. Neglecting the relatively small volume/weight of heptane during the fabrication process, MWCNTs solution (weight of MWCNT only taken in to account) was added to the PDMS base elastomer in varying weight percentages (0.5, 1.0, 1.5, 2.0, 2.5, 3.0, 3.5, 4.5 and 4.5 wt.%) again by using a horn tip VC 750 (Sonics Inc, USA.) programmable ultrasonic processor. The operating frequency was 42 kHz and the ultrasonic processor was operated in pulse mode (10 seconds on and 15 seconds off cycle), which provided mixing by repeatedly allowing the sample to settle back under the probe after each burst. The high frequency ultrasonication process was carried out for 2 minutes, which is much shorter than previous times of several hours needed for non-functionalized MWCNTs. We observed that we needed a longer relaxation time compared to the sonication time such as 30 seconds on and 5 seconds off cycle. Because of the temperature generated during the ultrasonication process melting of plastic beakers and breaking of glass beaker was observed at longer sonication times. The curing or crosslinking

agent was then added after the ultrasonication process was completed so as not to thermally set the polymer with the heat produced as a result of the ultrasonication mixing. The base elastomer and curing agent ratio were 10:1 as recommended by the supplier. Each nanocomposite (of varying wt.%) was then shear mixed at 500 rpm for two minutes or until heptane evaporated. The calculation of weight percentage takes in to account the curing agent whichwas added. The prepared nanocomposite samples were each placed into a vacuum chamber to remove air bubbles and excess solvent for 30 minutes. Figure 7 shows photographs of the different steps involved in fabricating the MWCNT-PDMS nanocomposite. By employing the fabrication process defined above, uniform dispersion of COOH- functionalized MWCNTs in the PDMS matrixwas achieved. Figure 8 shows this uniform dispersion. From these SEM micrographs, individual COOH- functionalized MWCNTs can be observed, indicating that the clumping of COOH- functionalized MWCNTs has been minimized in the PDMS matrix.

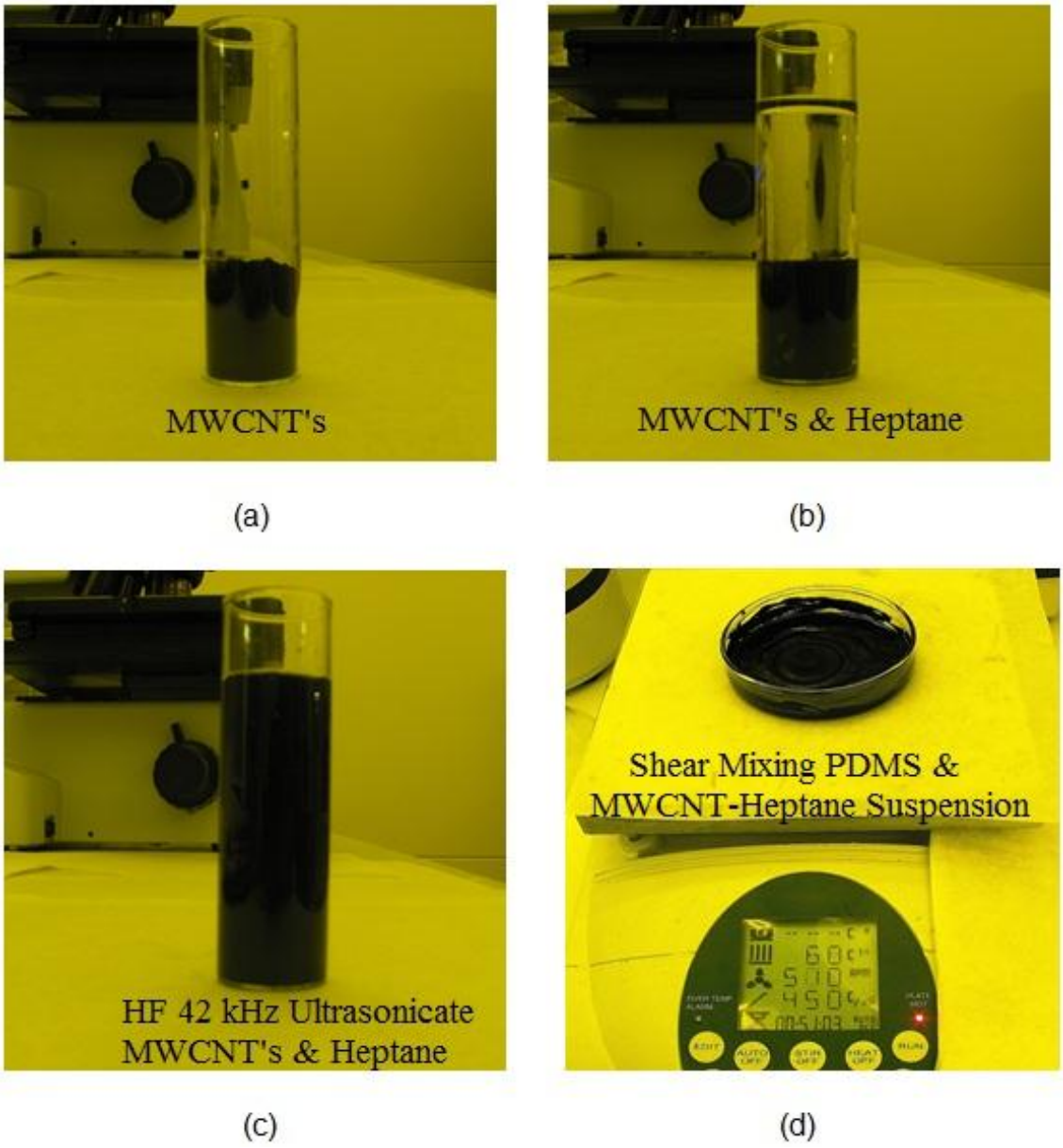

Figure 7 Photographs showing steps involved in fabrication of MWCNT-PDMS nanonanocomposites: a) MWCNT's; b) MWCNT's in heptane; c) high frequency ultrasonicted MWCNT's in heptane; d) shear mixing of MWCNT-PDMS using magnetic stirrer.

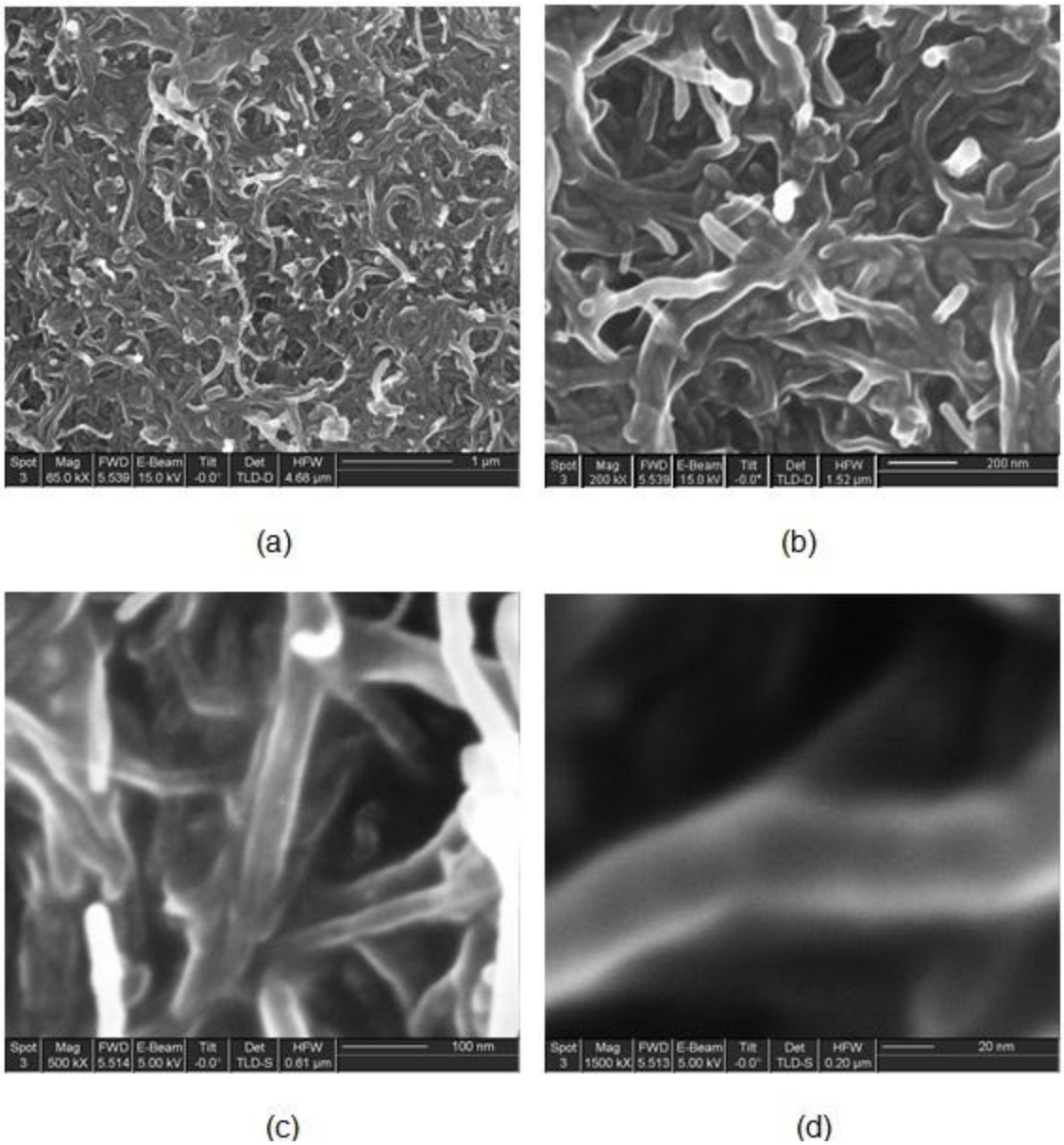

Figure 8 SEM photographs of COOH- functionalized MWCNTs at different (increasing) magnifications in PDMS showing uniform dispersal. Scale bar: a) 1µm ; b) 200 nm; c) 100nm; d) 20nm.

Electrically conducting Silver nanoparticle (Ag-n) doped PDMS nanocomposite

The Ag-n PDMS nanocomposites were fabricated by carefully weighing via digital balance the desired quantity of Ag-n (average diameter of 80 nm and 99.5% purity) and PDMS base elastomer. However, the Ag-n were first dispersed in heptaneby employing a horn tip VC 750 (Sonics Inc, USA.) programmable ultrasonic processor. Similarly to the MWCNT-PDMS nanocomposite fabrication process, both the Ag-n dispersion and base elastomer, were first manually stirred and again high frequency ultrasonicated for 2.5 minutes,. The crosslinking agent was addedafter the ultrasonication process in the ratio of 1:10 (i.e., 1 part of curing agent in 10 parts of base elastomer). Finally, the nanocomposite samples were shear mixed for 5 minutes or until the heptane evaporatedand finally put under vacuum for 30 minutes to remove any air bubbles. Twelve Ag-n PDMS samples were fabricated with weight percentage (wt.%) of Ag-n (15, 20, 25, 30, 31, 32, 33.5, 36, 37.5, 40, 45 and 50wt.%) in the PDMS matrix. Calculation of weight percentage takes in to account the crosslinking agent added but not the heptane. After these steps, the nanocomposite was ready to be micromolded. SEM analysis (figure 9) shows uniformly dispersed Silver nanoparticles in a PDMS polymer matrix. Individual nanoparticles can be seen in SEM graphs, indicating little or almost no agglomeration of silver nanoparticles in the prepared nanocomposite.

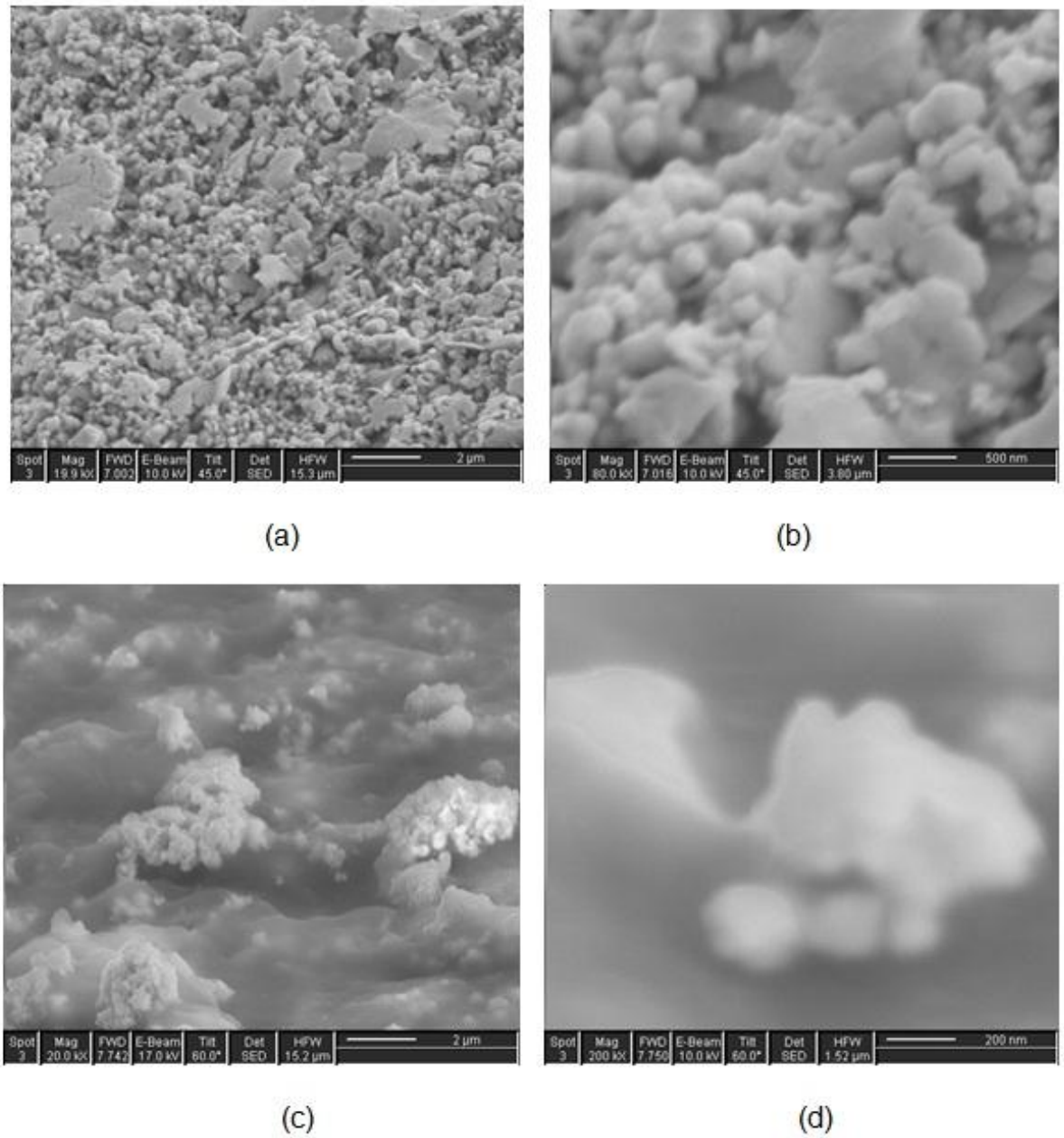

Figure 9 SEM graphs of Ag-n at different magnifications in PDMS. Scale bar: a) 2µm ; b) 500 nm; c) 2µm; d) 200nm

Soft magnetic and electrically conducting nickel nanoparticle doped PDMS.

The desired quantity (in this case 80 wt.%) of nickel nanoparticles with purity of 99.7+% and a diameter of 30-50nm, were first agitated by high frequency ultrasonication process in heptane. The nickel nanoparticle-heptane suspension was then dispersed ultrasonically in a PDMS base polymer matrix in varying weight percentages using a VC 750 (Sonic Inc.) programmable ultrasonic processor. Many processing steps are similar to steps as explained in the case of COOH-MWCNT PDMS and Ag-PDMS nanocomposite preparation. The ultrasonic processor was operated in pulse mode (10 seconds on and 15 seconds off cycle) for 2 minutes, which provided mixing by repeatedly allowing the sample to settle back under the probe after each burst. Later, curing agent was added and the nanocomposite was shear mixed until the heptane evaporated. Prior to micromolding, the prepared nanocomposite was placed into a vacuum chamber to remove air bubbles for 30 min.

Hard magnetic neodymium iron boron based composite[8]

This section describes thehard magnetic powder composition (NdFeB powder) and polymeric PDMS based composite and is divided into two sections:

1. Hard magnetic powder used

[8]The hard magnetic polymer described in this section is not a nanocomposite, as particle size is 5 micron in size.

2. NdFeB ($Nd_{0.7}Ce_{0.3})_{10.5}Fe_{83.9}B_{5.6}$) doped hard magnetic PDMS composite fabrication

Hard magnetic powder used

Magnetic powder used is MQFP-12-5. The powder is a finely milled, isotropic Nd-Fe-B magnetic material. It is fabricated by rapid solidification processing which imparts an α-Fe/Nd2Fe14B1 nanocomposite structure where the average grain size is 25-50nm. The nanostructure enables the powder to be milled to a D50 of 5 microns while still retaining excellent magnetic properties making the powder well suited to form into micromagnets deposited in a thin layer by mixing with an appropriate polymer. Because MQFP powders are isotropic such that it can be magnetized equally well in any direction, no consideration of magnetic alignment needs to be considered during the molding process. Magnetic orientation is applied after the molding.

Until now, the fabrication of micromagnets has been limited to lower strength ferrite powders or cumbersome micromachining of bulk magnetic materials. MQFP-12-5 offers up to 4 times the magnetic remanence of isotropic ferrite powders and 2 times the remanence of anisotropic ferrite powders. Bulk magnetic materials are limited in the amount of size reduction because they have micron-sized microstructures. As the size of the magnet approaches the grain size, then the resistance to demagnetization is much reduced, and the usefulness is less. Therefore more magnetic work in micromachines can be possible with MQFP.

The chemical composition of MQFP-12-5 is approximately $(Nd_{0.7}Ce_{0.3})_{10.5}Fe_{83.9}B_{5.6}$. Cerium is partially substituted for neodymium to reduce the magnetic anisotropy so that the resulting magnet can be more than 90% saturated with applied fields of only 15 kOe. An SEM micrograph of the powder is shown in Figure 10.

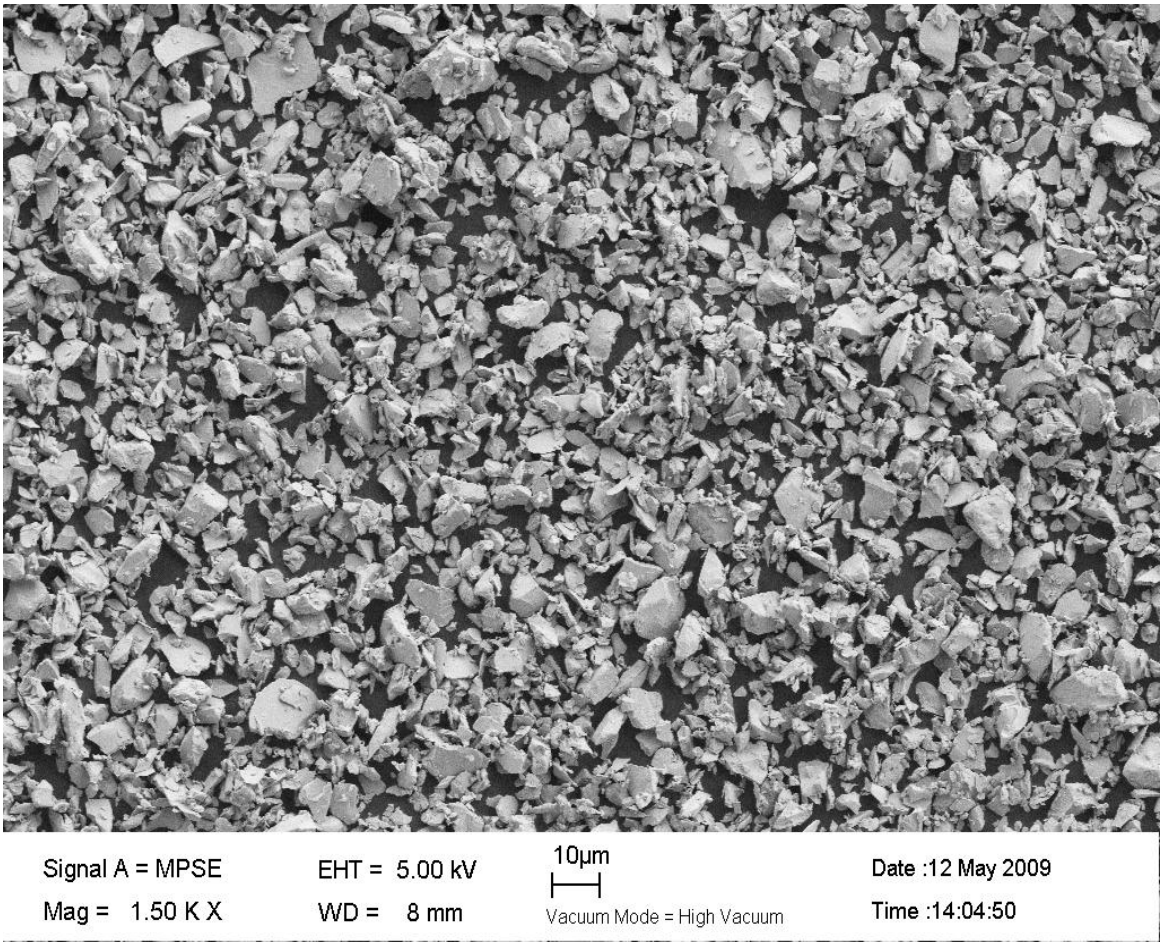

Figure 10[9] SEM micrograph of MQFP magnetic powder with an average particle size of 5µm.

[9]SEM micrograph provided by Magnequench Inc./ Neomaterials.

NdFeB ($Nd_{0.7}Ce_{0.3})_{10.5}Fe_{83.9}B_{5.6}$) doped hard magnetic PDMS[10]

The magnetic powder as prepared in the above section was first manually stirred in a PDMS base elastomer for 5 minutes, and then a horn tip ultrasonic probe was immersed in the composite operating at a frequency of 42 kHz in pulse mode (10 seconds on and 15 seconds off) for 4 hrs prior to adding curing agent. As recommended by the supplier (Dow Corning Inc. USA), the base elastomer and curing agent ratio was chosen to be 10:1. The prepared composite was placed into a vacuum chamber to remove air bubbles for 30 minutes. The hard magnetic nanocomposite was then ready to be micropatterened and magnetized.

Note that because of the large particle size (5-6 μm) solvent assisted dispersion is not required. Magnetic particleswere directly dispersed in PDMS polymer matrix and no agglomeration was observed after performing experiments with SQUID magnetometer. Those experiments and resultswill be discussed in Chapter 5 of this thesis.

3.2 SU-8 micromold fabrication

SU-8 is a negative tone, epoxy type, near UV (365nm) photo-patternable material that can be employed as a master for PDMS micromolding. It consists of a polymeric epoxy resin (Epon SU-8) in an organic solvent (gamma

[10]Adapter version of: A. Khosla, J. L. Korčok, B. L. Gray, D. B. Leznoff, J. W. Herchenroeder, D. Miller and Z. Chen, "Fabrication and testing of integrated permanent micromagnets for microfluidic systems", Proc. SPIE 7593, 759316 (2010); doi:10.1117/12.840942

Butyrolactone (GBL)) and a photoacid generator taken from the family of the triarylium-sulfonium salts. When this resin is photosensitized with a mixture of triarylsulfonium/hexafluroantimonate salt, the exposed regions polymerize, resulting in an extremely high crosslink density. Figure 11 shows chemical structure of SU-8.

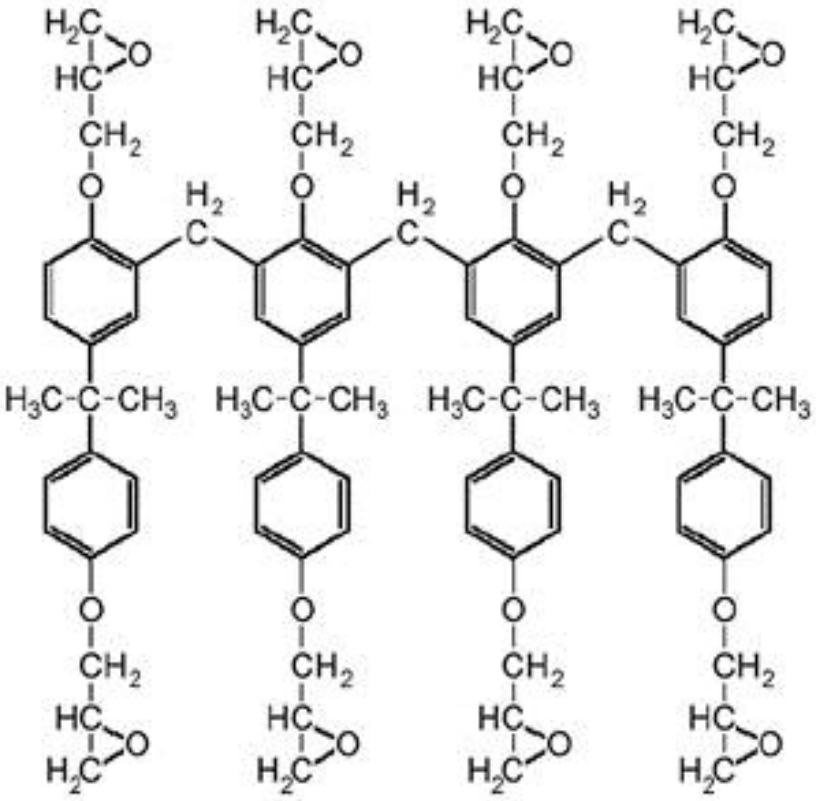

Figure 11 Chemical structure of SU-8 photoresist

The difference between SU-8 100 and SU-8 2005 is primarily their viscosities, which are 51500 cStand 45cSt, respectively [90]. In addition, the 2000 series (e.g., SU-8 2005, 3010) forms faster drying films. Figure 10(a-g) summarises the fabrication process used to produce SU-8 micromolds for

PDMS-nanocomposite micromolding. Different steps involved in producing the micromold are 1) substrate cleaning, 2) adhesion layer, 3) structural mold layer and patterning. All three steps are explained in detailin figure12.

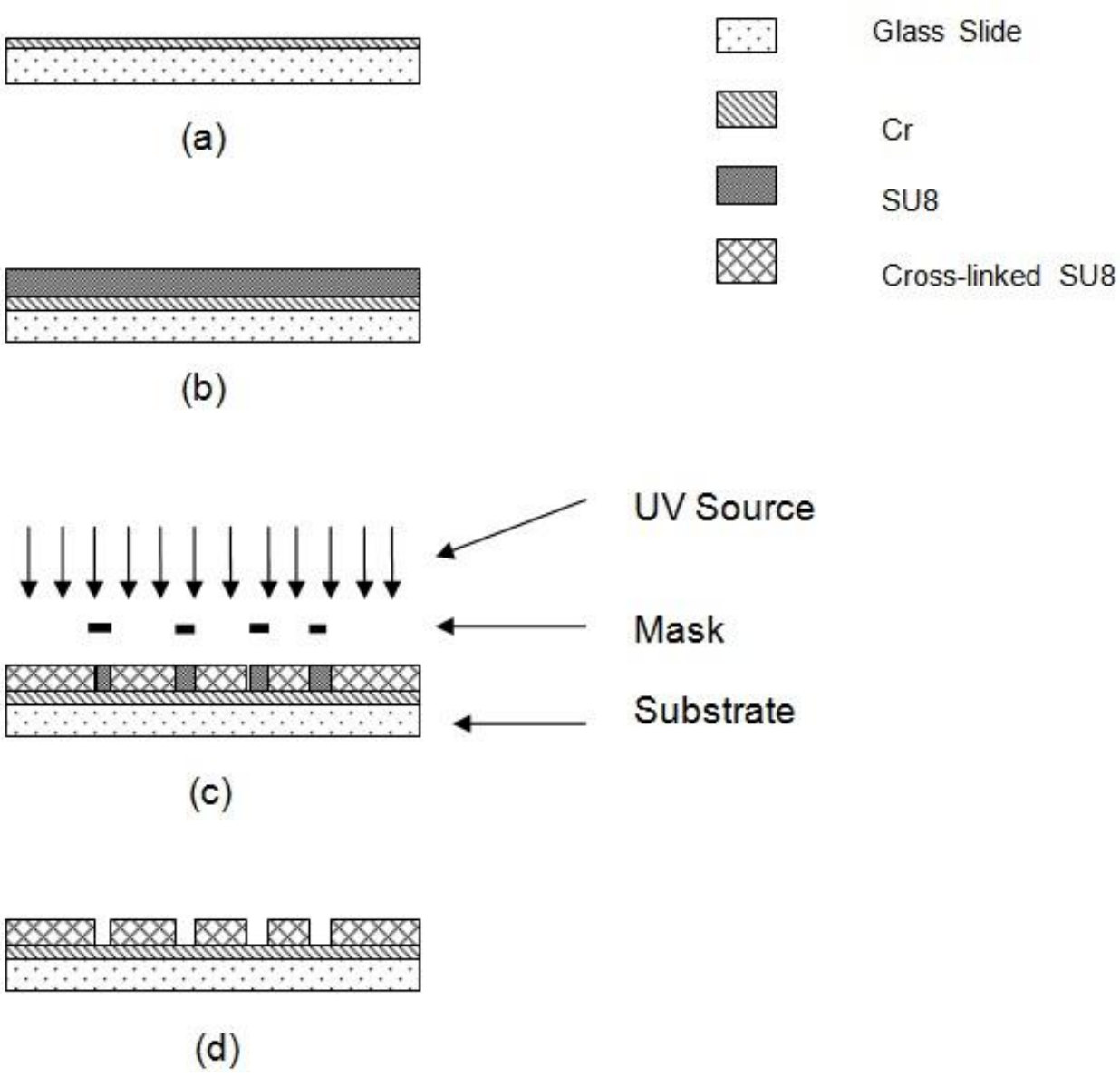

Figure 12 Fabrication process step for SU-8 micromold preparation via UV-light photopatterning of SU-8.

Substrate cleaning

Glass substrate

3 inch x 3 inch square, 1mm thick glass slides were used as substrates which were first cleaned in 100% Decon 90 Detergent using ultrasonic agitation for 5 minutes.The slides were then rinsed with de-ionized (DI) water, acetone, isopropyl alcohol (IPA), and DI water. The substrates were blow dried using nitrogen followed by dehydration baking for 20 minutes at 150°C in a convection oven. The slideswere then cooled to room temperature.

Silicon substrate

A 4-inch silicon wafer was RCA cleaned. The cleaning procedure involves the removal of insoluble organic contaminants, grease or silica gel, oxides, ionic and heavy metal contaminants.

The RCA cleaning procedure has three major steps:

1. Removal of insoluble organic contaminants

2. Removal of a thin silicon dioxide layer

3. Removal of ionic and heavy metal atomic contaminants

The wafer to be cleaned is soaked in DI water prior to start of the first step. Appendix 5 shows RCA process run sheet.

The first step also known as the organic clean removes insoluble contaminants. A solution of NH_4OH (ammonium hydroxide) + H_2O_2 (hydrogen peroxide) + H_2O (water) is prepared in the volume ratio 1:5:5. The prepared solution is introduced into a temperature controlled water bath and maintained at

75 ^{0}C (± 5 ^{0}C). The wafer soaked in DI water isdipped into this heated solution for duration of 10 minutes. Following this step the waferis rinsed by submerging them into a running DI water bath for 1 minute.

The second step known as the “oxide strip”; removes a thin silicon dioxide layer (about 10 Angstrom) formed in the organic clean and metallic contaminants, which may have accumulated from the previous step. A solution of HF (hydrofluoric acid) + H_2O (water) in the volume ratio of 1:50 is prepared. The waferis transferred from the running DI water bath into this solution for 15 seconds. This is immediately followed by submerging the wafer into a running DI water bath for 5 minutes to rinse any surface contaminants.

The final step, which is known as the “ionic clean”; removes ionic and heavy metal contaminants from the wafer. A solution of HCL (hydrochloric acid) + H_2O_2 (hydrogen peroxide) + H_2O (water) is prepared in the volume ratio of 1:1:6. The prepared solution isintroduced into a temperature controlled water bath and maintained at 75^{0}C (± 5^{0}C). The wafers are transferred from the running DI water bath into this solution for 10 minutes. Following this step the waferis rinsed by submerging them into a running DI water bath for 1 minute. Finally, the wafer is spun dried and/or blow-dried using nitrogen.The wafer is now ready to be used as substrate.

Adhesion layer

OmniCoat™ was used as a seed layer which was spin coated on the substrate (400 rpm for 15 seconds followed by 1200 rpm for 35 seconds) and

baked at a temperature of 200°C (ramp rate: 450°C /hr) on a hot plate (Tory Scientific, Model#HP30). A 5 µm thick adhesion layer of SU-8 2005 was spun on the substrate (1250 rpm for 35 seconds). The adhesion layer soft bake was performed at 90°C for 14 minutes (ramp rate: 450°C /hr). The substrate was cooled to room temperature, followed by a ultraviolet (UV) flood exposure for 90 seconds. All exposures in this work were carried out at near UV wavelengths (350-400 nm) using a Quintel Corporation Q-4000 contact mask aligner. The post exposure bake was carried out at a temperature of 90°C (ramp rate: 450°C/hr) for 14 minutes, followed by cooling to room temperature.

Micromold structural layer

Dehydration pre-bake was carried out at a temperature of 125^0C for 25 minutes. A 100 µm layer of SU-8 100 was spin coated (at 2250 rpm) on top of the adhesion layer, followed by soft baking at 90 °C for 80 minutes and cooling to room temperature. Desired structures were patterned using masked UV exposure for 60 seconds Full crosslinking of SU-8 100 was achieved by a post-exposure at a temperature of 60°C for 65 minutes (ramp rate: 300°C/hr) followed by cooling to room temperature. The structural layer was then developed in SU-8 Developer (Mircochem™) for 90 seconds in an ultrasonic bath. Figure 13 shows SU8-100 micropatterened of 4 inch Silicon wafer.

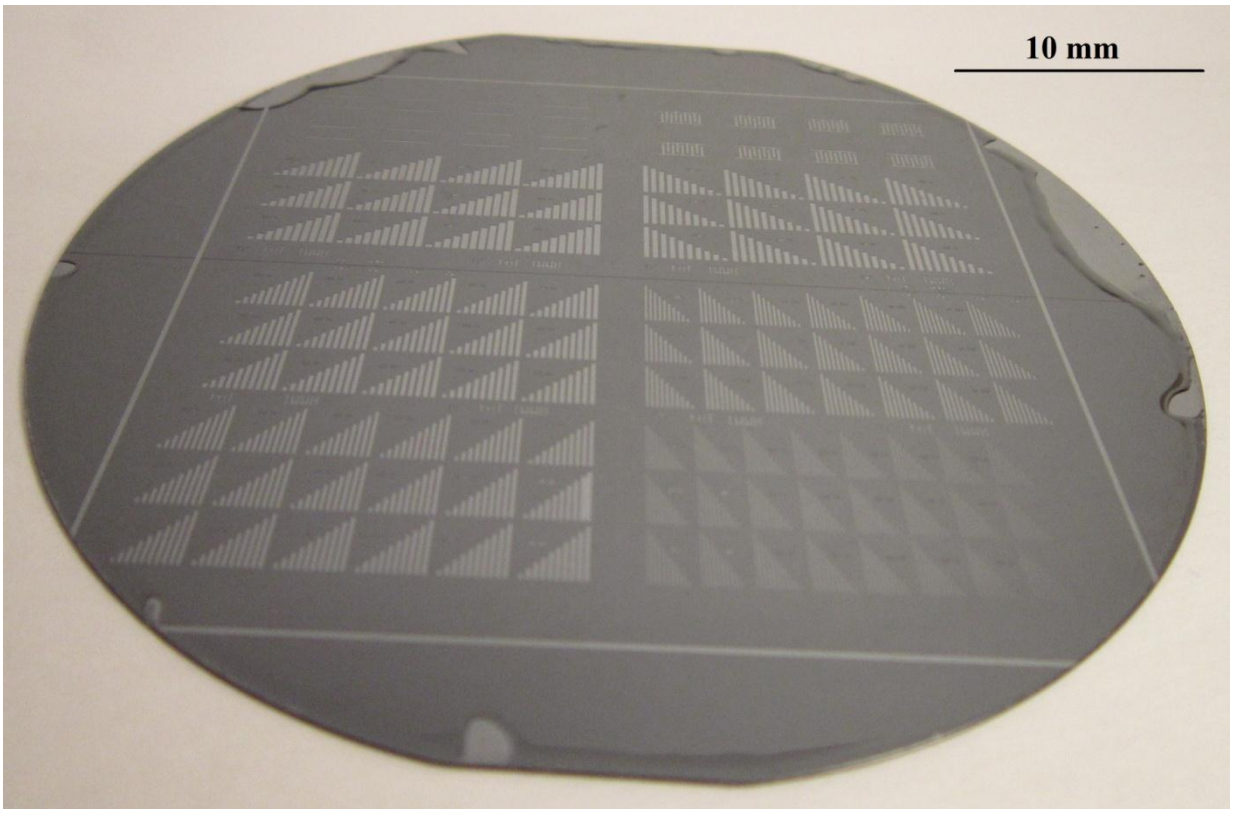

Figure 13 SU-8 micromold fabricated via UV-lightmicropattering of SU8 100 photoresist on 4 inch silicon wafer.

3.3 General hybrid nanocomposite micromolding process

This section describes a general hybrid micromolding process for all prepared nanocomposites. Examples of micromolded nanocomposites

structures; such as electrically conductive (MWCNT & Ag-n) and magnetic (Nickel & NdFeB) PDMS; are shown in figure 13 and 14.

The prepared composite(such as a) MWCNT-PDMS, c) Ag-n PDMS, 3) Ni-PDMSl, 4) NdFeB-PDMS) described in section 3.1 of this chapterare placed into a vacuum chamber to remove air bubbles for 30 minutes and poured on to a micromold which was fabricated using SU-8 100(described in section 3.2) and degassed for ten minutes. Excess composite was scraped off using the Damascene-like process from the surface of the mold using surgical knife (step by step fabrication process shown in figure 13). Undoped PDMS polymer was then poured on the surface and degassed. The silicon substrate is then kept on a hotplate at 75 °C for 1 hour and then peeled off from the mold. In some cases it became necessary to dilute the PDMS elastomer in an organic solvent like heptane or toluene and then ultrasonicate the desired quantity of nanoparticles. Note that ultrasonication should be carried out using an ultrasonic probe and not in an ultrasonic bath. Figure 15 and 16 show examples of fabricated different PDMS based multifunctional nanocomposite polymers on flexible undoped PDMS.

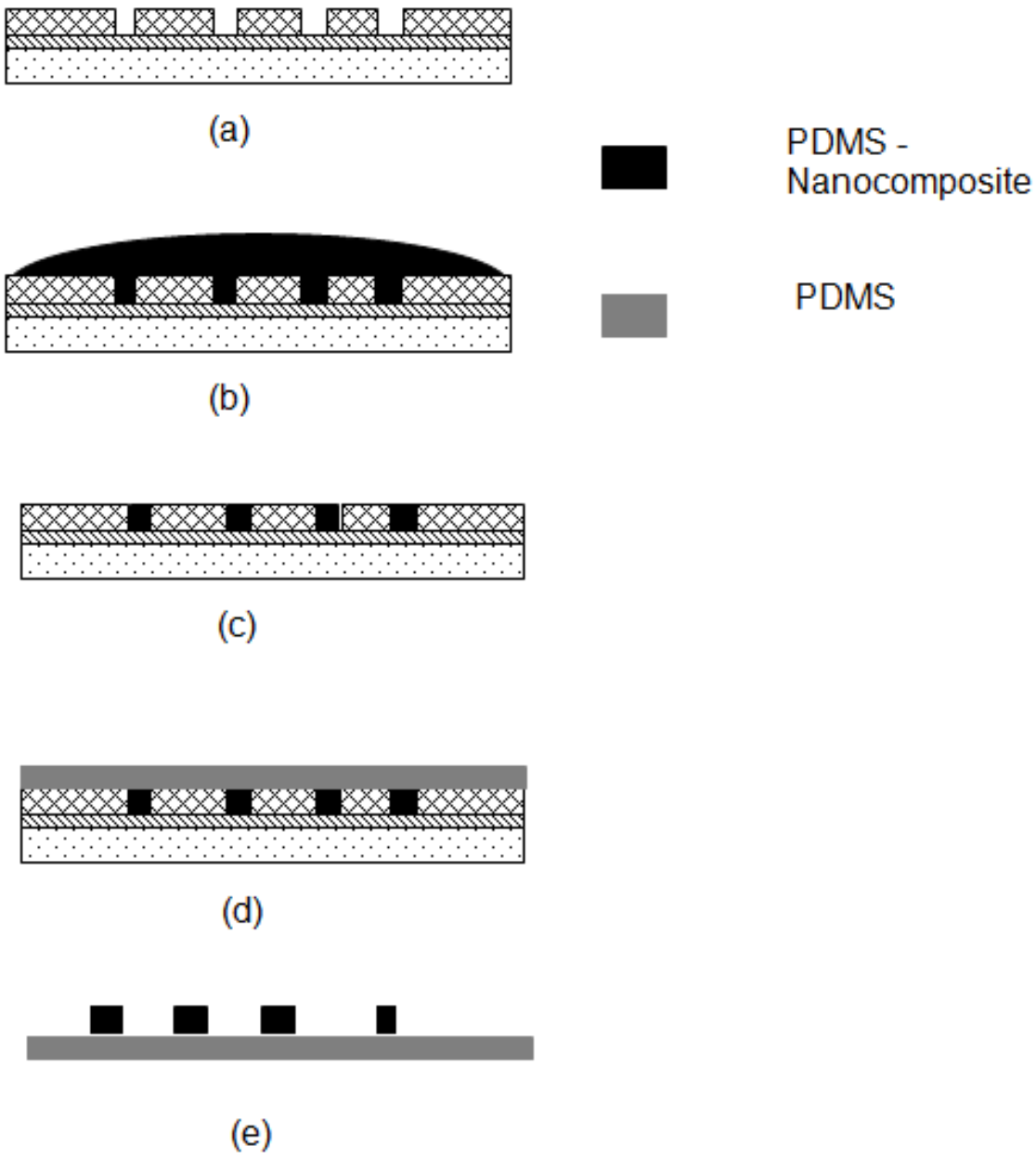

Figure 14 Hybrid fabrication process for combining micromolded nanocomposite with undoped PDMS polymer. A) SU-8 micromold, b) PDMS nanocomposite poured on SU-8 micromold, c) Excess nanocomposite scraped off from the surface of micromold, d) PDMS poured on the surface of mold, e) Pealed off nanocomposite microstructures on PDMS nonconductive/magnetic polymer

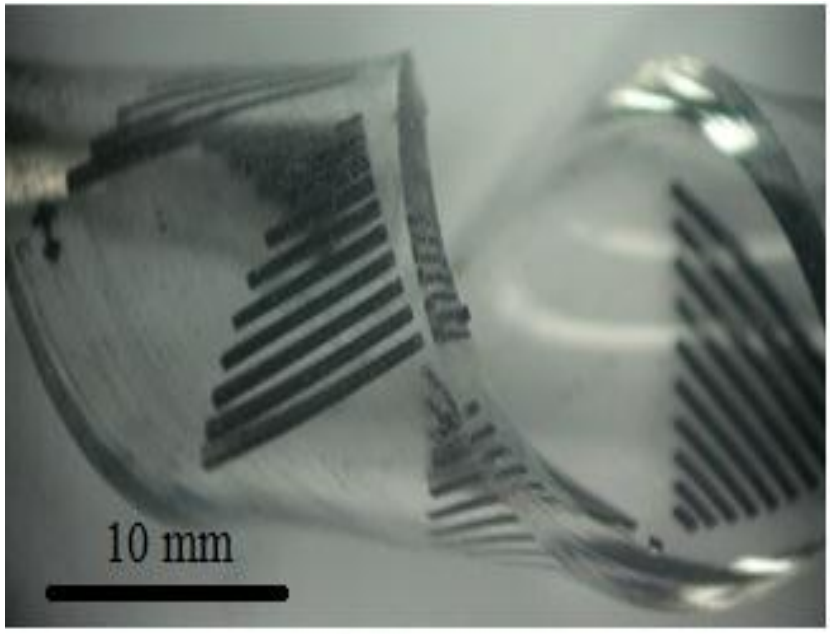

(a)

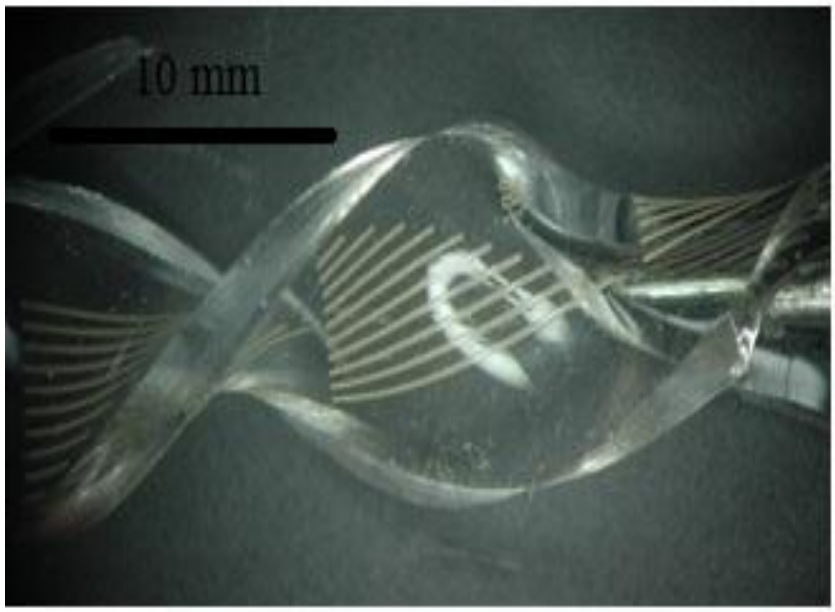

(b)

Figure 15 Optical micrographs of fabricated conductive microstructures on non-conducting PDMS: a) MWCNT-PDMS (4 wt.%)nanocomposite array of microelectrodes of lengths ranging from 1mm to 10mm, height of 30 µm and width of 100 µm; b) Ag-n PDMS (50 wt.%) array of m microelectrodes of lengths ranging from 1mm to 10mm height of 30 µm and width of 100 µm.

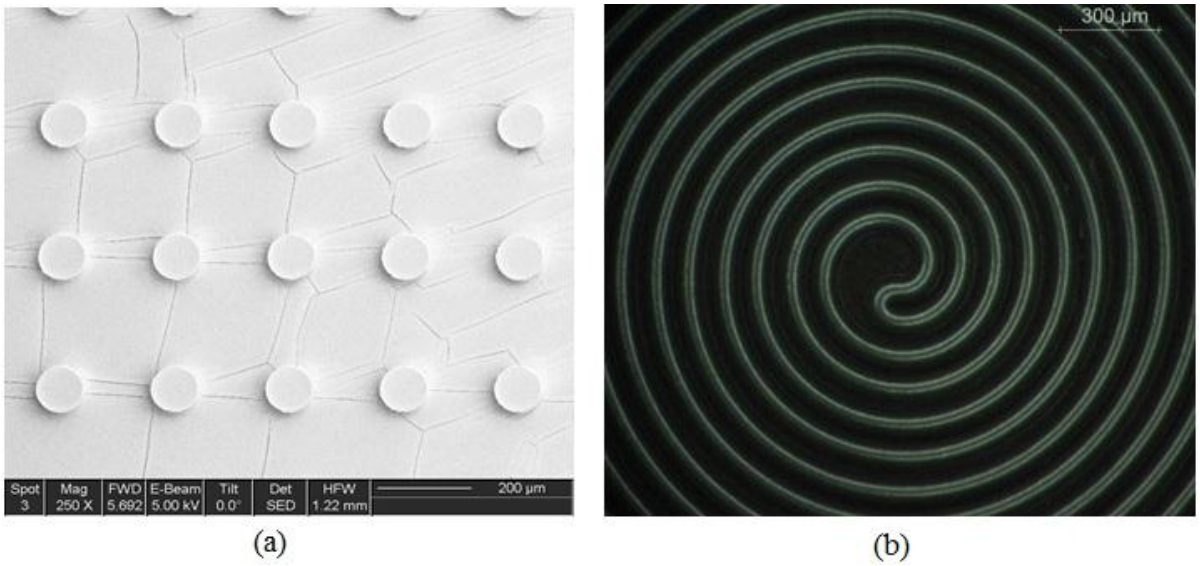

Figure 16 SEM and optical micrograph of: a) NdFeB micromolded hard micromagnets; b) 50nm nickel nanoparticle doped PDMS microcoils.

3.4 Summary, contributionsand discussion

In this chapter we have define a general fabrication process for PDMS based nanocomposites along with specific examples of four different nanocomposites which are; 1) multi walled carbon nanotubes, 2) silver, 3) nickel, 4) NdFeB. Note that for magnetic nanocomposites (nickel and NdFeB) use of a magnetic stirrer is not advisable.

SU-8, which is a negative tone photoresist,has been used as a structural micromold material. Omnicoat has been used as an adhesion promoter between silicon (or glass) wafers/substrates and SU-8 has been reported. Processing

parameters for SU-8 100 are discussed in detail. Appendix 6 outlines detailed processing steps for SU-8 100.

A novel hybrid process is introduced that enables hybrid systems with combined micropatterned PDMS based nanocomposites and undoped PDMS. In this process the nanocomposite is first poured on the SU-8 micromold and then degassed to remove air bubbles. The excess composite was scraped off using the Damascene-like process from the surface of the mold using surgical knife. Undoped PDMS is pored over the substrate, baked and peeled off from SU-8 substrate. This result in nanocomposite structures combined with nonconductive PDMS. Examples of hybrid microfabrication process are shown in section 3.3 of this chapter. SEM analysis of the fabricated MWCNT-PDMS and Ag-N PDMS nanocomposite indicate that nanoparticles are uniformly dispersed. Thus, the dispersion technique developed, which is a combination of high frequency ultrasonics and shear mixing, yields good dispersion.

This process alleviates problems with materials mismatch between flexible nonconductive polymers and metals or less flexible conductive polymers for soft (polymer) MEMS and flexible lab-on-chip systems. This new hybrid process is now being used by researchers at Engineering Science SFU, Concordia University and interest has been shown by industry to adopt his process such as lululemon, Timkin corporation and Montreal woollens.

However, it is noted that while SU-8 is an excellent micromold material for simple soft lithography, as well as the hybrid fabrication process for combining nanocomposite polymer with undoped PDMS discuss in detail is Section 3.3, it is

not without drawbacks. Some drawbacks associated with SU-8 as a nanocomposite micromold are as follows:

1. The SU-8 process is unstable for films thicker than 50 µm, meaning the same process does not yield same results and takes long time.
2. SU-8 is susceptible to traces of organic solvents presents in nanocomposites, which leads to swelling and deformation of the micromolds and leads to peeling off SU8.
3. Stiction of the nanocomposites to SU8 micromold can occur. The optical micrographs in figure 17 clearly show Ag-n PDMS composite sticking to the SU-8 micromold, making it difficult to peel off. This results inlow yield and fabrication of irregular and/or distorted structures.
4. Expensive, involves use of clean room, microelectronic photo-lithographic techniques and requires use of collimated UV source.

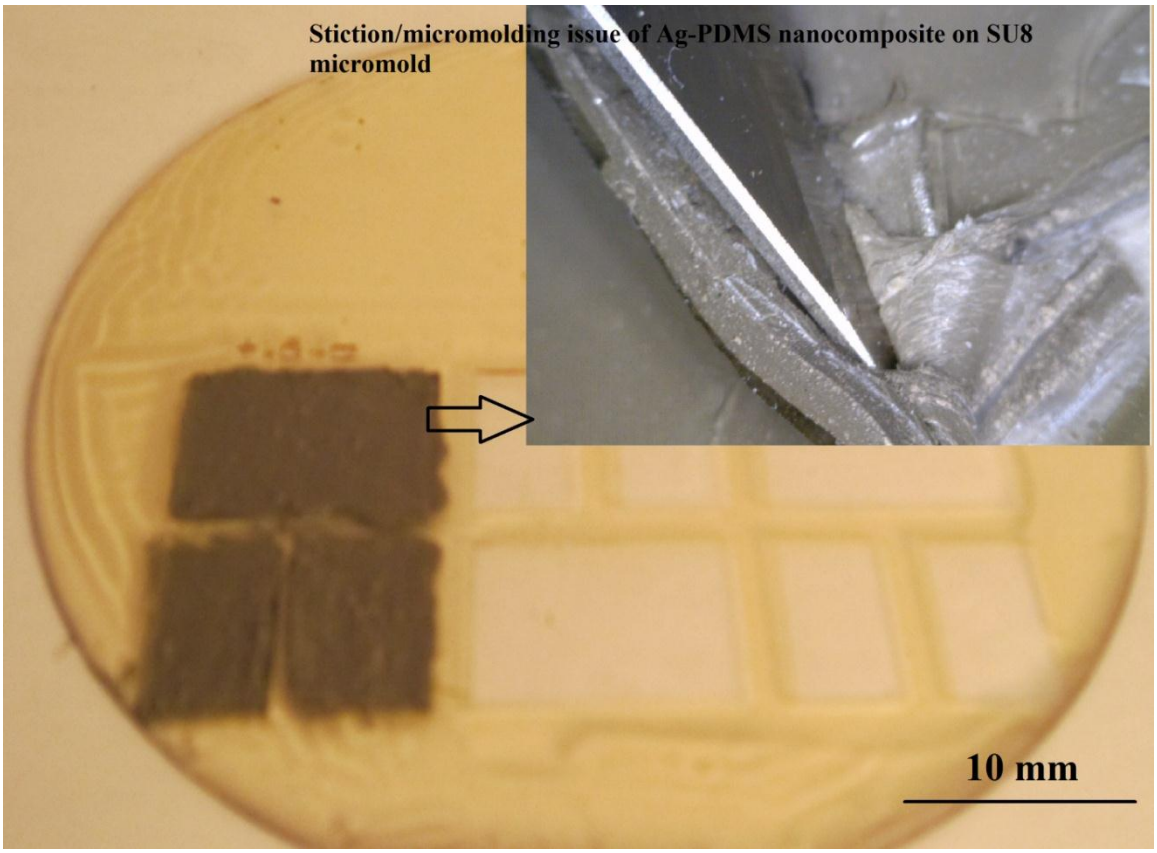

Figure 17 Optical micrograph of stiction of Ag-n PDMS nanocomposite to SU-8 micromold.

In order to elevate the above problems with SU-8, we investigated other materials which can be used as a micromold. Various lowcost materials were tried out including Polystyrene, S1318 PR, wax, COC, PMMA and polycarbonate.

However, we observed that PMMA works best as a micromold material because of its low cost, biocompatibility, chemical inertness, and optical properties. COC also showed excellent chemical internes but PMMA was chosen because of its availability from local sources. One of the challenges that needed to be overcome was to micromachine PMMA. One of the method used in Industry to micromachine PMMA is to use x-rays but this process very expensive.

We decided to try out CO_2 laser ablation and deep UV patterning of PMMA and test if it could be usedetch PMMA asmicromold and the feature size that can be obtained via both the process.

The next chapter describes both CO_2 laser and Deep UV micromachining of PMMA. Both the processes have their own advantages and disadvantages, and have been compared.

CHAPTER 4: PMMA AS MICROMOLD MATERIAL[11]

PMMA is an excellent choice for a micromolding master due to its high chemical inertness, mechanical strength and good dimensional stability. However, the use of PMMA as a positive tone resist or a mold usually involves a highly energetic and very expensive radiation source. One classical example is the use of synchrotron light (x-ray) for LIGA [91-101]. LIGA is a German acronym, standing for Lithographie, Galvanoformung, Abformung which translates to lithography, electroplating, and molding, for which the high cost x-ray source is required for the lithographic aspects of the process. Two low cost micromachining processes for PMMA are 1) Deep UV patterning; 2) CO_2 Laser ablation; for micromoldmaterials that are described in this chapter. These

[11]* Adapted version of:

[1] *A. Khosla et al, "Large scale micropatterning of multi-walled carbon nanotube/polydimethylsiloxane nanocomposite polymer on highly flexible 12×24 inch substrates", Proc. SPIE 7926, 79260L (2011)*

[2] *A. Khosla et al, "Preparation of nickel doped multi-functional micro-patternable polydimethylsiloxane nanocomposite polymer with characterization of its magnetic, electrical and mechanical properties for soft MEMS/Lab on a chip applications", Chapter 6: Polymer Nanotechnology Nanotech 2010 Vol. 1, Nanotechnology 2010: Advanced Materials, CNTs, Particles, Films and Composites ISBN:978-1-4398-3401-5*

processes described here, have been successfully demonstrated through this research over last four years.

4.1 Deep-UV lithography of commercial grade PMMA

PMMA patterningwith a latent image has been demonstrated using low-pressure mercury (germicidal) lamps [102-104], thus reducing drastically the cost associated with PMMA lithography. We utilized this low-cost, deep-UV lithography process, developed at IMMR, SFU by Marius et al. [105], for the fabrication of our micromolds which we then employ to moldour functional composite materials.

Figure 18 shows the basic fabrication sequence. The chosen structural material for the micromold was OPTIX®, a commercial acrylic purchased from PlaskoliteInc, Columbus, Ohio, USA.The irradiation source was a Stratalinker 2400UV crosslinker equipped with five low-pressure mercury lamps able to provide a nominal power of 4mW/cm^2 and a deep-UV spectrum with a maximum peak at 253.7 nm. In photolithography, collimated light is required for high aspect ratio patterning, however, the Stratalinker provides uncollimated illumination. To improve the resulting aspect ratio, a plastic grate made of 12.5 mm by 12.5 mm squares, each with a height of 13 mm, was set at a distance of 2 cm above the substrates during exposure. This way, only the light that hits the bottom plane of the grate at angles less than 46° with respect to the perpendicular on the surface are allowed through. Further, to even out the irradiation so that no square patterns are formed as a result of positioning, the grate above the substrateswas set on top of a rotational stage driven by a DC

motor, which was fed by a 9 Volt battery. The rotational frequency of the stage was approximately 0.125 Hz.

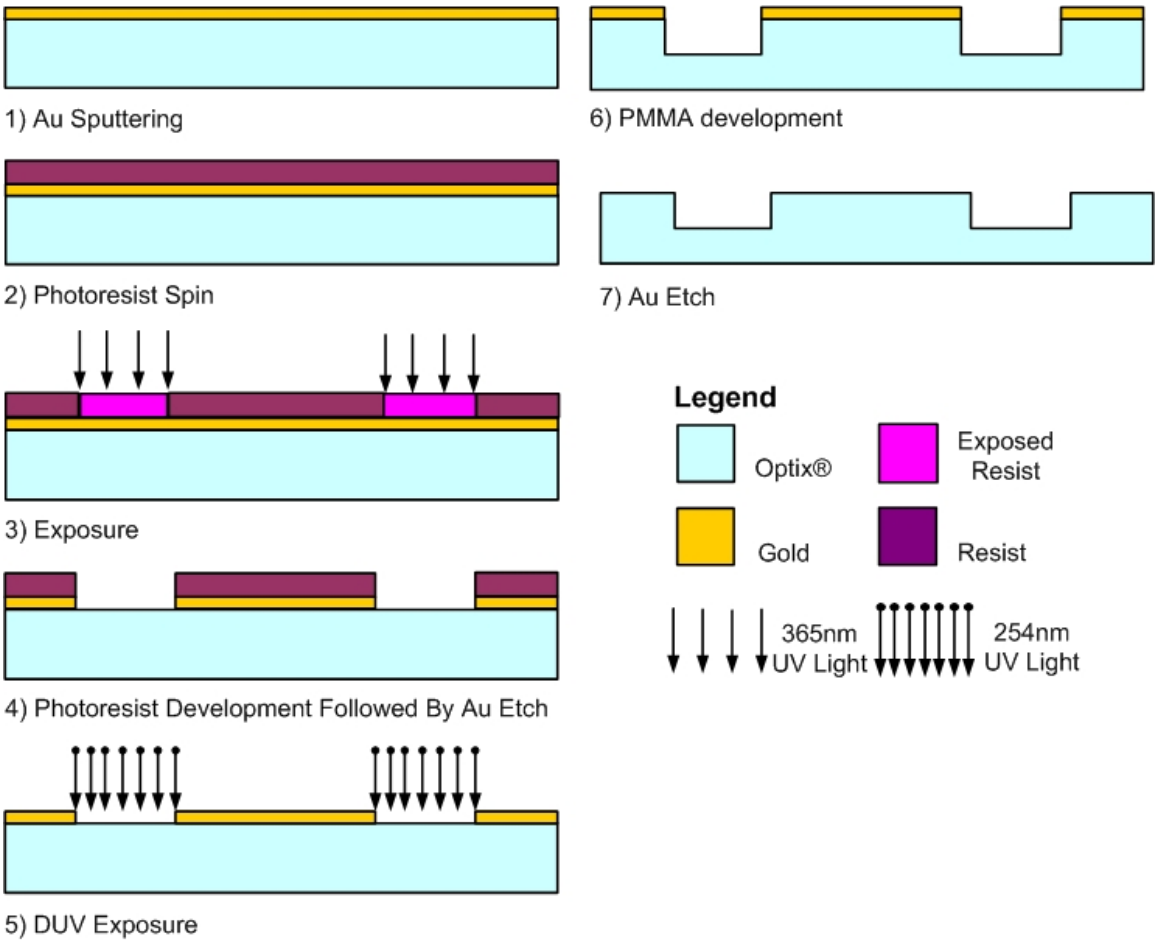

Figure 18[12] Deep-UV exposure of PMMA: fabrication process steps [104].

Prior to the following succession of steps, the acrylic was cut into 3 inch x 3 inch squares, cleaned with water and methanol, and then dried with a stream of nitrogen gas. A hard metal mask of 100nm of gold was sputtered on the PMMA

[12] Figure used with permission from Marius Haiducu [104].

substrate using a Corona Vacuum System sputtering system. After metal deposition, Shipley 1813 photoresist was spun on at 4000rpm for 30 seconds. Because the PMMA may warp if baked above 100°C, the photoresist baking temperature was kept below 75°C. The sample was exposed through a contact mask using an i-line source and developed in MF-319. The hard mask was etched using TFA gold etchant from Transene Company, Inc. Following the gold etch, the photoresist was removed using a 60 second blanket exposure followed by another development in MF-319, thus avoiding damage to the OPTIX® by strong organic solvents, such as acetone or photoresist stripper typically used to remove photoresist. At this point, the samples were exposed to deep UV using the hard mask for patterning, using a dose of 6650 Joules.

The samples were immersed in a developer bath consisting of 7:3 isopropyl alcohol (IPA) to de-ionized water (DI water) at 28°C for 1 hour. The temperature was maintained constant throughout the development and the bath was given a slight manual agitation. The development of the samples was quenched in an ultrasonic IPA bath at room temperature (~18°C) for 10 seconds, followed by an IPA rinse for another 10 seconds. This quenching was necessary to prevent the re-deposition of the partially dissolved PMMA. After removing the gold mask using TFA gold etchant, rinsing with DI water, and blowing the samples dry with nitrogen gas, the depth of the etched channels were measured using an Alpha-step 500 profilometer and found to be 100μm deep and a width of 20μm. Figure 19 shows SEM micrographs deep UV lithographically patterend PMMA. The Deep UV micromachining gives an anisotropic etching profile.

However, no adhesion/ stiction problems of nanocomposite were observed. Sub-micron features are possible,but they are highly dependent on the UV source and etching accuracy of the gold hard mask. Figure 18shows micromolded nanocomposite structures obtained using UV-patterned PMMA molds. It is clearly visible from SEM micrographs that the micromolded structures are curved; this is due to the anisotropic etch of the PMMA micromold as explained by figure 20.

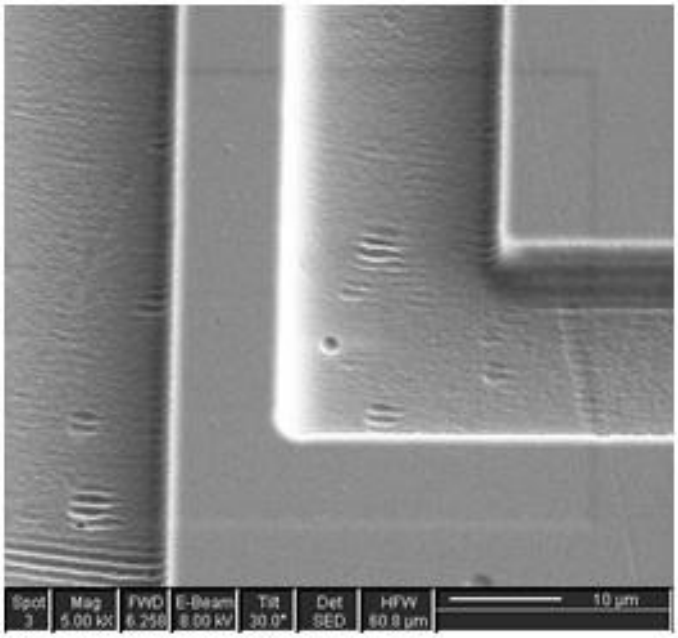

(a)

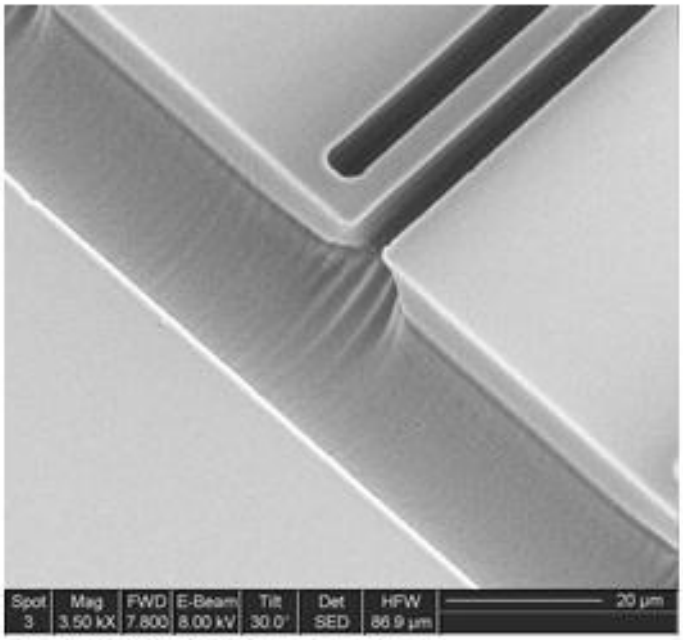

(b)

Figure 19[13] SEM micrographs of Deep UV patterned PMMA

[13] SEM micrographs used with permission from Marius Haiducu [105].

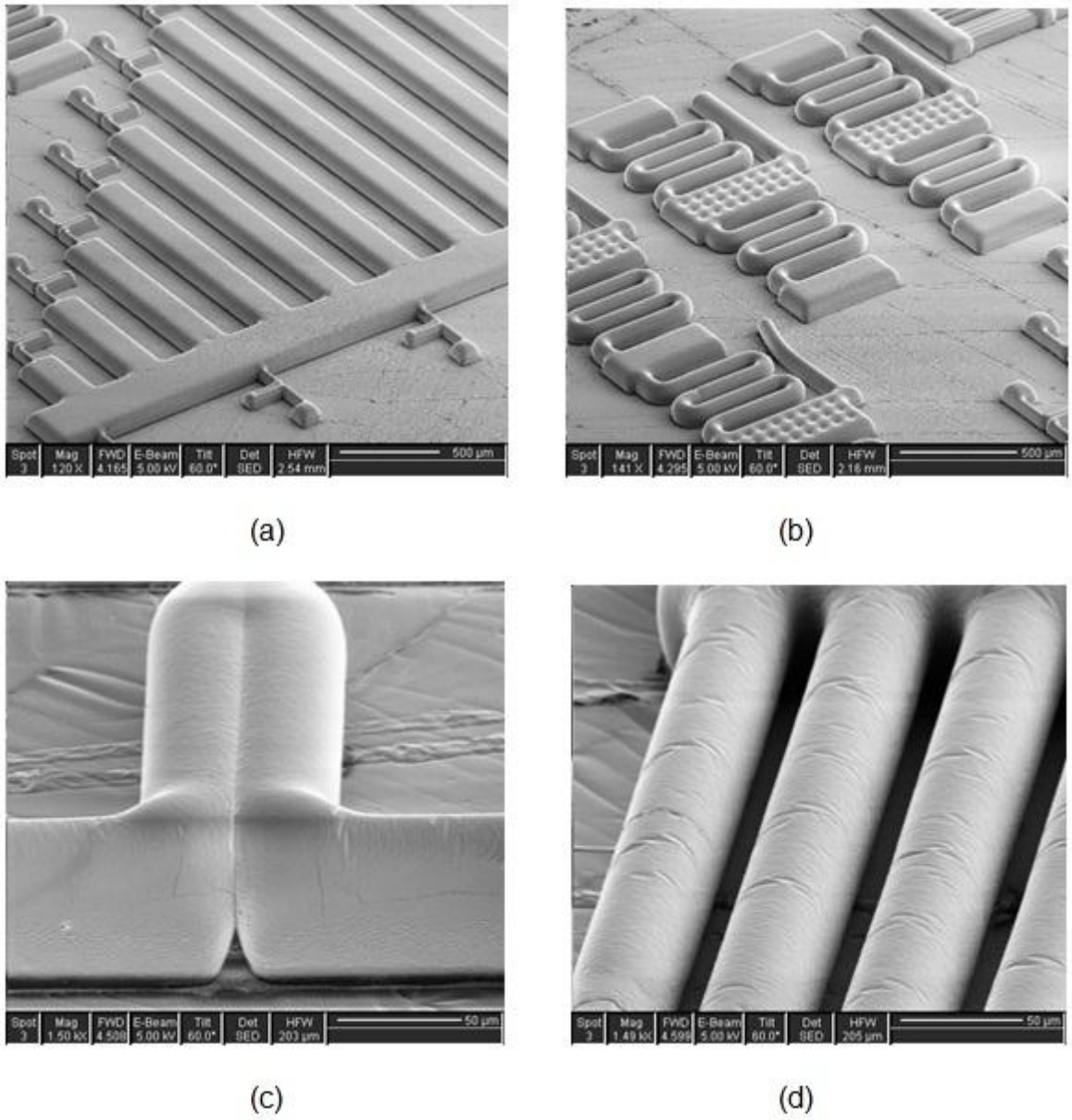

Figure 20 SEM micrographs of micromolded magnetic nanocomposite: a) cantilevers; b) bridges; c) cantilever tip/edge; d) parallel bridges.

4.2 CO_2 laser ablation of PMMA

Large-area molds for micro-patterning were fabricated by laser etching 5-mm thick, 12 inch x 24 inch PMMA sheets using the Universal Laser System's VersaLASER© laser ablation system. The system has a CO_2 laser cartridge with a maximum rated power of 60 watts that produces an invisible infrared beam at a wavelength of 10.6 μm. According to the manufacturer, the system is rated to run at the maximum raster beam speed of 1143 mm/s (45 in/s). The movement of the mirrors and lens assembly is achieved by a motor and controlled by operating software (UPS). The laser system works with vector and raster modes to produce lines and filled shapes, respectively. In this work, the system was set to vector mode for single pass ablation. The control factors that determine the channel depth and width are laser power and speed of ablation, which are set as a percentage via the control software. A CO_2 laser emits infrared radiation at a wavelength of 10.6 μm. PMMA has a high absorptance[14] of about 0.92 in the infrared. PMMA also combines a low heat capacity with a low heat conductance, which means that any absorbed heat will result in a rapidly rising temperature. This means that the CO_2-laser beam ablates the PMMA photothermally. Unlike UV lasers, a CO_2 laser emits radiation continuously. Wherever the focused laser beam meets the PMMA surface, the temperature of the irradiated spot rises rapidly, that the PMMA first melts and then decompose, leaving an V-shape groove. Figure 21 and 22 shows a cross-sectional area and top view of a

[14]Absorptance is different from absorbance and is defined as: The ratio of the radiant flux absorbed by a body to that incident upon it.

samplechannel etched by the above mentioned laser system. The channels have a V groove due to the temperature distribution within the PMMA substrateThe relationship between laser power and the channel depth is illustrated in figure 23. From figure 23 that the channel depth increases linearly with the power and decreases exponentially with the beam speed. We observed that the effect of beam speed and power on the channel/groove width is not significant. However, it varies almost linearly with both beam speed and power. Hence, by varying beam speed and power we can achieve different depths and aspect ratios.

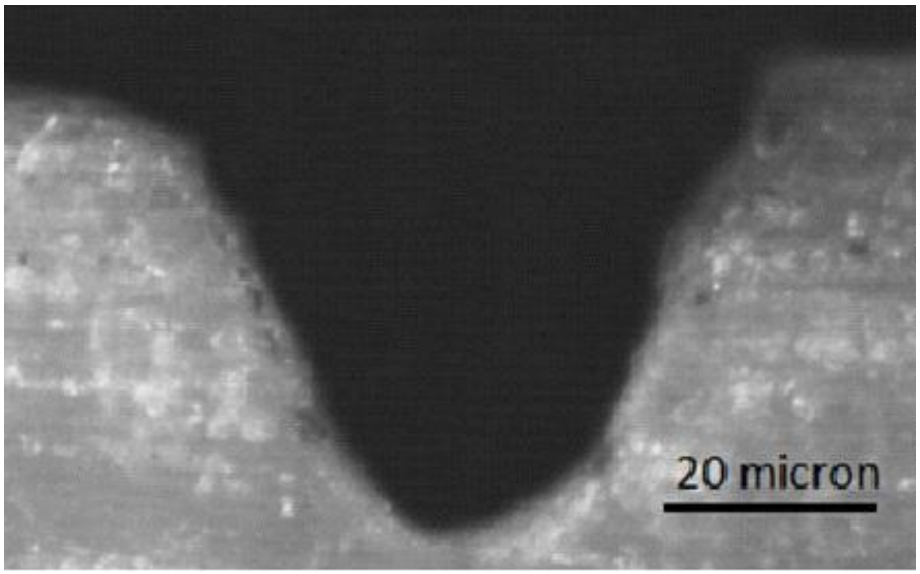

Figure 21 Cross-sectional area of CO_2 laser etched PMMA.

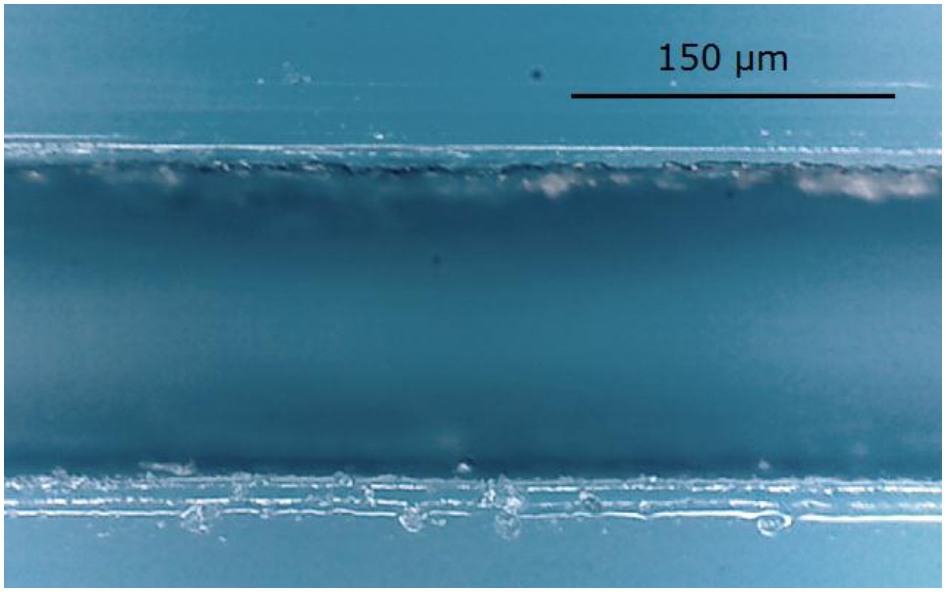

Figure 22 Optical micro graph top view of 150µm CO_2 Laser etch PMMA

In order to achieve a feature size of 400 µm we operated the laser system 45% of speed and 35% of power. For structures less than 100 µm it is observed that high speed and low power provide better results. Feature size of less than 20 µm is difficult to achieve by CO_2 laser ablation technique.

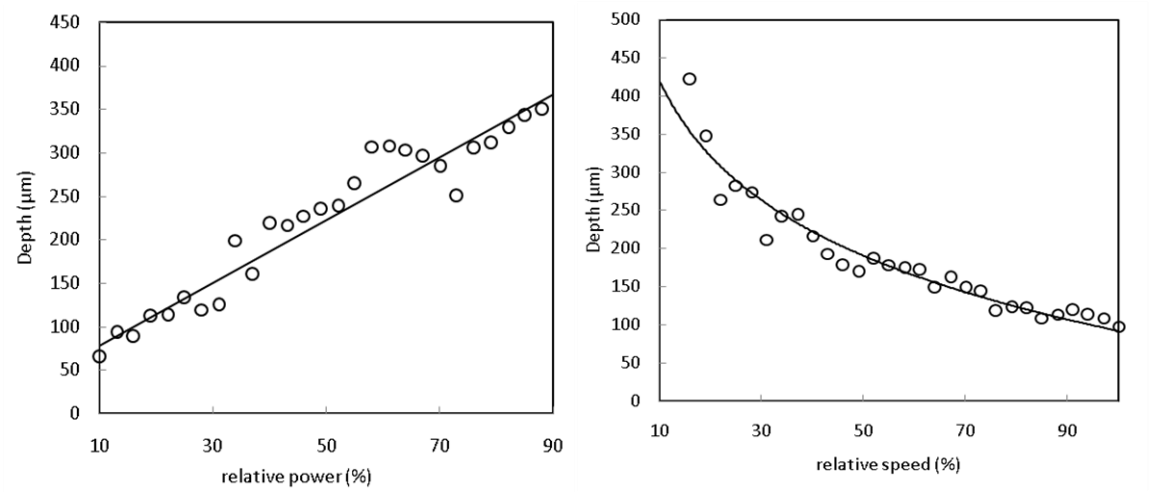

Figure 23 Effect of laser power (a) and beam speed (b) on the channel depth. The relative values are based on the maximum laser power of 65 W and beam speed of 1143 mm/s. Data points are measurement results and solid lines are fitting curves. The substrate material is 5mm thick.

Figure 24 shows a 12 inch x 24 inch laser etched PMMA 5mm thick micromold substrate and MWCNT-PDMS nanocomposite micropatterened on a flexible undoped PDMS.This was carried out using the hybrid micromolding process reported in chapter 3 for use with smaller (3inch x 3 inch) micromold substrates. The prepared nanocomposite was poured on to the 12 inch x 24 inch large-scalemicromold. Excess MWCNT-PDMS composite were scraped off using a Damascene-like process from the surface of the mold using a surgical knife. The surface of the substrate is then cleaned with IPA. Undoped, degassed PDMS polymer is then poured on the surface of the nano-composite filled mold. Finally, the PDMS is cured overnight (12 hours) or under an infrared lamp for 3 hours and peeled off from the mold.

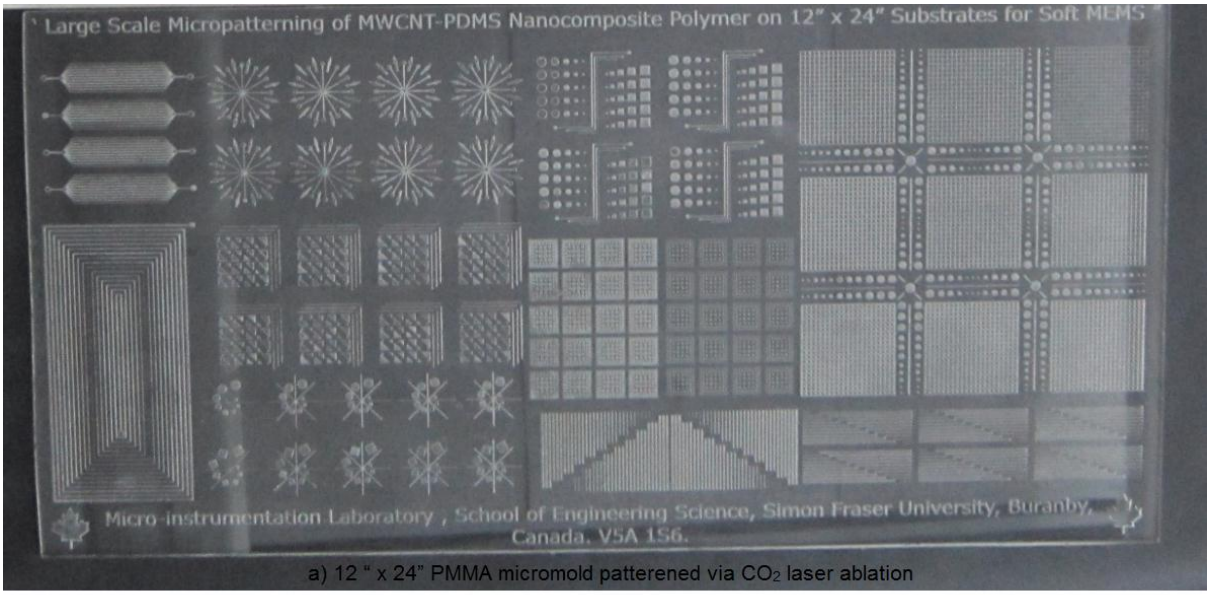

a) 12 " x 24" PMMA micromold patterened via CO_2 laser ablation

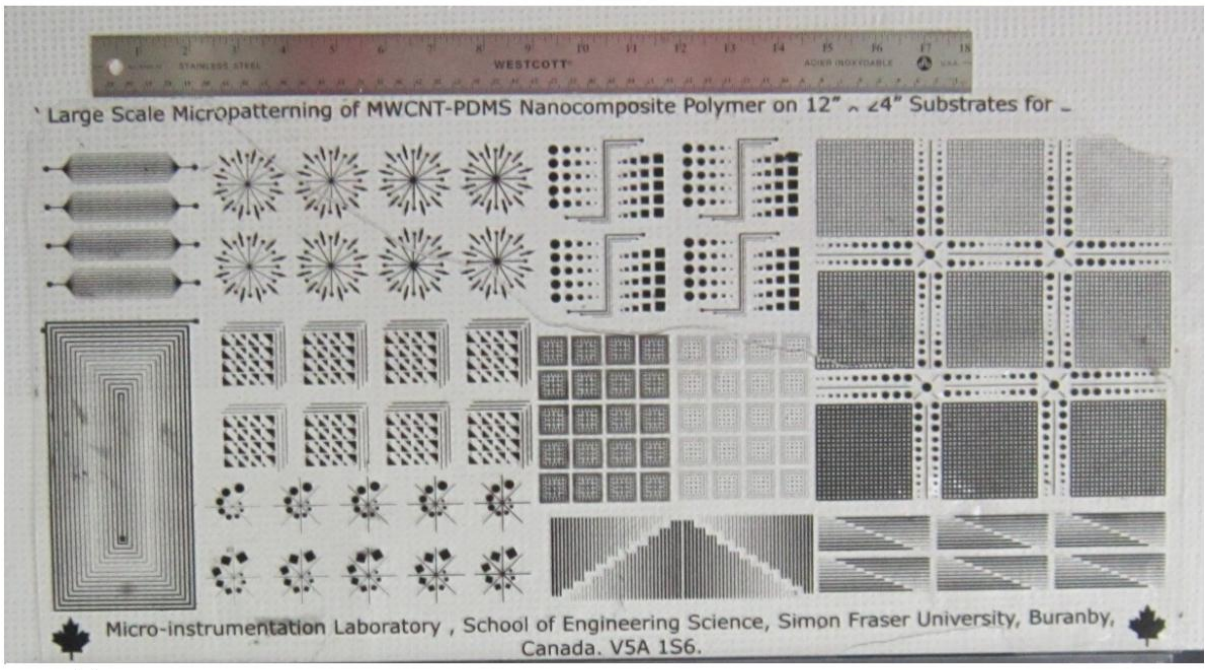

b) MWCNT-PDMS nano composite-Hybrid microfabrication process against a 12 inch x 24 inch PMMA micromold

Figure 24 Optical micrograph of large scale micro patterning of MWCNT-PDMS nano composite-Hybrid microfabrication process against a 12 inch x 24 inch substrate.

4.3 Summary, contributions and discussion

In this chapter we have successfully shown micromachining of nanocompositemicromolds using commercial grade PMMA by DEEP UV photolithography and CO_2 laser micromachining. PMMA for use as a micromold material has been reported for the first time. A novel low cost, large scale, hybrid micro-molding technique on 12 " x 24" PMMA micromoldspatterened via CO_2 laser ablation has also been successfully demonstrated for the first time. This allows us to batch fabricate very large numbers of micromolded devices at the same time, or very large continuous structures such as long lines for electronic routing on large substrates. Not only does this potentially reduce manufacturing cost through larger batch fabrication, it enables the construction of new very large area devices such as electrode arrays, electrical wires, micromagnets, magnetic wires [104, 105].Table 2 compares Deep UV vs CO_2 micromaching of PMMA.

The Deep UV photolithographic process of etching commercial grade PMMA is a very interesting technology and leads to smoother etched surfaces as compared to CO_2 laser ablation. However, one of the drawbacks is the Deep UV is the exposure time required in the process and can last up to 15 hours in order to achieve a depth of 100 µm. The process has been tried for 4 inch PMMA substrates but has the potential to be scaled up to larger substrates such as 12" inch x 24" inch PMMA sheets. For such large substrates, deposition of a hard mask (e.g., for 4 inch PMMA sheet, sputtered gold was used a hard mask) and

spin coating is not possible. However, in Appendix 7 we have shown another low cost technique, whichhas the potential to be used for large scale Deep UV micromachining of PMMA to be used for micromoldmolding. We have employed use of commercial grade PMMA mirrors, which have a 7 µm aluminium coating at the back. Etching of aluminium has been demonstrated for 4 inch PMMA mirrors. However, large-scale fabrication has not been demonstrated as yet because it is impossible to spin coat photoresists on large substrates using currently available equipment. Using a dry film photoresists can be a potential solution.; this work is under investigation.

Table 2 Comparison Deep UV vs CO_2 micromaching of PMMA

	Deep UV	**CO_2**
Etched surface	**smooth**	**rough**
Etch profile	**Anisotropic etch**	**V shape etch**
Etching	**Wet chemical**	**Dry**
Feature size	**2 µm - 5 µm** (Limited by resolution of DEEP UV exposure and hard mask)	**50 µm**
Submicron features	**Possible but not demonstrated.**	**Not Possible**
Etching time (4x4 inch)	**~15 hrs for 100 µm depth**	**10 -15 min. for 100 µm depth**
Large-scale fabrication	**Possible but not demonstrated**	**demonstrated**

CHAPTER 5: RESULTS AND DISCUSSION[15]

In this chapter, the properties and results of different PDMS based nanocomposites that are described in chapter3 are discussed. The PDMS nanocomposites are as follows 1) MWCNT-PDMS, 2) Ag-n PDMS, 3) Ni-PDMS, 4) NdFeB-PDMS. Along with results, devices fabricated using these nanocomposites are also described and characterized, and include devices such as ribbon cables, microelectrodes, and hard micromagnets.

[15]Adapted version of:

[1] *A. Khosla and B. L Gray; "Preparation, characterization and micromolding of multi-walled carbon nanotube polydimethylsiloxane conducting nanocomposite polymer", Materials Letters Volume 63, Issues 13-14, 31 May 2009, Pages 1203-1206*

[2] *A. Khosla and B. L. Gray, " Preparation, Micro-Patterning and Electrical Characterization of Functionalized Carbon-Nanotube Polydimethylsiloxane Nanocomposite Polymer", Macromolecular Symposia: Special Issue: Polymers and Organic Chemistry, Volume 297, Issue 1, pages 210–218, November-2010*

[3] *A. Khosla, B. L Gray "Properties of Conductive Micromoldable Thermosetting Polymer for Electronic Routing in Highly Flexible Microfluidic Systems" SPIE Proceedings Vol. 7593, Microfluidics, BioMEMS, and Medical Microsystems VIII*

[4] *A. Khosla, B. L Gray "Fabrication of Multiwalled Carbon Nanotube Polydimethylsiloxne Nanocomposite Polymer Flexible Microelectrodes for Microfluidics and MEMS." SPIE Proceedings Vol. 7642 Electroactive Polymer Actuators and Devices (EAPAD) 2010.*

[5] *A. Khosla, B.L. Gray, "CONDUCTIVE ELASTOMERIC MATERIAL AND USES THEREFOR" US Patent No. 61/113998*

[6] *A. Khosla, B. L Gray, J. L. Korčok, D. B. Leznoff, "NOVEL MAGNETIC NANOCOMPOSITES WITH PREPARATION AND METHODS OF PATTERNING SAME". US Patent No. 61/288,244*

5.1 Electrically conductive MWCNT-PDMS results and discussion

In this section, the electrical properties of the fabricated MWCNT-PDMS nanocomposite is discussed, such as determination of percolation threshold and calculated resistivity values for MWCNT-PDMS structures. MWCNT-PDMS ribbon cables were fabricated as example strcuturesand the effect of bending of the cables is also been discussed.

Resistivity and percolation threshold measurements

The evolution of the electrical resistivity of COOH- functionalized MWCNTs in PDMS as a function of weight percentage and temperature has been determined using the set up illustrated in figure 25. An HP-3478A multimeter was set to operate in four point probe mode in order to eliminate any contact resistance. The HP-3478A multimeter passes a known current through the sample using the “input” leads and measures the voltage across the sample using the “sense” leads. The resistance between the “sense” leads is then calculated using Ohm’s Law. Because the sense leads are not drawing any current, the effects of contact resistance are eliminated, thus giving only the resistance of the bulk material.

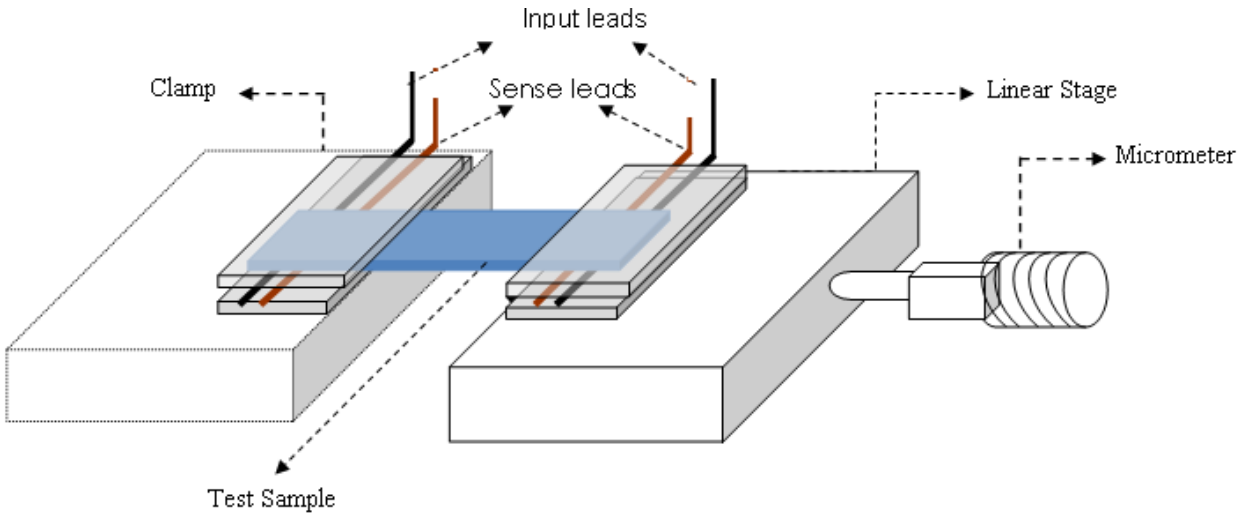

Figure 25 Test fixture to measure the resistivity of MWCNT-PDMS nanocomposite samples

As can be seen from figure 26, it is observed that the resistivity increases slowly up to 1.5 wt-%. However, after this point the conductivity increases rapidly, which corresponds to the resistivity decreasing. This behavior of conductivity variation can be explained in terms of the percolation theory as discussed in Chapter 2 section 2.6;to review: at lower concentrations of functionalized MWCNTs, the percolation paths are not completely set up by the MWCNT network. As the concentration of MWCNTs in the composite increases, the percolation paths via conducting MWCNTs are set up, and the MWCNTs control the conductivity of the nanocomposite matrix. The concentration of MWCNTs required for insulator conductor-transition is referred as threshold concentration or percolation limit, which was 1.5 wt.% for the functionalized MWCNT-PDMS nanocomposite shown in figure 24. The resistivity level achieved at 2 wt.% was approximately 62 Ω-cm.

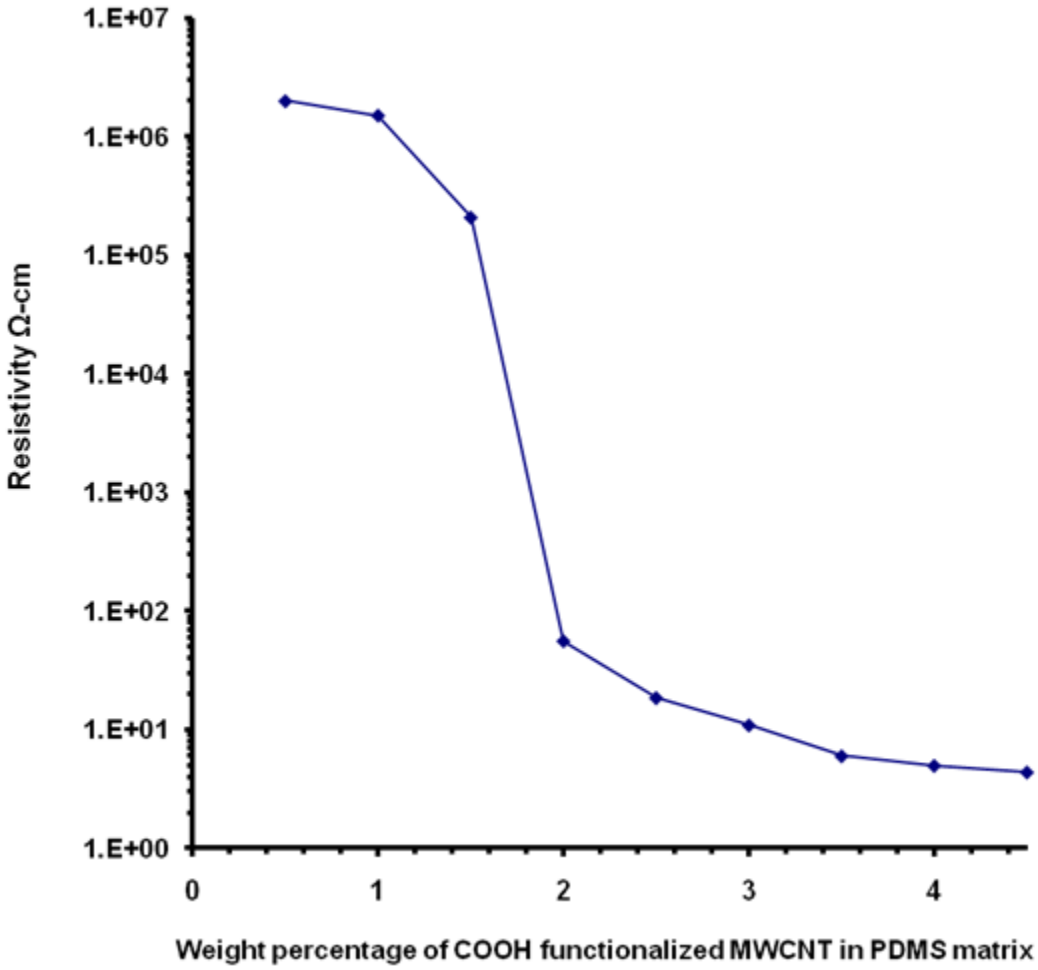

Figure 26 Resistivity verses COOH- functionalized MWCNT wt.% in the PDMS matrix

MWCNT-PDMS microribbon cable fabrication and testing

The hybrid microfabrication process defined in section 3.3 of chapter 3was employed to fabricated the nanocomposite employed in making ribbon cables. A step by step fabrication process is shown pictorially in figure 27. The fabricated ribbon cables had lengths of 25 cm, height of 150 µm and width of 150 µm. A total of 45 ribbon cables were fabricated with doping level of 4 wt.% of MWCNT in PDMS matrix. The average resistivity of for micro-fabricated ribbon cables is $2.02E^{-05}$KΩm.

Table 3shows that standard deviation and relative standard deviation of the fabricated 45 ribbon cables, are both small. This confirms our ability to fabricate ribbon cables with consistent resistivity values.

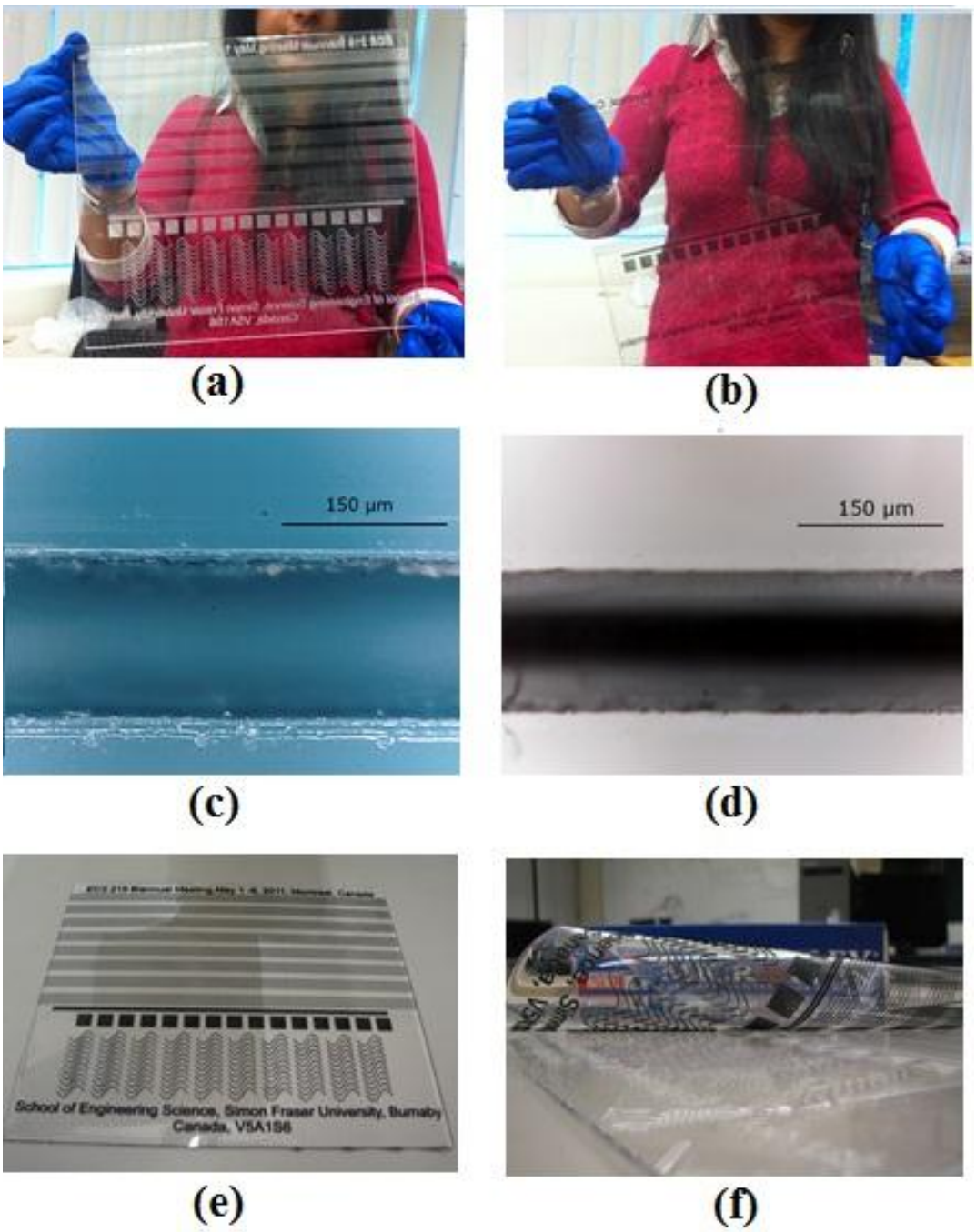

Figure 27 Microribboncabel fabrication: a) laser etched PMMA micromold; b) PMMA micromold after Damascene-like process, filled with MWCNT-PDMS nanocomposite; c) optical micrograph of etched PMMA; d) demolded MWCNT-PDMS ribbon cable close up; e) cured PDMS on PMM

Table 3 Standard and relativestandard deviation of resistivity of 45 ribbon cables

Parameter	Resistivity in Ω-m
Median	168
Mean	170
Standard deviation	10.449
Relative standard deviation:	0.0622

The fabricated ribbon cables were subjected to change in orientation in order to study the effect of bending of ribbon cables on resistivity. We compared three orientations; 1) curved in, 2) and curved out as defined in figure 28.

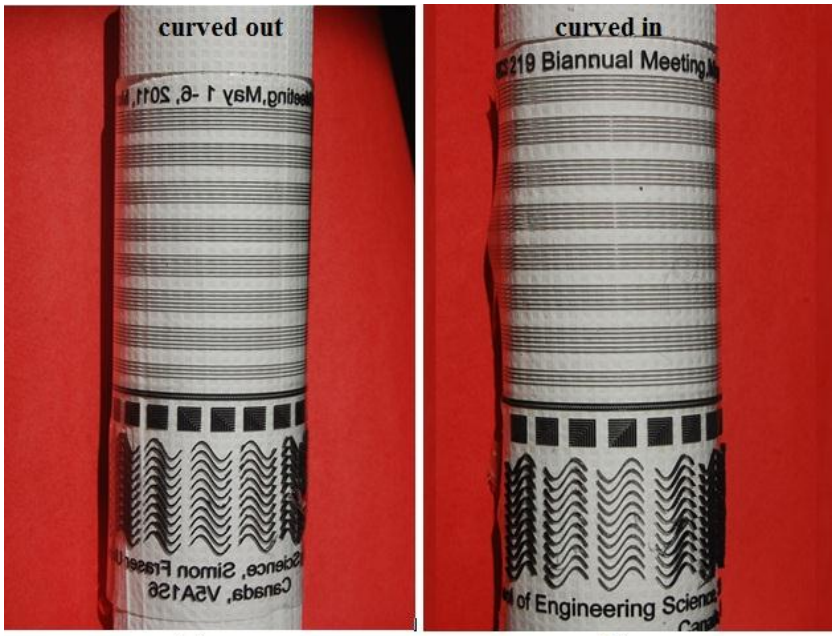

Figure 28 Micro ribbon cables (a) curved in (b) curved out. For the curved in structures, the ribbon cable structures are on the surface on the inside curve, and the opposite (on the outside of the rolled sheet) for the outside curved.

The decrease in average resistance, shown in Table 4, due to “curving in”was found to be 5.24 kΩ, while the increase in average resistance due to “curving out” was similarly 7.6 kΩ.

Table 4 Effects on resistance of MWCNT-PDMS microribbon cables due to curving

	Absolute change	Relative change
Decrease due to curving in	5.24 kΩ	0.0317
Increase due to curving out	7.60 kΩ	0.0442

These results suggest an interesting phenomenon concerning the electrical properties of our nanomaterial. These results indicate that the MWCNT-PDMS nanocomposite polymer is piezoresistive. This piezoresitive response is consistent with the results of others [111].

Negative Temperature Coefficient of Resistivity Results

It is observed that the MWCNT-PDMS nanocomposites show a negative temperature coefficient of resistivity (NTCR), which has been characterized for three different weight percentages (1.5, 2 and 2.5 wt-%) as shown in figure 29. Negative temperature coefficients are of interest because they can be exploited

for on-chip temperature sensors for, e.g., measuring local temperature during on-chip chemical reactions for lab on a chip devices.

The functionalized MWCNT-PDMS nanocomposite samples were loaded onto the four probe test fixture (figure 25) and placed in the thermal chamber. The temperature was increased in steps of 20^0C up to a maximum temperature of 300^0C and the corresponding value of resistance was recorded at each temperature. A clear trend is observed from the values obtained and shown in figure 30: for every 20^0C rise in temperature, a predictable trend is that there is a decrease in resistivity with an increase in temperature, thus showing a negative temperature coefficient of resistivity.

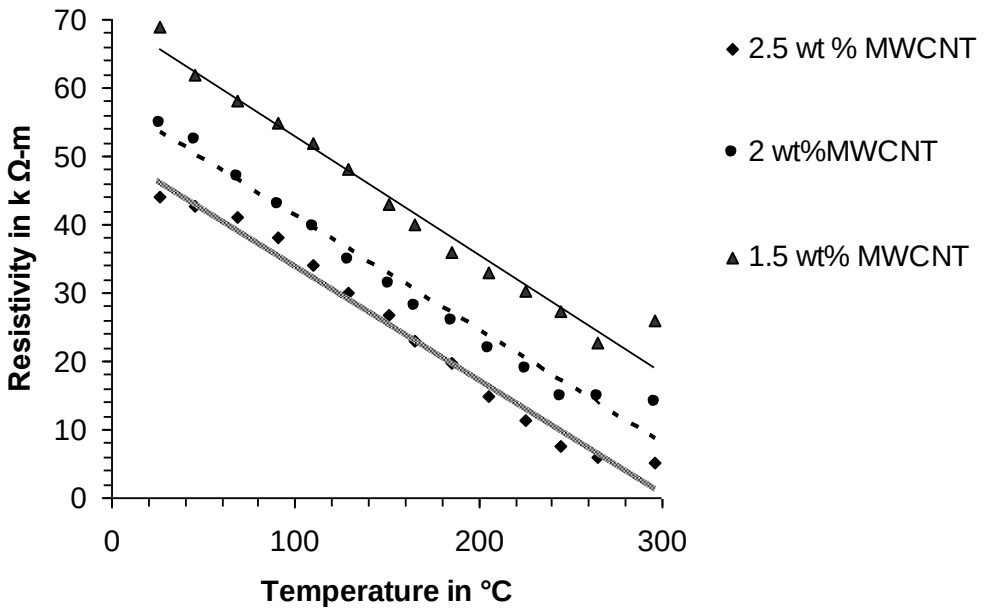

Figure 29 Negative temperature coefficient of resistivity of COOH- functionalized MWCNT in PDMS for different weight percentages of nanotubes.

Summary

We have successfully demonstrated the preparation, improved micropatterning, nanoparticle dispersion analysis, and electrical property characterization of COOH- functionalized mutli-walled carbon nanotube (MWCNT) and polydimethylsiloxane (PDMS) conductive nanocomposite polymers that can be employed for lab on a chip applications. SEM analysis shows that COOH- functionalized MWCNT are well dispersed with little observable agglomeration. Although the purchased MWCNTs were COOH-functionalized, some amount clumping or bundling was still observed on initial mixing with PDMS base, and hence, we additionally employed high frequency

ultrasonic dispersion method in order to achieve de-agglomeration, leading to fairly uniform dispersion and improved resistivity.

The electrical and temperature dependent properties of the nanocomposites have been characterized as a function of weight percentage (wt.%) of COOH- functionalized MWCNTs in the PDMS matrix. It is observed that a percolation threshold occurs at approximately 1.5 wt.%. The current nanocomposites show lower resistivity (62 Ω-cm or better) at 2 wt.% than our previously reported value of 100 Ω-cm at 2 wt.% of MWCNT's in PDMS matrix. As mentioned, this is likely due to a combination of dispersion uniformity and aspect ratio, although the functionalized nanotubes were of inferior grade (and much less expensive).

We have also shown successfully microfabrication of MWCNT-PDMS ribbon cables with a result that the ribbon cables show a pizeoresistive response on bending.

5.2 Electrically conductive Ag-n-PDMS results and discussion

Percolation threshold and electrical properties

In order to characterize the electrical properties of the Ag-PDMS nanocomposites, thick films 3cm x 1 cm x 0.01cm in size with twelve different weight percentages of Ag-n (15, 20, 25, 30, 31, 32, 33.5, 36, 37.5, 40, 45 and 50wt%) were prepared and tested using an HP-3478A multimeter which was operated in four point probe mode in order to eliminate any contact resistance in

a similar way as explained in section 5.1 of this chapter. The effect of Ag-n concentration on electrical properties is shown in figure 31 (a). It is observed that as the concentration of Ag-n in the PDMS increases, the percolation paths via Ag-n are set up and the Ag-n control the conductivity of the nanocomposite matrix with the result that the resistivity decreases sharply at 32.5 wt%, which is referred to as percolation threshold as explained in chapter 2.Figure 30 showsoptical micrographs of fabricated array of microelectrodes of lengths ranging from 1mm to 10mm.

Figure 30 Optical micrographs of fabricated microelectrodes on nonconducting PDMS: array of microelectrodes of lengths ranging from 1mm to 10mm

The current–voltage (I–V) characteristic of each micromolded electrode, which gives the current through the micromolded structure as a relation to the voltage across it, was measured using an HP 4155C Semiconductor Parameter Analyzer (SPA). The results are shown in Figure 31 (b). The SPA was

programmed to operate in two terminal device mode, with a sweep voltage of 0–1 V in steps of 0.01 V. The corresponding current values were recorded for five microelectrodes with different lengths (*l* = 1mm, 2mm, 3mm, 4mm and 5mm) with

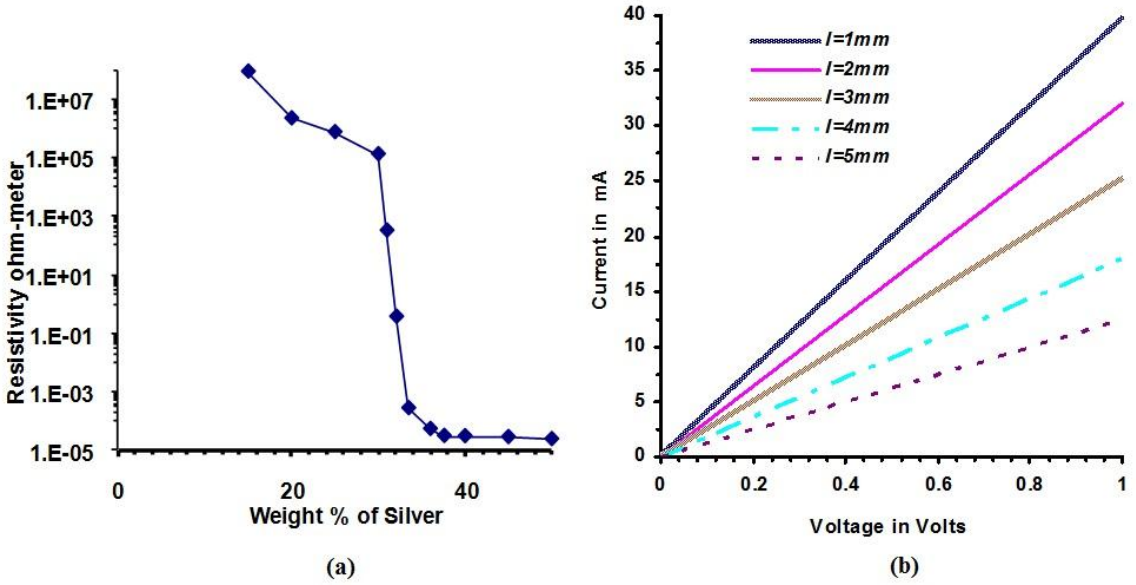

Figure 31 Electrical properties of Ag-n PDMS nanocomposite micropatternable polymer: a) resistivity vs. weight percentage of silver nanoparticles in PDMS matrix; b) I-V characteristics of microelectrodes of different lengths.

Aheight of 30 µm and width of 100 µm.The wt.% of Ag-n in this case was 50 % in PDMS. The contact to these electrodes was carefully made using micro-manipulators. It can be clearly seen from the graph that for the microelectrode with *l*=1mm, a current of 40mA is easily achievable at 1 V which is good for signal routing applications for MEMS and microfluidic applications. The resistivity level achieved at 50 weight percentage is equal to 2.3×10^{-5} Ω-m which is better than bulk carbon. As all the electrodes were fabricated on the same substrate, all the dimensions of the electrodes are the same except the length *l*. As the length

of the electrode increases the resistance increases ($R \propto l$), hence there is a drop in the value of current as is expected.

Summary

We have demonstrated the preparation and microfabrication via soft lithography of conducting Ag-n–PDMS-based nanocomposite highly conductive microelectrodes and electronic routing. The percolation threshold achieved for the silver nanoparticle and PDMS composites was 32 wt% of Ag-n in the PDMS matrix. We have successfully shown that we can micromold Ag-n-PDMS nanocomposite structures on a non conducting PDMS substrate, demonstrating both microelectrodes. The height and width of all the microelectrodes was the same (30μm,100μm, respectively), with lengths ranging from 1mm to 10mm, and resistance varying as expected with length. Allelectrodes maintained conductivity under physical deformation such as twisting and bending. It was also observed that current in the range of 15mA to 40mA was easily achieved at 1 volt depending on the length of the fabricated microelectrodes. This demonstrated process alleviates problems with materials mismatch between flexible nonconductive polymers and metals or less flexible conductive polymers for soft (polymer) MEMS and flexible lab-on-chip systems. Further experimentation is needed to characterize the smallest feature size, aspect ratio, and resolution, although unfilled PDMS has been micromolded with features smaller than 50 nm. Further experimentation is also needed to build up sequential layers of electronic routing.

5.3 Soft magnetic Ni-PDMS nanocomposite properties and testing[16]

Magnetic characterization

The magnetic properties of Ni-PDMS nanocomposites were obtainedby SQUID magnetometry and were compared to pure nickel nanoparticles. Magnetometry measurements were carried out on a Quantum Design MPMS-XL-7SSQUID magnetometer. Ni-PDMS samples, as well as the pure (30-50 nm) Ni nanoparticles, were packed in polycarbonate capsules and mounted in low-background diamagnetic straws. For each sample, magnetization (M) vs. field (H) hysteresis measurements were obtained at 300 K in fields between +2 T and -2 T, taking data every 25-200 G at low fields (< 0.2 T) and 1000-5000 G at higher fields. The pure Ni nanoparticles were found to have a saturation magnetization, M_{sat}, of 46.0 emu/g. The coercivity, H_c, is 105 G, indicating that the material is a soft magnet. The shapes of the hysteresis loops, fields at which saturation occurs, and coercive fields are identical for all Ni-PDMS composites, verifying

[16] *A. Khosla, J. L Karcock, B. L Gray and D. B Leznoffl, "Preparation of nickel doped multi-functional micro-patternable polydimethylsiloxane nanocomposite polymer with characterization of its magnetic, electrical and mechanical properties for soft MEMS/Lab on a chip applications", Chapter 6: Polymer Nanotechnology Nanotech 2010 Vol. 1, Nanotechnology 2010: Advanced Materials, CNTs, Particles, Films and Composites ISBN:978-1-4398-3401-5*

Compositions Including Magnetic Materials: Inventors: Bonnie Gray (Vancouver, CA) Daniel B. Leznoff (Vancouver, CA) Jasmine L. Korcok (Maidstone, CA) AjitKhosla (New Westminster, CA)Assignees: Simon Fraser University, IPC8 Class: AH01F126FI, USPC Class: 4302701, Class name: Radiation sensitive composition or product or process of making, Publication date: 06/23/2011, Patent application number: 20110151377

that the incorporation of the nanoparticles into PDMS films did not change their fundamental magnetic properties. As expected, M_{sat} values per gram of nanocomposite correlate linearly with the wt.% of Ni in PDMS (Figure 33), with the 45.5 % sample having the largest saturation magnetization, at 21.0 emu/g as compared to the pure Ni Nanoparticles which had a saturation magnetization of 45.7 emu/g (shown in figure 32 as the 100 wt.% point).

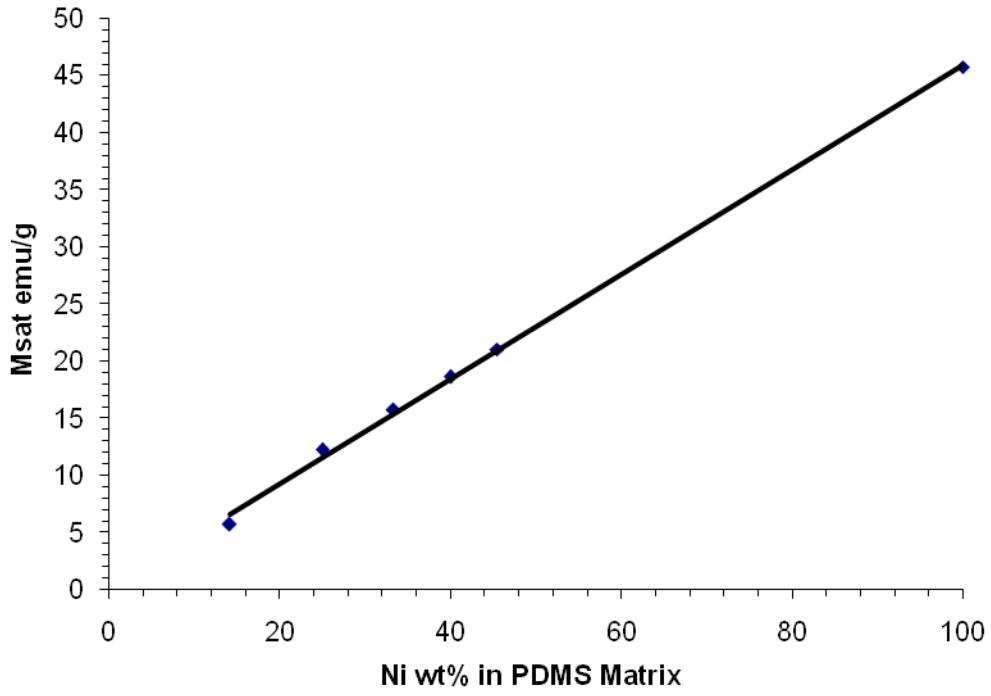

Figure 32 Saturation magnetization (Msat) per gram of composite as a function of mass percent of Ni in the Ni-PDMS composites.

Mechanical characterization

Young's Modulus measurements were done using an Instron +3340 Series Single Column System. A total of ten test specimens were fabricated with varying weight percentage of nickel nanoparticles in PDMS (eg. 0, 14.06, 25, 30 …55), with each sample having a gage length of 75 mm, a width of 25 mm, and a thickness of 1mm. Tests were carried out employing the ASTM (E8-04) Standard Test Method. After the sample was loaded into the testing apparatus and the strain gauge attached to the specimen, all variables were cleared and the speed of the grips was set to 15 mm/minute. Each specimen was pulled until failure while data was collected by a computer acquisition system. The measured Young's Modulus of pure PDMS was found to be 0.59 Mpa, which lies well within the range of earlier reported values of 0.36-0.87Mpa. Figure 33 shows results of Young's Modulus for all fabricated nanocomposites. The Young's Modulus increases with increasing wt.% of nickel nanoparticles in the PDMS matrix. Thus, doping the PDMS with nickel nanoparticles results in materials with higher Young's Modulus. However, after 60 wt. % the nanocomposite could not be easily micromolded because of increased viscosity at high fill levels. It was observed that the Young Modulus's is an approximately linear function of filler loading up to 50 wt%, and can be particularly enhanced. The curve levels off slightly above 50 wt%, although still increases. The results obtained are in accordance with the experimental values previously reported by other

researchers on nanocomposite polymers doped with 200nm silver nano composites previously reported [106].

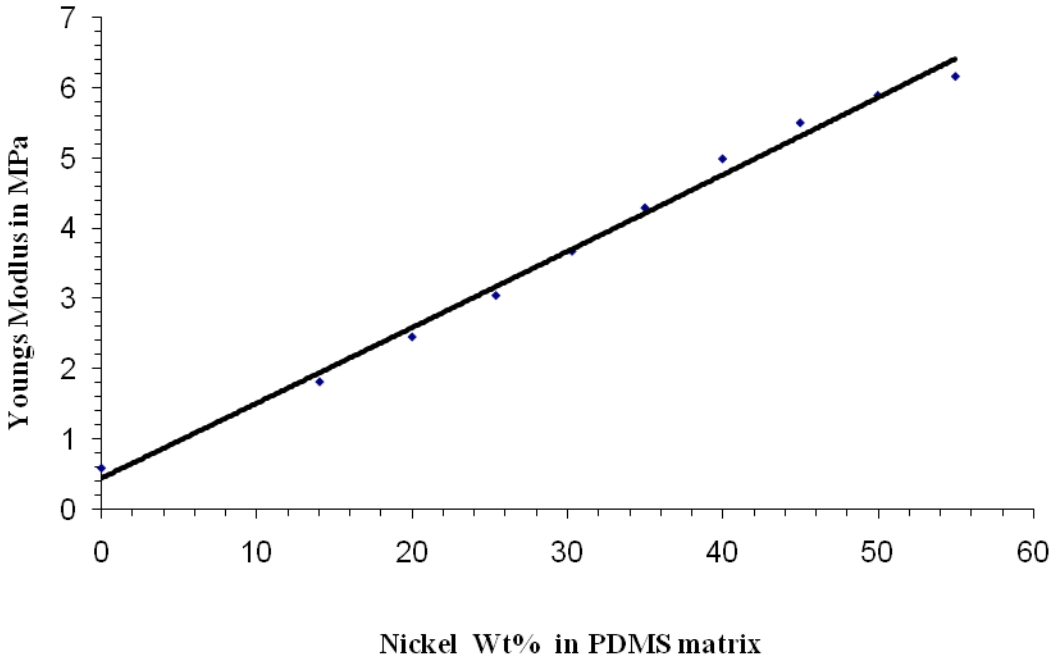

Figure 33 Young Modulus's versus nickel weight percentage (Wt%) in PDMS matrix

Electrical characterization

The direct current (DC) electrical properties of 10 mm x 5mm x 1mm films of the Ni-PDMS nanocomposite were measure using an HP3748A digital multimeter, which was set to operate in a four probe mode to eliminate the contact resistance as previously described. Figure 34 shows the resulting resistivity of nickel nanoparticle doped PDMS with varying weight percentage. It

can be clearly seen that the resistivity decreases with increasing nickel nanoparticle weight percentage. It is observed that up to 40 weight percent the resistivity decreases slowly. However, after this point, which is the percolation threshold, the resistivity decreases rapidly and can be explained in terms of percolation theory. At lower concentrations the nickel nanoparticle percolation paths are not set up and as the concentration is increased the percolation paths are set up by the conducting nickel nanoparticles. At this point the nickel nanoparticles control the conductivity of the nanocomposite. The percolation threshold was observed to be equal to 41 wt% for the Ni-PDMS nanocomposite.

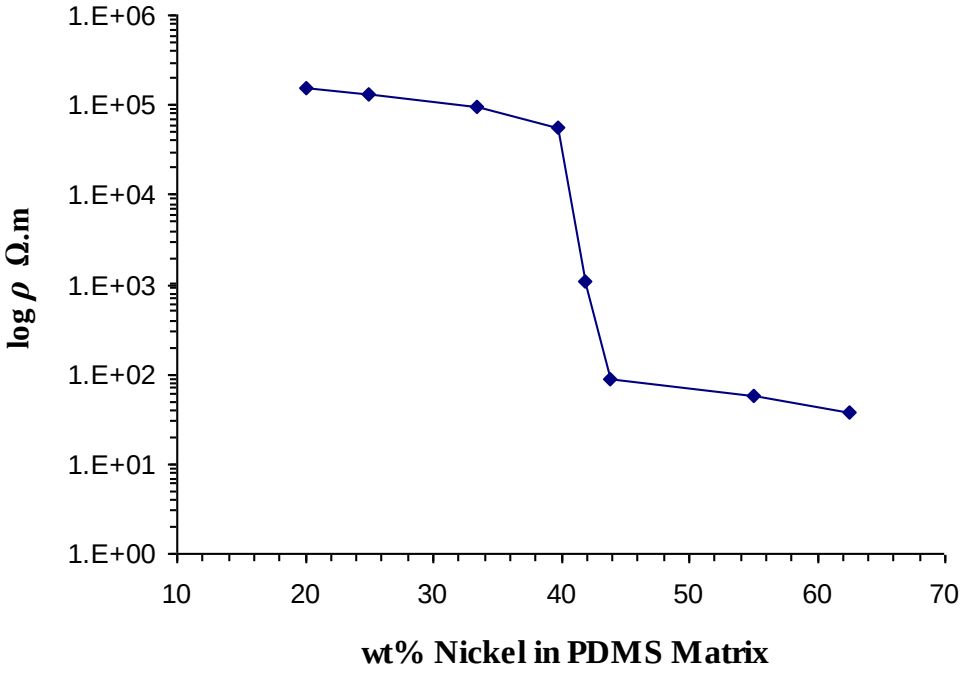

Figure 34 Resisitivity versus nickel wt. % in PDMS matrix.

Summary

The electrical, magnetic and mechanical properties of micropatternable nickel nanoparticle (30-50nm) doped polydimethylsiloxane have been characterized as a function of weight percentage of nickel nanoparticles in the PDMS matrix. It is observed that a percolation threshold occurs at approximately 41 weight percentage and the highest saturation magnetization occurs at 45.2 weight percentage. It was also observed that beyond 60 weight percentage, the nanocomposite becomes difficult to micropattern. The fabricated nanocomposite has superior mechanical properties, with a higher Young's Modulus than undoped PDMS; the relationship between Young's Modulus and nanoparticle doping was found to be approximately linear. We have been successfully able to micromold the prepared 89anocomposite down to features sizes of 20μm (limited by the photomask resolution limit), using a fabrication process similar to unfilled PDMS. The multifunction material can be not only used to solve the signal routing problem in μTAS but also shows promise as a magnetically actuated material for fluid control components such as microvalves and pumps. Further work will involve incorporating this novel material in developing microheaters, microvalves and micropumps for all polymer in lab on a chip devices.

5.4 NdFeB-PDMS and micromagnet testing

Micromagnets characterization

The magnetic-PDMS composite with 75 weight percentage on NdFeB in PDMS matrix was fabricated as defined in chapter 3 and disc magnets 50 micron in diameter and 30 micron in height were fabricate via the process defined in chapter 3, section 3.3. The magnetic properties of the micromolded permanent magnets shown in figure 35(a) were measured using a Quantum Design MPMS-XL-7S SQUID magnetometer. A typical coercivity (H_c) and remanent magnetization (M_r) hysteresis loop at 300 K between -20 kOe and +20 kOeis shown in figure 35(b). The hysteresis loop was found to be quite reproducible; different samples from the same magnetic polymer batch did not show much variation (Table 4), indicating that the MQFP particles were homogenously dispersed in the PDMS matrix for all samples. The coercivity, H_{ci}, was 5260 ± 30 Oe, confirming that the property of the magnetic powder was unchanged upon micromolding into the composite material since the pure 5 micron NdFeB powder (without polymer matrix) has an H_{ci} = 5325 Oe. The pure powder also has a remanent magnetization, M_r = 80.68 emu/g, whereas the remanent magnetization of the 75 wt% micromolded permanent magnets, M_r, was 60.10 emu/g on average verifying the 75 wt.% of the magnetic powder into the micromolded permanent magnets, hence uniform dispersion.

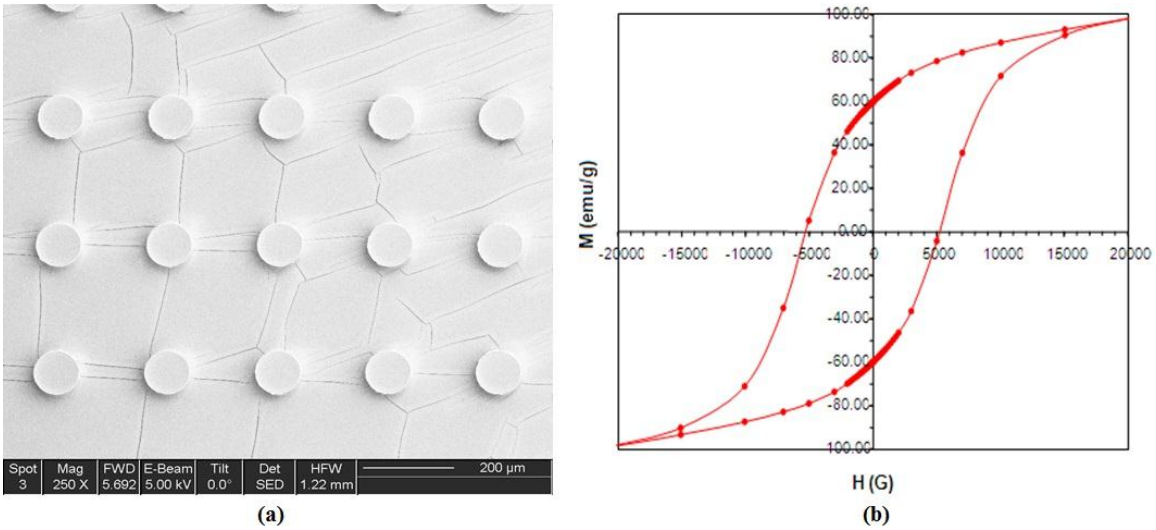

Figure 35 a) SEM micrograph of an array of micromolded magnets and b) typical remanent magnetization (M) vs. coercitvity (H) hysteresis loop of a micromagnetic polymer sample at 300 K

Table 5[17] Coercivity (Hc) and remanent magnetization (Mr) of five different 50µm, height 30µm micromolded magnet samples.

Magnet	1	2	3	4	5	Average +/- one standard deviation
H_c (G)	5245	5280	5260	5290	5225	5260 +/- 23.4
M_r (emu/g)	59.64	65.19	58.91	57.17	59.61	59.7 +/- 2.7

[17]It should be noted that these calculations in Table 5, do not take in to account self demagnitzation of the tested micromagnets or samples.

Summary

We have successfully fabricated, polydimethylsiloxane bonded, permanent disc magnets via soft lithography with a diameter of 50μm, height of 30μm, by ultrasonically agitating MQFP-12-5 powder in an uncured polymer matrix. All the fabricated micromagnets from the same magnetic composite show similar magnetic properties, suggesting that the dispersion of MQFP-12-5 in the PDMS matrix is homogeneous. The micro magnets show average remanent magnetization (M_r) of 60.10 emu/g and coercivity (H_{ci}) of 5260Oe at 75 weight percentage of magnetic powder in PDMS matrix, with standard deviations of 2.7 and 23.4 respectively. Further work will involve integration of these developed micromagnets in micro pumps, valves, micromotors and generators for MEMS and microfluidic applications on flexible PDMS, investigation of other sizes and materials for magnetic particle, and investigation of other flexible polymer matricies.

5.5 Summary table for properties of multifunctional Nanocomposites

The following tables summarize the properties of the nanocomposite polymers developed for this thesis.

Table 6 Multifunctional nanocomposite polymers & properties

Multifunctional nanocomposite polymers & properties				
Nanocomposites **Properties**	**MWCNT-PDMS**	**Ag-n PDMS**	**Ni-PDMS**	**MQFP-5 PDMS (NdFeB)**
Resistivity	0.62 Ω-m	2.3×10^{-5} Ω-m	5.9×10^{-3} Ω-m	✘
Percolation threshold	1.5 wt.%	32 wt.%	41.5 wt.%	✘
Dispersion technique	Organic solvent assisted	Organic solvent assisted	Organic solvent assisted	No organic solvents required
Remanent magnetization (Mr)	✘	✘	✘	60.10 emu/g (@ 75 wt.%)
Saturation magnetization (Msat)	✘	✘	21.0 emu/g (@41.5 wt.%)	✘
Micromolding	✓	✓	✓	✓
Repeatability	✓	✓	✓	✓
NTCR	✓	✘	✘	✘

Table 7 Comparison of electrical resistivity of bulk elements verses nanocomposites

#	Element	Bulk: electrical resistivity Ω-m	Nanocomposite: electrically resistivity Ω-m
1	Silver	1.59×10^{-8}	1.59×10^{-8} @50 wt.% (Particle Size: 80-500nm)
2	Carbon	5×10^{-4} to 8×10^{-4}	0.62 @ 22 wt.% MWCNT size:outer diameter of 10nm and length of 30μm
3	Nickel	6.99×10^{-8}	5.9×10^{-3} @ 60 wt. % Particle Size: 30-50nm

CHAPTER 6: FUTURE WORK AND CONCLUSION

6.1 Future work

In the course of the work described in the thesis, several possible improvements were identified for future work.

Feature size

It is important to determine thesmallest feature size, aspect ratio, and resolution, of the fabricated nanocomposites. This is highly dependent on the nanoparticle size used to fabricate the nanocomposites and also how well we are able to fabricate the micro- or nano- mold. However, it has been reported that unfilled PDMS has been micromolded with features smaller than 50 nm, so we expect that our nanomaterials may be employed for features less than one micrometer, provided sufficiently small nanoparticles used .

PMMA etching improvements

Improving PMMA laser ablation is critical as it can be seenfrom figure 19 that etched PMMA has a V-groove profile. Processes need to be developed in order to reduce or eliminate this profile. Initial experiments carried out to reduce the V groove are promising. An exposure to flame for 30 seconds, which is a combination of nitrogen and oxygen, tends to reduce and smoothens the V-

groove profile. However, this process needs to be characterized.DEEP UV patterning is a promising technique for micromolding nanocomposites. However, further experimentation is needed in order to determine if submicron or nano features can be achieved through this process.

Cyclic olefin copolymer as structural mold material

Commercial grade cyclic olefin copolymer (COC)has the potential to be explored as a new micromold material because of its better chemical resistant properties as compared to PMMA. However, laser ablation is possible but other technique such as UV lithography needs to be explored.

Other microfabrication techniques

Screen-printingis being explored as a new low cost microfabrication technique for micropatterning nanocomposites. Our initial results show that these nanocomposites can be fabricated on substrates such as kapton, fabrics, PDMS, PMMA etc. However, further experimentation is required to determine the minimum feature size, whichcan be obtained by screen-printing for the nanocomposites. Also, the long working time needed to keep screens clear of cured material limits the potential thermosetting polymer ratios and types, which also needs to be optimized. Furthermore, nanoimprint lithography also needs to be explored for the developed nanocomposites.

Device fabrication

Work is under progress in order to build sequential layers for electronic routing for multilayer lab on a chip devices using the developed electrically

conducting nanocomposites.Also, work is being carried out in order to characterize and integrate MWCNT-PDMS nanocomposite polymer to develop on-chip temperature sensors for MEMS and microfluidic applications.

Daniel Hilbich, and Mona Rabar at Microinstrumentation Laboratory at SFU are carrying out integration of the developed magnetic materials, to fabricate micromagnets for micropumps and valves. Applications such as, micromotors, and generators for MEMS and microfluidic applications are also worth exploring.

6.2 Contributions

This work has resulted in a number of publications and patents. The “Preparation, characterization and micromolding of multi-walled carbon nanotube polydimethylsiloxane conducting nanocomposite polymer” published in materials letters has been cited over 24 times since February 2009. It was also rated among top 25 papers for the year 2009. The work done on multifunctional nanocomposites has resulted in 3 patents, over 40 papers and not only attracted industrial collaborations such as Magnequench Inc, Job Mastermagnets, McKesson, Timkin Corporation, Design sportswear, Montreal Woollens, Pinnacle consultancy, BJA enterprise, Lululemon etc., but also has brought in money and support from industry.

Furthermore, many of the multifunctional nanocomposite polymers described in this thesis are now being used by other researchers at SFU, in development of microstructures and systems as part of their own thesis works

and being presented at prestigious international conferences. Thus, the materials and techniques described here-in are already in use within SFU and elsewhere such as University of Waterloo, Ontario and University of Concordia, Montreal; showing widespread applicability to the field of soft-MEMS research.

The quality of the research work done on multifunctional nanocomposites, has resulted in the author's nomination to the Executive Committee of Electro-Chemical Society- Sensor Division, as well as to that of the SPIE Smart Structures and Materials, even though the author is still a student.The author has been Invited 7 times to present his research work on multifunctional nanocomposite polymers, at various renowned institutions and conferences, including, Lawrence Berkeley National Laboratory, the U.S. Department of Energy, Berkeley, California (April 2011); McGill University and Concordia University, Montreal; the University of South Florida and the SPIE conference on Smart Structures and Materials (March 2011).A part of this work has also led to an invited journal paper, "Preparation, Micro-Patterning and Electrical Characterization of Functionalized Carbon-Nanotube Polydimethylsiloxane Nanocomposite Polymer", Macromolecular Symposia: Special Issue: Polymers and Organic Chemistry, Volume 297, Issue 1, pages 210–218, November-2010. A second invited journal paper is under preparation on "Micromagnets and medicine" to be submitted to the Journal of Nanotechnology in Engineering and Medicine, American Society of Mechanical Engineers. The author is humbled by and grateful for this recognition, but also excited that his work is generating such international interest in a variety of technical societies, industry, and laboratories.

6.3 Conclusion

This thesis has described a general preparation, characterization and fabrication process for various PDMS based nanoparticle doped multifunctional nanocomposite polymers. These developed nanocomposite polymers allows manufacture of flexible PDMS based active microfluidics and MEMS devices. Four different types of PDMS based multifunctional nanocomposite polymers have been developed, containing the following particles; 1) multi walled carbon nanotubes, 2) silver, 3) nickel, 4) NdFeB. We have successfully demonstrated integration and micropatterning of the developed multifunctional nanocomposite polymers (electrically conductive and magnetic) structures in bulk PDMS. This is extremely important for signal routing, interfacing to signal processing electronics, for powering active devices, and actuation purposes. A new hybrid microfabrication process is also for the first time demonstrated for combining micromolded nanocomposite with undoped PDMS polymer.

Poly(methyl methacrylate) (PMMA) is also explored as a new molding substrate, as opposed to SU-8. PMMA offers high chemical resistance as compared to SU-8. This is important because one of the processing steps involved in fabrication includes using organic solvents such as heptane. SU-8 is venerable to organic solvents, which results in stiction of nano composites to the mold and SU-8 swelling. We have described two different processes for micromachining PMMA, DEEP UV photolithography and CO_2 laser ablation. We have successfully demonstrated that PMMA can be used for small and large area

microfabrication such that 12 inch by 24inch flexible sheets containing active nanoomposite polymer devices can be realized on a large scale.

We have demonstrated use of these new developed PDMS based nanocomposite polymers, hybrid microfabrication process in order to fabricate microelectrodes, ribbon cables and permanent micromagnets as example devices. A summary of the properties of the developed nanocomposites is shown in table 6, chapter 5, and section 5.5.

Adopting the processes described in this thesis lead to development of flexible microfluidics and MEMS.

APPENDICES

Appendix 1 Positive mask layout for electrodes fabricated in figures 13 and 32

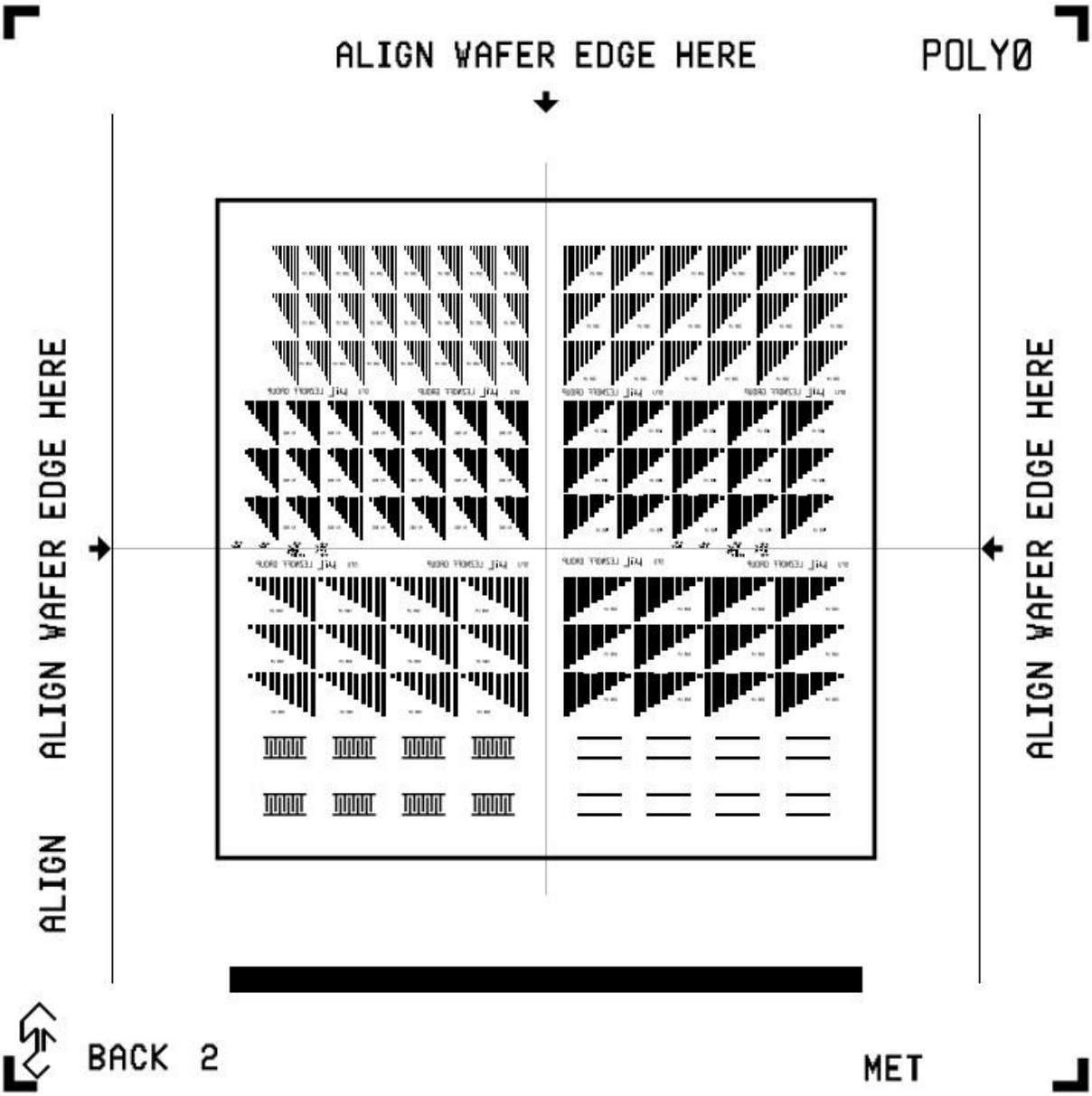

Appendix 2 Negative mask layout for electrodes fabricated in figures 13 and 32

Appendix 3 Layout of .cdr file for CO_2 laser ablation of 12inch x 24 inch large scale PMMA micromold

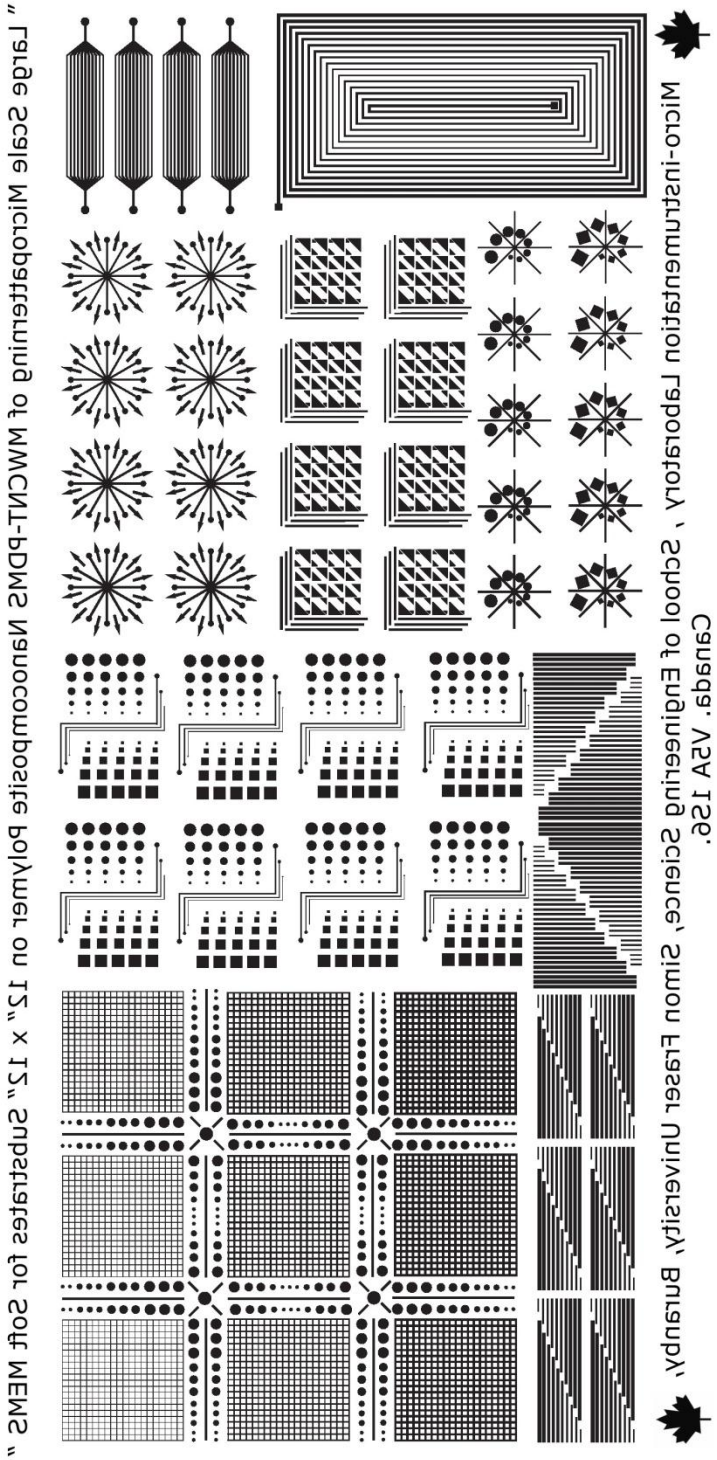

Appendix 4 Layout of .cdr file for CO_2 laser ablation of PMMA micromold for ribbon cables

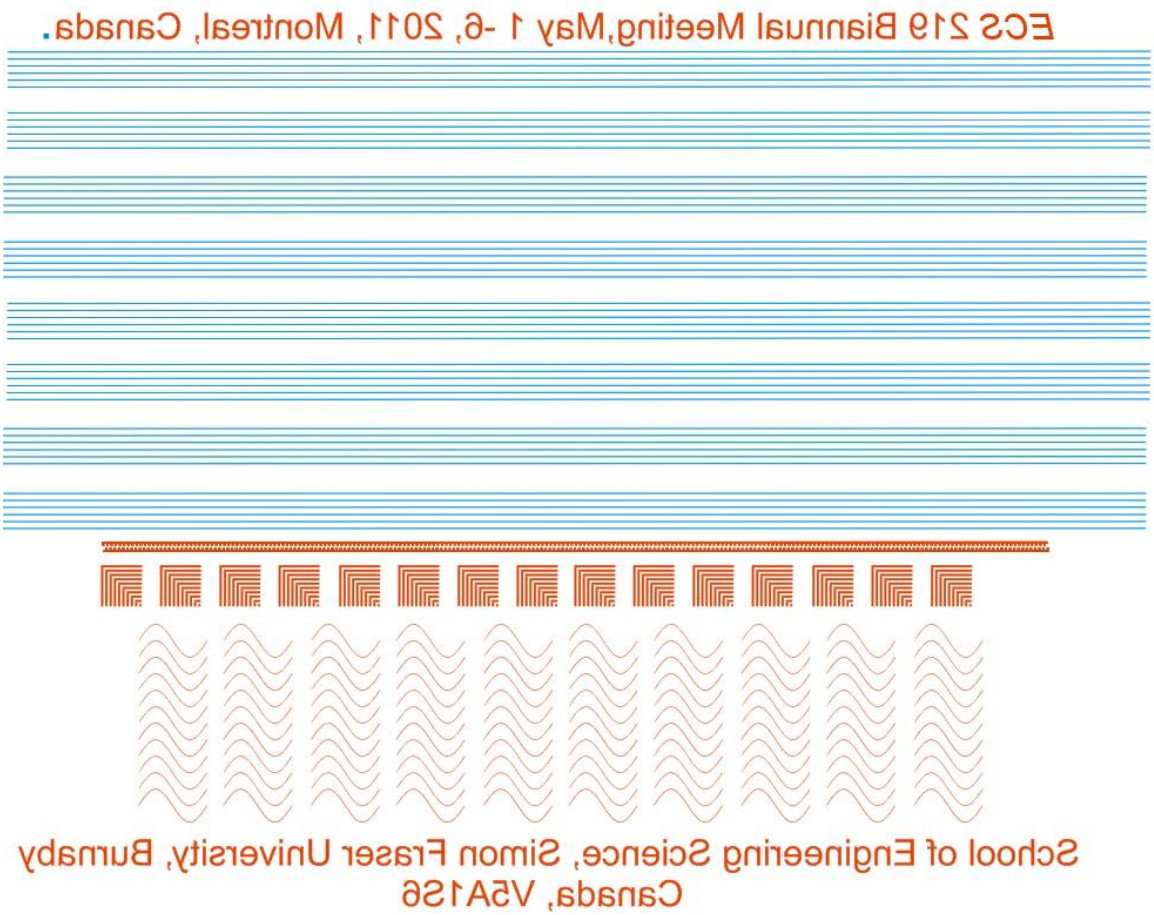

Appendix 5 RCA run sheet: cleaning Silicon and glass substrates

PROCESS BATCH SHEET (RCA clean, mod'd for oxidized wafers) **Iss 7** **Pg____of____**

ENSC Batch No._____Wafers Started_____Date_____
Material_____Orientation_____Size_____Thickness_____
Resistivity_____Type_____
Wafer Vendor_____Vendor Batch #_____SFU P.O._____

Process Step #	Process Conditions	Oper & Wafer #	Comments
_____A	**RCA SC-1 Clean (Organics)** Temp = 80 +/- 5C Time = 10 minutes DI H2O 5 parts (1000mL) NH4OH, 30% 1 part (200 mL) H2O2, 50% 1 part (200 mL)* *Volumes are sufficient to cover 8 wafers in dippers in 2000 mL glass beaker, major flats up.		Hydrate wafers in DI water before placing in SC-1. Heat water for SC-1. Add NH4OH and then H2O2. Stabilize temperature. Remove wafers from water, place in SC-1, and start timing if temp in range.
_____B	**DI Water Rinse** > 3 minutes in running DI water		
_____C	**HF Dip (Native Oxide Strip)** Temp = Room temp Time = 30 seconds DI H2O **100** parts (1600 mL)* HF **1** part (16 mL) *Volumes sufficient to cover 8 wafers in dippers in a 2 L plastic beaker, major flats up.		This is the modified step. Either leave out this step completely or reduce concentration from 10:1 to 100:1 as shown.
_____D	**DI Water Rinse** > 3 minutes in running DI water		
_____E	**RCA SC-2 Clean (Metals)** Temp = 80 +/- 5C Time = 10 minutes DI H2O 6 parts (1050 mL) HCl 1 part (175 mL) H2O2 1 part (175 mL)* *Volumes for 2 L glass beaker		Heat the water. Add HCl and then H2O2. Note that the addition of the HCl can raise the temperature of the solution significantly. Stabilize the temperature. Remove wafers from rinse, place in SC-2, and start timing if temp in range.
_____F	**DI Water Dump Rinse** > 5 min in beaker of running DI H2O. Dump H2O. Repeat twice		
_____G	**Spin Dry** Spin at max RPM until dry (false colours disappear). Check for water on back. Repeat spin or blow with dry N2 if needed.		

Appendix 6 Thick SU8 100 processing parameters

1. **Clean Glass Slide:**
    - Wash with soap, rinse with water (4 times). Use Decon 90 microclean solution.
    - Rinse with Acetone, IPA and DI Water
    - Blow dry using nitrogen Gun.
    - Prebake 120 ^{o}C for 20 minutes
    - Cool down at room temperature.

   Or Perform RCA clean

2. **SU8 Adhesion layer:**
    - Sputter chrome ~5nm (there are other ways to do it eg. Omnicoat)

3. **SU8-100 layer**:
    - Spin coat @1250 rpm (75 seconds).
    - Wait for 5 minutes before baking

4. **Soft Bake (Remove Solvents):** Use Hotplate
    - Start 50 ^{o}C for 5 minutes
    - Prebake* 65 ^{o}C 20 minutes
    - Softbake90 ^{o}C for 60minutes
    - Cool/ramp down 50 ^{o}C for 10 minutes.

*If excessive bubbling occurs at 65 ^{o}C ramp soft bake step75C for 1 hour.

5. **Align & Expose:** (MASK)
    - Time 52 seconds

6. **Post Exposure Bake (PEB):** for full cross-linking. (use hotplate)
    - Start 50 ^{o}C for 5 minutes
    - Post Exposure Bake 65 ^{o}C 32 minutes (ramp hotplate at 40C/hr)
    - Raise the temperature to 80 ^{o}C for 10 minutes. If you see wrinkles, drop the temperature to 65 ^{o}C
    - Cool to room temperature.
    - Perform a pin prick test.
7. **Develop:** Use SU8 developer , develop to end point.
8. **IPA Rinse:** Soak in IPA, Agitate well. If white film is apparent develop for some more time.
9. **Dry:** Using nitrogen gun.
10. **Inspect:** Use microscope with yellow light look for cracking, white film etc.

Comments:

Appendix 7 Commercial Plexiglass mirrors and MEMS: New approach toward low cost polymer microsystems

This extra chapter describes a new approach to fabricate low cost metallization on PMMA substrates based on commercially available Mirrored-Extruded Acrylic (mirrored Plexiglass / mirrored PMMA). The patterned metal could be subsequently employed as a mask for deep-UV PMMA micropatterning of polymer-MEMS devices. The process presented eliminates the use of sputtered metals and can be scaled up to substrates of sizes 12 inch x 24 inch or larger for batch fabrication. Mirrored Extruded Acrylic has a coating of 6 micron thick vacuum metalized aluminum or copper with an adhesive backing. We have discovered that the adhesive backing can be easily etched away by using ethanol, exposing the aluminum or copper, which can be micropatterned by standard photolithographic processes. We have fabricated various microstructures in aluminum, including microelectrodes and Van de Paw structures. Resistivity measurements show that the resistivity of the micro-machined aluminum is equal to lower than 4.8×10^{-6} Ω-m, which is sufficient for sensor electrodes or signal routing applications for MEMS/ MST devices.

Introduction

Over the last two decades, micro total analysis system (μ-TAS) devices have been investigated by many researchers world wide. Many materials have been employed to fabricate such devices, with some of the most common materials being glass, polydimethyalsiloxane (PDMS), SU-8, Cyclic Olefin

Copolymer (COC) and poly(methyl methacrylate) (PMMA). Typical fabrication methods involve using relatively expensive techniques and equipment such as photolithography, x-ray lithography, injection molding and hot embossing [107].

PMMA has a great potential to be used for μ-TAS devices because of it low cost, biocompatibility, chemical inertness and optical properties [108]. PMMA is a commonly used polymer in MEMS and microfluidics [109, 110]. However, typical PMMA processing involves hot embossing using relatively expensive equipment. Thus, there is great incentive to develop low cost micromachining processes for PMMA. Marius, et. al., showed low cost micromachining of commercial grade PMMA by deep UV radiation [111]. However, a hard mask was required which involved sputtering of gold and then micropatterning it.

This paper presents a new approach to fabricate low cost metallization on PMMA substrates based on commercially available Mirrored-Extruded Acrylic (mirrored Plexiglass / mirrored PMMA). The patterned metal could be subsequently employed as a mask for deep-UV PMMA micropatterning of polymer-MEMS devices. Our technique eliminates the need for metal sputtering and is scalable up to substrates as large as 24 x 24 inch. Furthermore, the metal is thicker than conventionally deposited metal and similar in thickness to electroplated metal, making it an excellent mask for deep UV patterning of PMMA microstructures. The patterned metal can be additionally employed for signal routing purposes, or for integrated microelectrodes or microcoils. Large scale machining of these mirrors is also possible for EMI shielding purposes for aerospace applications [112].

Experimental

Micromachining Mirrored-Extruded Acrylic

The commercially available acrylic mirrors have a coating of 6 micron thick vacuum metalized aluminum with an adhesive backing. Mirrored-Extruded Acrylic sheets 12 inch x 24 inch in size were diced in to 4 inch circular substrates using a Universal Versa laser system in order to fit into our photolithographic aligner. Mirrored-Extruded Acrylic was bought from Industrial Plastics and Paints Inc., Canada. Shipley 1813 photoresist was bought from MicroChem, USA.

The first task was to etch the adhesive backing in order to expose the aluminum. We found that ethanol was the perfect solvent for this purpose. The substrates were dipped in ethanol and the adhesive backing was completely removed after 20 minutes. The adhesive backing swells and is easily peeled off from the substrate exposing the aluminum coating. This step was followed by rinsing the substrate with IPA, DI water and blow drying using nitrogen. A dehydration bake was performed for 45 minutes at 70 ^{o}C. The substrates were then cooled down to room temperature. We note that it is important not to raise the temperature above 70 ^{o}C as after this temperature the substrate starts to deform. Shipley 1813 photoresist was spin coated at 5000 rpm on the cooled down dehydrated substrate and baked for 6 minutes at 70 ^{o}C. The substrate was aligned and exposed using a mask aligner and the desired micropatterns transferred to the photoresist. The metal patterning was then accomplished using wet chemical etching using Aluminum Etchant type A manufactured by

TranseneCompany Inc USA. The substrate was dipped in the aluminum etchant which was heated to a temperature of 50^0C. It was observed that the time required to etch the 6µm thick aluminum was 74 seconds. The fabrication process steps are shown in figure 36. It should be noted that acetone should not be used at any step of the fabrication process as PMMA is vulnerable to acetone. This is the reason that after micromachining of aluminum we flood expose the substrate and develop it again in MF Developer in order to remove the photoresist on the micromachined aluminum structures. The smallest feature size achievable using our process was 5 microns. Figure 37 shows some resulting fabricated aluminum micro-structures.

Electrical properties

Eelectrodes with varying widths from 200 µm to 600 µm, in increments of 100 µm were fabricated. The lengths varied from 500 µm to 5000 µm, in increments of 500 µm. We employed a two point probe method in order test the electrical properties of the fabricated electrodes. The heads of the probes were placed and positioned as near to the edges of each rectangular structure as possible; the purpose of this was to ensure that the length dependence of resistance was mapped/measured as accurately as possible. Care was taken to avoid damaging the structures with the sharp multi-tester head by limiting the pressure applied to the probe on the structure. This method of testing was repeated over all groups/groupings of electrodes present on the substrate. All lengths, widths and heights of electrodes were measured using a digital caliper and micrometer, respectively, both accurate up to 3 decimal places. Our

experiments showed that the resistance increases as length increases, as expected. Resistance also increased as width decreased. The data shows a resistivity for the aluminum ranging from 3.60 X 10^{-6} to 4.45 X 10^{-6}. This compares to pure aluminum with a resistivity of 2.62 x 10^{-8} [113].

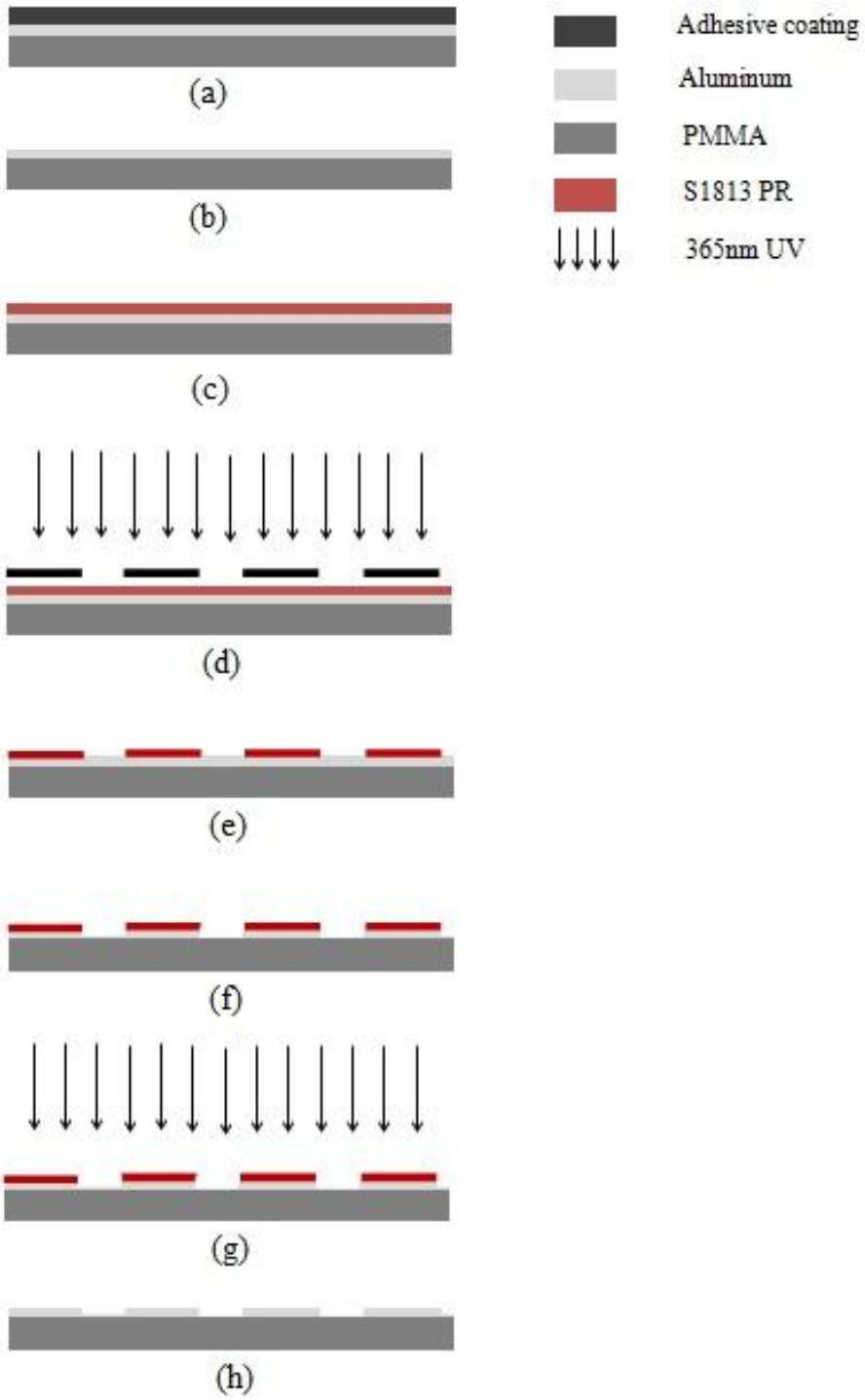

Figure 36 Fabrication flow for micromachining Mirrored-Extruded Acrylic metal

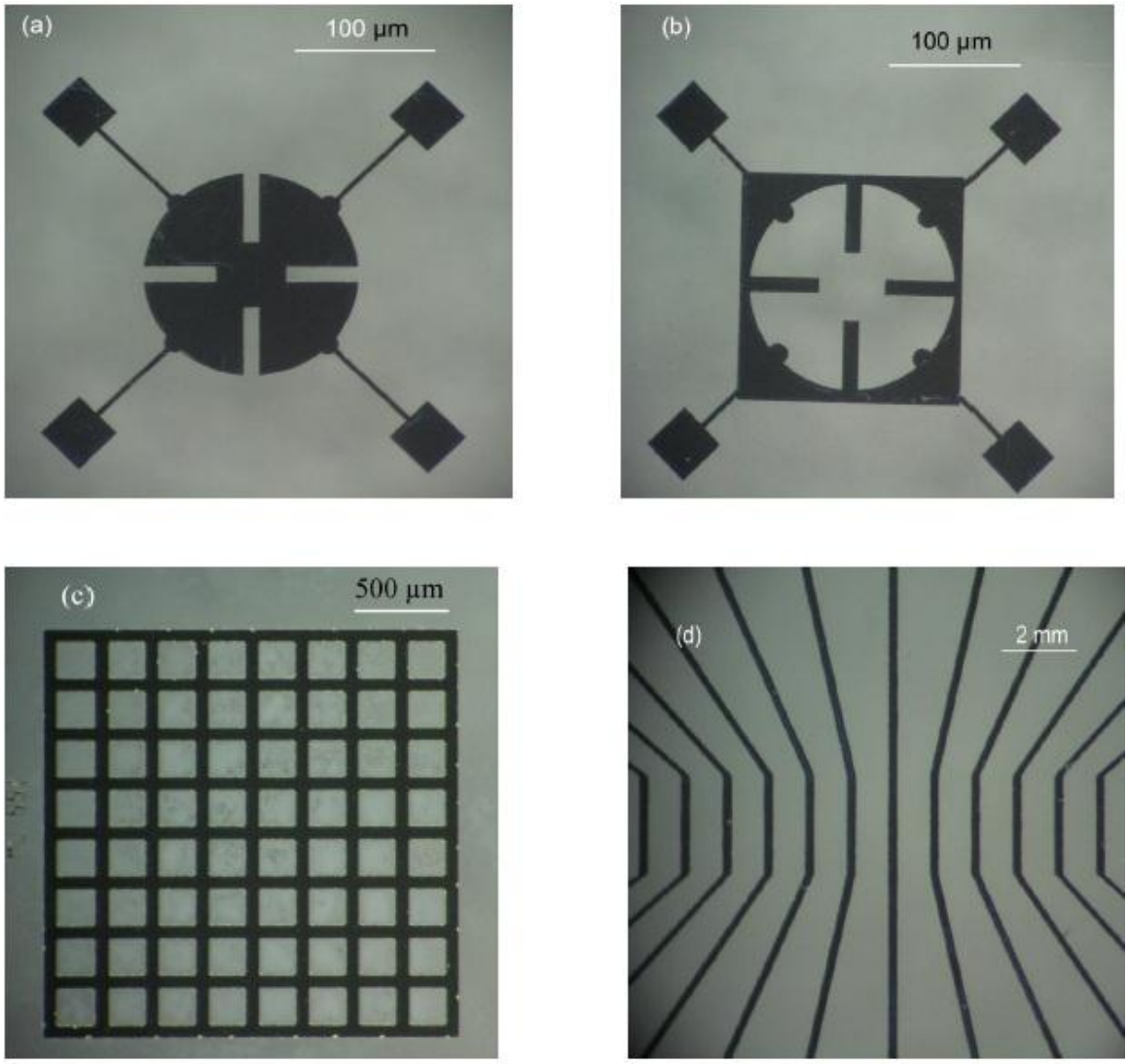

Figure 37 Micrographs of micromachined extruded mirrored acrylic aluminium.

Summary

In this work,we have presented a new approach to fabricate low cost PMMA MEMS devices based on commercially available Mirrored-Extruded Acrylic (mirrored Plexiglass / mirrored PMMA) mirrors. The process that we have presented eliminates the use of sputtered metals and can be scaled up to substrates of 12 inch x 24 inch or larger. The metal already present on extruded mirrored acrylic is micro-patterned by standard photolithographic processes. The patterned metal could be subsequently employed as a mask for deep-UV PMMA micropatterning of polymer-MEMS devices [114]. We have fabricated various microstructures in aluminum, including microelectrodes and Van de Paw structures. Electrical measurements show that the resistivity of the micro-machined aluminum is equal to lower than 4.8×10^{-6} Ω-m, which is sufficient for sensor electrodes or signal routing applications for MEMS/ MST devices.

REFERENCE LIST

[1] http://www.nanowerk.com/nanotechnology/introduction/introduction_to_nanotechnology_1.html (Date accessed: 8/14/20011)

[2] Guozhong Cao, “Nanostructures & Nanomaterials: Synthesis, Properties & Applications”, chapter 1,Imperial College Press; 1 edition (April 30, 2004), ISBN-10: 1860944809, ISBN-13: 978-1860944802

[3] http://biomedthai.blogspot.com/2009/06/what-is-nanotechnology3.html (Date accessed: 8/14/20011)

[4] http://www.nano.org.uk/news/293/, (Date accessed: 8/14/20011)

[5] http://www.tahan.com/charlie/nanosociety/course201/nanos/MP.pdf (Date accessed: 8/14/20011)

[6] http://www.nanosysinc.com/what_we_do/led_backlighting/ (Date accessed: 8/14/20011)

[7] http://cientifica.eu/blog/white-papers/nanotechcleantech/ (Date accessed: 8/14/20011)

[8] http://ge.geglobalresearch.com/blog/creating-anti-icing-surfaces/ (Date accessed: 8/14/20011)

[9] Ramsey M.Stevens,Cattien V. Nguyen,andM.Meyyappan, "Carbon Nanotube Scanning Probe for Imaging in Aqueous Environment" IEEE transactions on Nanobioscience,Vol.3, No.1,March 2004

[10] http://www.gizmag.com/go/5192/ (Date accessed: 8/14/20011)

[11] http://www.nanowerk.com/news/newsid=6258.php (Date accessed: 8/14/20011)

[12] Chang Gyuhwang, "Nanotechnology Enables a New Memory Growth Model" Proceedings of the IEEE,Vol.91,No.11,November 2003

[13] http://www.appliednanotech.net/tech/cnt_displays.php (Date accessed: 8/14/20011)

[14] http://www.freewebs.com/jayaramco/doc/Selected_Appz_of_Nanotechnology_in_Textiles.pdf

[15] http://www.tahan.com/charlie/nanosociety/course201/nanos/AJ.pdf

[16] http://ammtiac.alionscience.com/pdf/AMPQ6_1ART03.pdf
(Date accessed: 8/14/20011)

[17] ShuPeng, James O'Keeffe, Chengyu Wei, K. Cho, "Carbon Nanotube Chemical and Mechanical Sensors".Conference Paper for the 3rd International Workshop on Structural Health Monitoring

[18] http://hansmalab.physics.ucsb.edu/phys150/nanotech.pdf
(Date accessed: 8/14/20011)

[19] http://www.nanocompositech.com/review-nanocomposite.htm
(Date accessed: 8/14/20011)

[20] RupaliGangopadhyay and Amitabha De, “Conducting Polymer Nanocomposites: A Brief Overview”, Chem. Mater., 2000, 12 (3), pp 608–622

[21] RabihZaouk, Benjamin Y. Park and Marc J. Madou, “Microfluidic Techniques: Introduction to Microfabrication Techniques”, Volume 32, ISSN 1064-3745, 2008

[22] Xia Younan, Whitesides George M.; Annu Rev Mater Sci 1998; Vol 28: Pages153–84

[23] Masayuki Matsubara, Kenji Chayama, Joji Urakawa, Yasuhiko Shibutani, Yoshihide Tanaka, Sahori Takeda and Shinichi Wakida;. In: Atmospheric and Biological Environmental Monitoring, Pages 275-284, Edition 1, Year 2009, Springer Netherlands, ISBN 978-1-4020-9673-0 (Print)

[24] B. Xu, F. Arias, S. T. Brittain, X.-M. Zhao, B. Grzybowski, S. Torquato, G. M. Whitesides Advanced Materials Oct 1999, Volume 11 Issue 14, Pages 1186 – 1189

[25] Hidenori Nagai et. al. in: Atmospheric and Biological Environmental Monitoring, Pages 275-284, Edition 1, Year 2009, Springer Netherlands, ISBN 978-1-4020-9673-0 (Print)

[26] J. El-Ali, I.R. Perch-Nielsen, C.R. Poulsen, D.D. Bang, P. Telleman, A.Wolff; Sensors and Actuators A, Volume 110 (2004), Pages 3–10

[27] Suyan Xiao, Lu fengChe, XinxinLi,Yuelin Wang, Microelectronics Journal, Volume 38 (2007), Pages 360–364

[28] Carbon Nanotubes: Basic Concepts and Physical Properties, 2004, WILEY-VCH, Verlng GmbH & Co. KGaA

[29] J. Lu , M. Lu , A. Bermak, Y.-K. Lee, , Proceedings of the 7th IEEE International Conference on Nanotechnology, Hong Kong, (August 2 - 5, 2007) 1240-1243.

[30] C. Liu, Mater. Res. Soc. Symp. Proc., 947 (2007) A07-01.

[31] J. Engel, J. Chen, N. Chen, S. Pandya, C. Liu, 19th IEEE International Conference on Micro Electro Mechanical Systems, Istanbul., (2006)

[32] A. Khosla and B.L. Gray, Materials Letters Volume 63, Issues 13-14, 31 May 2009, Pages 1203-1206

[33] Guan Wang, Zhongkui Tan, Xueqing Liu, Vladimir Samuilov, and Michael Dudley, Mater. Res. Soc. Symp. Proc. Vol. 963, 2007, pages 0963-Q20-24.

[34] http://www.azonano.com/details.asp?ArticleID=1563#1

[35] http://www1.dowcorning.com/DataFiles/090007c88020bcca.pdf

[36] T. Ueda, B.L. Gray, Yuchun Chen and Paul Li, Proceedings SPIE vol. 6886. January 2008

[37] Wen Dai, Kun Lian and WanjunWang;MicrosystTechnol Volume 11(2005), Pages 526–534

[38] S. M Westwood, S Jaffer, B. L Gray; J. Micromechanics Microengineering Vol. 18, 2008;Pages: 064014

[39] B.J.Last and D.J. Thouless, Phys Rev Lett 27 (1971), Pages.1719–1721.

[40] D. Stauffer, A. Aharony, Introduction to percolation theory, 2nded., Philadelphia, Taylor and Francis, 1994

[41] Moonho Lee Mina Yoo Sensors, 2002. Proceedings of IEEE Volume: 1, Pages: 56- 61

[42] H. Sato and M. Sano; Colloids and Surfaces A: Physicochemical and Engineering Aspects Volume 322, Issues 1-3 (2008), Pages 103-107

[43] R. Andrews, D. Jacques, M. Minot, T. Rantell, Macromolecular Materials and Engineering, volume 287, Issue6, (2002) 287-395

[44] Y. A Kim, T Hayashi, Y Fukai, M Endo; Chemical Physics Letters, Volume. 355, issue 3-4, Pages 279-284

[45] M. Inyo, T. Tahara, T. Iwaki, F. Iskandar, C.-J. Hogan, Jr., and K. Okuyama, J. Colloid Interface Sci., Volume304 (2006), Pages 535–40

[46] S. V Ahir and E. M Terentjev, Polymeric Nanostructures and Their Applications; Chapter 3, Volume 1 (2006), Pages 1-48, ISBN:1-5888-068-3

[47] Cynthia A. Mitchell, Jeffrey L. Bahr, SivaramArepalli, James M. Tour, and RamananKrishnamoorti; Macromolecules, Volume35 (23)(2002,), Pages 8825–8830

[48] Jacob C. Kearns, Robert L. Shambaugh; Journal of Applied Polymer Science, Volume 86, Issue 8 (2002), Pages 2079-2084

[49] F. J. Fuchs, In 45th Annual Technical Conference of Society of.Vacuum Coaters ISSN 0737–5921, 64–67 (2002).

[50] K. L. Lu, M. Lago, Y. K. Chen, M. L. H. Green, P. J. F. HarrisS. C. Tsang; Carbon, Volume 34, Issue 6, 1996, Pages 814-816

[51] M. L Kovarik , S C Jacobson; Anal Chem Vol. 79 (2007), Pages 1655–60.

[52] N Pamme : Lab Chip, 2006, vol. 6, pages 24-38

[53] T. Speliotisa et al: Journal of Magnetism and Magnetic Materials 316, 2007, Pages 120–123

[54] P. Saravanan et al, Journal of Magnetism and Magnetic Materials 321 (2009), Pages 3138–3143.

[55] Naigang Wang et al: Journal of Applied Physics, 103, 07E109 (2008).

[56] B. M. Dutoit et al: Sensors and Actuators A: Physical Volume 77, Issue 3, 2 November 1999, Pages 178-182

[57] B. Pawlowskia et al :Journal of Magnetism and Magnetic Materials Volume 265, Issue 3, October 2003, Pages 337-344.

[58] A. Walthe et al: Journal of Magnetism and Magnetic Materials Volume 321, Issue 6, March 2009, Pages 590-594.

[59] O. Cugat et al: Sensors and Actuators A: Physical, Volume 129, Issues 1-2, 24 May 2006, Pages 265-269

[60] Younan Xia and George M. Whitesides, Annu Rev Mater Sci 28 (1998), pages 153–184

[61] A.J Gallant et al: Infrared and Millimeter Waves, 2007 and the 2007 15th International Conference on Terahertz Electronics. IRMMW-THz., vol., no2-., pp.982-983, Sept. 2007

[62] A. Khosla and B. L.Gray: Materials Letters Volume 63, Issues 13-14, 2009, Pages 1203-1206.

[63] http://www.magnequench.com/

[64] http://www.microchem.com/products/su_eight.htm
(Date accessed: 8/14/20011)

[65] Wen Dai, Kun Lian and WanjunWang;MicrosystTechnol Volume 11(2005), Pages 526–534

[66] Jacob C. Kearns, Robert L. Shambaugh; Journal of Applied Polymer Science, Volume 86, Issue 8 (2002), Pages 2079-2084

[67] Sandler, M.S.P. Shaffer, T. Prasse, W. Bauhofer, K. Schulte and A.H. Windle, Polymer 40 (1999), p. 5967.

[68] M.S.P. Shaffer and A.H. Windle, Adv Mater 11 (11) (1999), p. 938.

[69] Younan Xia and George M. Whitesides, Annu Rev Mater Sci 28 (1998), pp. 153–184.

[70] J.C. McDonald and G.M. Whitesides, Electrophoresis 21 (1) (2000), pp. 27–40. [12] Westwood S, Jaffer S, Gray BL. J. Micromech. Microeng. 18 064014, 2008 [9pp]

[71] http://www.microchem.com/products/su_eight.htm.

[72] B.J. Last and D.J. Thouless, Phys Rev Lett 27 (1971), pp. 1719–1721

[73] S. Jaffer and B.L. Gray, J Micromechanics Microengineering 18 (2008), p. 035043.

[74] S.M. Westwood, S. Jaffer and B.L. Gray, J Micromechanics Microengineering 18 (2008), p. 064014 (9 pp.)

[75] M.L. Kovarik and S.C. Jacobson, Anal Chem 79 (2007), pp. 1655–166

[76] Moonho Lee Mina Yoo Sensors, 2002. Proceedings of IEEE Volume: 1, Pages: 56- 61

[77] H. Sato and M. Sano; Colloids and Surfaces A: Physicochemical and Engineering Aspects Volume 322, Issues 1-3 (2008), Pages 103-107

[78] R. Andrews, D. Jacques, M. Minot, T. Rantell, Macromolecular Materials and Engineering, volume 287, Issue6, (2002) 287-395

[79] Y. A Kim, T Hayashi, Y Fukai, M Endo; Chemical Physics Letters, Volume. 355, issue 3-4, Pages 279-284

[80] M. Inyo, T. Tahara, T. Iwaki, F. Iskandar, C.-J. Hogan, Jr., and K. Okuyama, J. Colloid Interface Sci., Volume304 (2006), Pages 535–40

[81] S. V Ahir and E. M Terentjev, Polymeric Nanostructures and Their Applications; Chapter 3, Volume 1 (2006), Pages 1-48, ISBN:1-5888-068-3

[82] Cynthia A. Mitchell, Jeffrey L. Bahr, SivaramArepalli, James M. Tour, and RamananKrishnamoorti; Macromolecules, Volume35 (23)(2002,), Pages 8825–8830

[83] Jacob C. Kearns, Robert L. Shambaugh; Journal of Applied Polymer Science, Volume 86, Issue 8 (2002), Pages 2079-2088

[84] O. Rötting , W. Röpke, H. Becker and C. Gärtner, “Polymer microfabrication technologies”, Microsystem Technology Volume 8, Number 1, 32-36.

[85] H.M. Zidan and M. Abu-Elnader,“Structural and optical properties of pure PMMA and metal chloride-doped PMMA films”, Physica B: Condensed Matter Volume 355, Issues 1-4, 31 January 2005, Pages 308-317

[86] Feature sizes of 60 µm in the positive photoresist and 10 µm in the negative photoresist have been successfully achieved.

[87] Laurie Brown, Terry Koerner, J. Hugh Horton and Richard D. Oleschuk ," Fabrication and characterization of poly(methylmethacrylate) microfluidic devices bonded using surface modifications and solvents”, Lab Chip, 2006, 6, 66-73

[88] Marius Haiducu, M.ASc Thesis, “LOW COST MICROFLUIDICS ON COMMERCIAL GRADE POLY(METHYL METHACRYLATE) (PMMA) USING DEEP UV PATTERNING”. http://ir.lib.sfu.ca/dspace/bitstream/1892/11156/1/ETD4626.pdf

[89] http://www.tangram.co.uk/TI-Polymer-PMMA.html

[90] Serway, Raymond A. “Principles of Physics” (2nd ed ed.), (1998). Fort Worth, Texas; London: Saunders College Pub.p. 602.ISBN 0-03-020457-7.

[91] O. Rötting , W. Röpke, H. Becker and C. Gärtner, “Polymer microfabrication technologies”, Microsystem Technology Volume 8, Number 1, 32-36.

[92] H.M. Zidan and M. Abu-Elnader,“Structural and optical properties of pure PMMA and metal chloride-doped PMMA films”, Physica B: Condensed Matter Volume 355, Issues 1-4, 31 January 2005, Pages 308-317

[93] Laurie Brown, Terry Koerner, J. Hugh Horton and Richard D. Oleschuk ," Fabrication and characterization of poly(methylmethacrylate) microfluidic devices bonded using surface modifications and solvents”, Lab Chip, 2006,6, 66-73

[94] Marius Haiducu, M.ASc Thesis, “LOW COST MICROFLUIDICS ON COMMERCIAL GRADE POLY(METHYL METHACRYLATE) (PMMA) USING DEEP UV PATTERNING”

http://ir.lib.sfu.ca/dspace/bitstream/1892/11156/1/ETD4626.pdf

[95] http://www.tangram.co.uk/TI-Polymer-PMMA.htmlSerway, Raymond A. “Principles of Physics” (2nd ed ed.), (1998). Fort Worth, Texas; London: Saunders College Pub. p. 602. ISBN 0-03-020457-7.

[96] S. Yasin, D.G. Hasko, and H. Ahmed. Fabrication of <5 nm width lines in poly(methylmethacrylate) resist using a water:isopropyl alcohol developer and ultrasonically-assisted development. Applied Physics Letters, 78(18):2760–2762, 2001.

[97] M.A. Mohsin and M.G. Cowie. Enhanced sensitivity in the electron beam resist poly(methyl methacrylate) using improved solvent developer. Polymer, 29(12):2130–2135, 1988.

[98] E. Lavallée, J. Beauvais, and J. Beerens. Electron beam lithography of nanostructures using 2-propanol:water and 2-propanol:methyl isobutyl ketone as developers for polymethylmethacrylate. Journal of Vacuum Science and Technology B, 16(3):1255–1257,1998.

[99] E.A. Dobisz, S.L. Brandow, R. Bass, and J. Mitterender.Effects of molecular properties on nanolithography in polymethyl methacrylate. Journal of Vacuum Science and Technology B, 18(1):107–111, 2000.

[100]J.S. Greeneich. Developer characteristics of poly-(methyl methacrylate) electron resist. Journal of the Electrochemical Society, 122(7):970–976, 1975.

[101]S. Yasin, M.N. Khalid, and D.G. Hasko. Reduction in roughness of resist features in pmma due to the absence of a rinse. Japanese Journal of Applied Physics, 43(10):6984–6987, 2004.

[102]J.S. Papanu, D.W. Hess, D.S. Soane, and A.T. Bell. Dissolution of thin poly(methyl methacrylate) films in ketones, binary ketone/alcohol mixtures, and hydroxy ketones. Journal of the Electrochemical Society, 136(10):3077–3083, 198

[103]O. Rötting , W. Röpke, H. Becker and C. Gärtner, “Polymer microfabrication technologies”, Microsystem Technology Volume 8, Number 1, 32-36.

[104] H.M. Zidan and M. Abu-Elnader,“Structural and optical properties of pure PMMA and metal chloride-doped PMMA films”, Physica B: Condensed Matter Volume 355, Issues 1-4, 31 January 2005, Pages 308-317

[105] Laurie Brown, Terry Koerner, J. Hugh Horton and Richard D. Oleschuk ," Fabrication and characterization of poly(methylmethacrylate) microfluidic devices bonded using surface modifications and solvents”, Lab Chip, 2006,6, 66-73

[106]http://www.tangram.co.uk/TI-Polymer-PMMA.html

[107]Serway, Raymond A. “Principles of Physics” (2nd ed ed.), (1998). Fort Worth, Texas; London: Saunders College Pub. p. 602. ISBN 0-03-020457-7.

[108]Serway, Raymond A. "Principles of Physics" (2nd ed ed.), (1998). Fort Worth, Texas; London: Saunders College Pub.p. 602.ISBN 0-03-020457-7.

[109]Y. A Kim, T Hayashi, Y Fukai, M Endo; Chemical Physics Letters, Volume. 355, issue 3-4, Pages 279-284

[110]M. Inyo, T. Tahara, T. Iwaki, F. Iskandar, C.-J. Hogan, Jr., and K. Okuyama, J. Colloid Interface Sci., Volume304 (2006), Pages 535–40

[111]S. V Ahir and E. M Terentjev, Polymeric Nanostructures and Their Applications; Chapter 3, Volume 1 (2006), Pages 1-48, ISBN:1-5888-068-3

[112]Cynthia A. Mitchell, Jeffrey L. Bahr, SivaramArepalli, James M. Tour, and RamananKrishnamoorti; Macromolecules, Volume35 (23)(2002,), Pages 8825–8830

[113]Jacob C. Kearns, Robert L. Shambaugh; Journal of Applied Polymer Science, Volume 86, Issue 8 (2002), Pages 2079-2088

[114]Marius Haiducu, M.ASc Thesis, "LOW COST MICROFLUIDICS ON COMMERCIAL GRADE POLY(METHYL METHACRYLATE) (PMMA) USING DEEP UV PATTERNING".